NORTHWESTERN UNIVERSITY

DISSECTING THE ROLE OF C53 IN REGULATION OF
CELL CYCLE AND CELL DEATH

A DISSERTATION

SUBMITTED TO THE GRADUATE SCHOOL
IN PARTIAL FULFILLMENT OF THE REQUIREMENTS

for the degree

DOCTOR OF PHILOSOPHY

Field of (Integrated Graduate Program in the Life Sciences)

By

Hai Jiang

EVANSTON, ILLINOIS

(December 2006)

ABSTRACT

DISSECTING THE ROLE OF C53 IN REGULATION OF
CELL CYCLE AND CELL DEATH

Hai Jiang

Regulation of cell cycle and cell death are critical for normal cellular proliferation, tissue homeostasis, animal development, and the pathogenesis of human diseases such as cancer. Irregularities in cell cycle and cell death may result in tumorigenesis. In this dissertation, I describe my studies of a novel gene C53, which we found to play pivotal roles in cell cycle and cell death.

First, C53 suppresses the G2/M DNA damage checkpoint via inhibiting the activation and kinase activity of checkpoint kinase 1 and checkpoint kinase 2. When treated with genotoxins, cells overexpressing C53 cannot adopt G2 arrest; instead they proceed into mitosis and subsequently die during mitosis. Depletion of C53 leads to sustained G2 arrest and reduces cell death from genotoxins. C53 also regulates mitotic entry during unperturbed cell cycle. Overexpression of C53 leads to unscheduled Cdk1 activation and uneven chromatin condensation, while C53 depletion causes delays in Cdk1 activation and mitotic entry.

Second, C53 plays important roles in various stages of mitosis. C53 depletion causes many mitotic defects, including inability to separate centrosomes, mono-polar spindle, rosette-like chromosome arrangement, chromosome lagging, incomplete cytokinesis, and irregularly shaped daughter nuclei. Interestingly, most of these defects resemble those caused by Plk1 depletion. Further studies revealed C53 and Plk1 co-localize with each other at various stages of M phase. C53 interacts with the kinase domain of Plk1 and is a Plk1 substrate. Plk1-mediated phosphorylation of C53 may be important for its functions during M phase.

Third, C53 is a caspase substrate, with three caspase cleavage sites sequentially cleaved during apoptosis. Cleavage of C53 into C53-C1 promotes etoposide-induced cell death. In addition, overexpression of C53-C3 caused nuclear deformities.

Taken together, these findings demonstrate important functions of C53 during cell cycle and cell death, and provide valuable information for future studies of this novel gene.

Acknowledgements

This thesis was completed in Dr. Honglin Li's lab at the Neurobiology department at Children's Memorial Research Center (CMRC). Over the years, CMRC and the Neurobiology department have given us great supports and encouragements, without which I couldn't have done this research. The person I want to thank most is my mentor Dr. Honglin Li, for his guidance and unwavering support, and for being such a wonderful friend over the last six years. I'd like to thank members of my thesis committee, Dr. Lester Binder, Dr. H. William Schnaper, Dr. Vincent Cryns and Dr. Francis Szele for their invaluable critics and suggestions, which prompted me to realize several new aspects of my thesis project. Moreover, I want to thank Dr. Cryns and Dr. Francis for reagents and equipment sharing, especially Dr. Francis, who generously granted me unlimited access to the time lapse video microscopy, which enabled me to make several important findings of this new protein. Numerous people contributed to and helped on this project. I want to express my great thankfulness to Dr. Jianchun Wu, a post Doctoral fellow in the lab, for her help and collaboration. Dr. Shouqing Luo, a former post Doctoral fellow, identified caspase cleavage sites of this protein and his contribution is deeply appreciated. Former summer students Kunal Karmali, Chen He, Emma Yan, and former technician Grace Wang contributed in many research projects. Former and present post Doctoral fellows Dr. Xin Tong and Dr. Wending Yang also helped me on this project. The research communities at CMRC, especially Dr. Bernard Mirkin and faculties in the

List of Abbreviations

53BP1   p53 binding protein 1

9-1-1 complex   Rad9-Rad1-Hus1 complex

APC/C   Anaphase-Promoting Complex/cyclosome

ATM   ataxia-telagiectasia-mutated

ATR   ATM and Rad3 related

C-terminal   carboxy-terminal

CAK   Cdk activating kinase

Cdk1   cyclin-dependent kinase 1

Chk1   checkpoint kinase 1

Chk2   checkpoint kinase 2

CIAP1   cellular inhibitor of apoptosis 1

DSBs   DNA double strand breaks

FADD   FAS-associated death domain protein

FHA domain   forkhead-associated domain

MRN complex   Mre11-Rad50-Nbs1 complex

N-terminal   amino-terminal

PBD   polo-box domain

PCM   pericentriolar material

Plk1   polo-like kinase 1

Plkk1   Plk kinase-1

PKA   protein kinase A

RNAi   RNA interference

siRNA   small interfering RNA

shRNA   small hairpin RNA

TRAIL   TNF-Related Apoptosis Inducing Ligand

UCC   uneven chromatin condensation

XIAP   X-chromosome-linked inhibitor of apoptosis

Table of Contents

List of Figures and Illustrations

Chapter I Introduction

1.1 The cell cycle

In all living organisms, cells reproduce themselves through repeated rounds of cell growth and division. The orderly sequence of events to achieve cell growth and division is called the cell cycle, which is critical for normal cell proliferation, tissue homeostasis and animal development. The mammalian cell cycle is defined by four major phases. During G1 phase, cell monitors internal and external environment and grows in size. During S phase, DNA is replicated. At G2 phase, cell cycle ceases briefly and the status of chromosome duplication and integrity is monitored. In the following M phase, cell undergoes nuclear division (mitosis) and cytoplasmic division (cytokinesis), and two daughter cells are produced, each inheriting a set of genomic material identical to the previous generation. Failure to faithfully replicate and segregate genetic materials leads to the formation of aberrant daughter cells and contributes to the malignancy of many human cancers.

1.2 Cell cycle checkpoints and DNA damage response

Given the importance of genetic information, cells have developed sophisticated surveillance mechanisms to ensure the faithful inheritance of genetic material between generations. Such mechanisms, called "cell cycle checkpoints", constantly monitor cell cycle progression and ensure that a later event of the cell cycle begins only when the preceding event is finished. There are four major checkpoints in the mammalian cell cycle: the G1/S checkpoint, the intra-S checkpoint, the G2/M checkpoint, and the spindle

assembly checkpoint. Each of these checkpoints is indispensable for the orderly progression of cell cycle. Once activated, cell cycle checkpoints utilize a large network, consisting of multiple kinases, phosphatases, and Ubiquitin ligase complexes to halt the progression of the cell cycle, thereby allowing time for cells to carry out repair. If the damages are beyond repair, cells either stay permanently in cell cycle arrest, or elicit cell death program to eliminate themselves.

One major case of checkpoint activation is when DNA damage is induced inside cells. The DNA damage checkpoint signaling pathway involves participations of DNA damage sensors, signaling transducers and effectors (Figure 1A). The conserved Rad9-Rad1-Hus1 (9-1-1) complex and Mre11-Rad50-Nbs1 (MRN) complex sense DNA damage [1,2] and recruit two related and conserved proteins of the phosphoinositide 3-kinase-like family, ATM (ataxia-telagiectasia-mutated) and ATR (ATM and Rad3 related). Acting as signal transducers, these two kinases phosphorylate and activate downstream targets such as checkpoint kinase 1 (Chk1) [3,4] and checkpoint kinase 2 (Chk2) [5], p53 [6,7], BRCA1 [8,9], H2AX [10], and 53BP1 [11,12].

Among these ATM/ATR substrates, Chk1 and Chk2 are the major kinases relaying DNA damage signals to downstream effectors [13]. The mammalian Chk1 and Chk2 are structurally unrelated yet functionally overlapping serine/threonine kinases that play critical roles in relaying checkpoint signaling in response to various genotoxic insults (Bartek and Lukas, 2003). Chk2 is the homologue of yeast Rad53 and Cds1 that contains a SQ cluster domain at its N-terminus, a phospho-amino acid binding motif called the FHA (forkhead-associated) domain and the kinase domain (Figure 1B). Chk2 appears to be largely inactive in the absence of DNA damage. It is activated mainly by

A

B
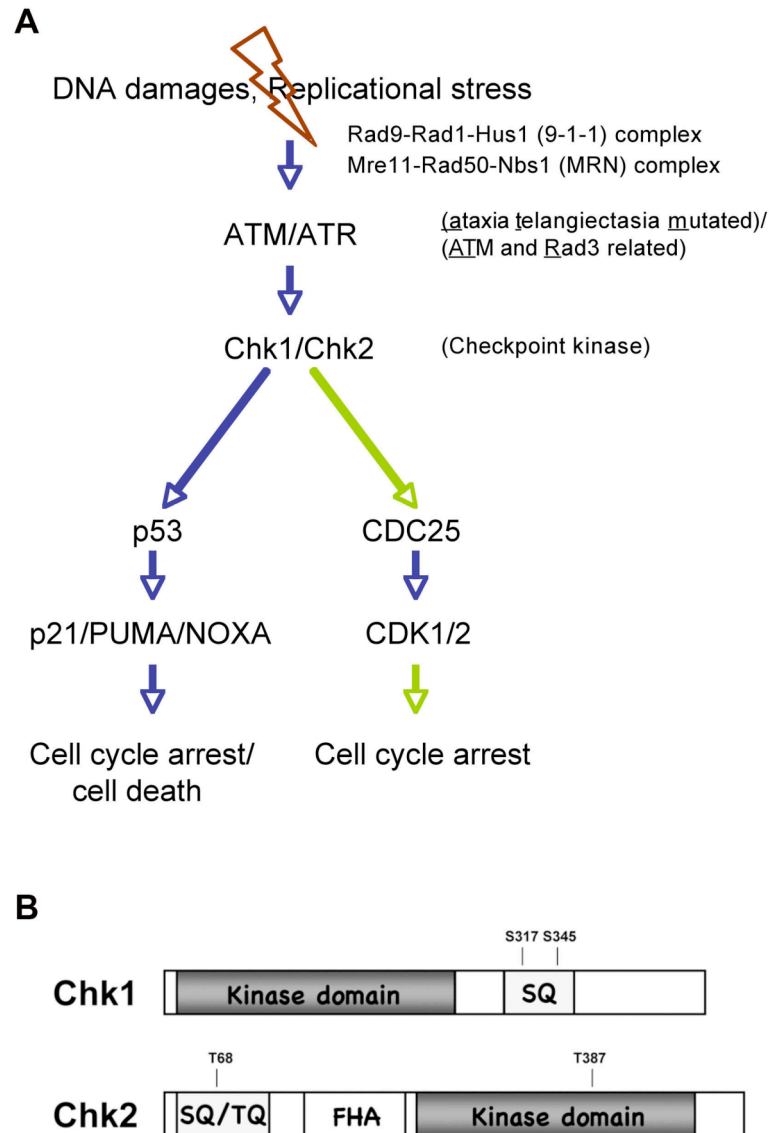
Figure 1 DNA damage response and Checkpoint kinases

A. Depiction of DNA damage responses.
B. Structures of human Chk1 and Chk2. In Chk1, SQ, a serine/glutamine-rich region with two ATM/ATR phosphorylation sites S317 and S345). In Chk2, SQ/TQ, a serine/glutamine and threonine/glutamine rich region with ATM/ATR phosphorylation site (T68). FHA, a forkhead-associated domain required for Chk2 homodimerization and other protein-protein interactions. T387 is an autophosphorylation site.

ATM-mediated phosphorylation of residue Thr68 at the SQ domain in response to DNA double-strand breaks (DSBs) [5]. In contrast, Chk1 is a labile protein, and is active even in unperturbed cell cycle. It contains a kinase domain at its N-terminus and a SQ cluster at its C-terminus (Figure 1B). Chk1 is usually activated by ATR-mediated phosphorylation of Ser317 and Ser345 in response to UV and replication stress [4]. Recently, Zhang *et al* reported that phosphorylation of Chk1 induced by genotoxic stress promotes its degradation by the ubiquitin-proteasome pathway [14]. Despite the original concept of ATM-Chk2 and ATR-Chk1 axis, various cross-talk among these kinases has been reported, exemplified by the phosphorylation of Chk1 by ATM in response to ionizing radiation [3].

Once activated, Chk1 and Chk2 phosphorylate various substrates to elicit proper DNA damage responses. One prominent substrate of Chk1 and Chk2 is p53 [15], which can be stabilized by such phosphorylation. p53 then upregulates p21 [16], an inhibitor of cyclin dependent kinase 1 and 2, to halt the cell cycle for repair. If the DNA damage is too severe and beyond repair, p53 transcriptional targets such as PUMA [17] and Noxa [18] then elicit the mitochondrial apoptotic pathway to induce programmed cell death. Meanwhile, Chk1 and Chk2 also phosphorylate and inactivate Cdc25 [19], which will also lead to cell cycle arrest.

The DNA damage checkpoint network is essential for maintenance of replication accuracy and genome stability, and defects in DNA damage response are largely responsible for tumorigenesis and genome instability of cancer cells [20,21]. Bartkova *et al* [22] and Gorgoulis *et al* [23] recently provided evidence that the DNA damage response such as activation of ATM and Chk2 was induced in human precancerous lesions and oncogene-driven tissue culture cells. This DNA damage response delays or

prevents progression towards full-blown cancer. Inactivation or mutations compromising this response may allow cell proliferation and increase genomic instability and tumorigenesis. ATM deficiency leads to genome instability and predisposition to cancer [24], while many genetic alterations of Chk1 and Chk2 have been found in many types of familial and sporadic cancers [13]. These evidence strongly suggest the importance of DNA damage checkpoint to prevent tumorigenesis. However, as will be explained later, in tumor cells where p53 is lost or mutated, DNA damage checkpoints can greatly reduce the effectiveness of anti-cancer therapies. Therefore, abrogation of DNA damage checkpoints may represent a novel approach to sensitize tumor cells to conventional cancer treatment [25].

1.3 The G2/M checkpoint and its importance for chemotherapy

The Cdk1/cyclin B1 kinase complex is the driving force of mitotic entry [26-28]. Once activated, Cdk1/cyclin B1 phosphorylates various substrates, inducing condensin [29] and nuclear lamin [30], to induce multiple changes, such as chromosome condensation and nuclear membrane breakdown. Before M phase of the cell cycle, Cdk1 is kept inactive by two inhibitory phosphorylations on its N-terminus. These two phosphorylations, p-T-14 and p-Y-15, carried out by two kinases Wee1 and Myt1, block the ATP binding of Cdk1 and renders it inactive [31-33]. At the onset of mitosis, phosphates of the Cdc25 family, such as Cdc25B and Cdc25C remove these two inhibitory phosphorylations [34]. Phosphorylation by CAK ensues and the core enzyme Cdk1 becomes active [35,36]. Meanwhile, cyclin B1 transcription increases during late G2 phase [37] and phosphorylation of cyclin B1 facilitates the nuclear accumulation of

Cdk1/Cyclin B1 [38]. Together, these events lead to the activation of Cdk1/Cyclin B1 complex, which then drives cell into mitosis.

The activation state of Cdk1/cyclin B1 is the major target of the G2/M checkpoint and is under constant and accurate control. Before the completion of DNA replication, Cdk1/cylin B1 needs to be kept inactive; otherwise cells will proceed into mitosis prematurely, producing daughter cells with incomplete genetic material. Such inhibition of Cdk1/clycin B1 also occurs when cells detect genomic damages [20], thereby enabling DNA damage repair during the G2 phase.

The majority of human solid tumors do not have a functional p53-signaling pathway. These cells, when treated with genotoxic stress, especially those inducing chromosome breaks (e.g., ionizing irradiation, etoposide, Camptothecin and Doxorubicin), do not undergo p53-mediated cell death or cell cycle arrest. Instead, they are arrested at G2 due to the function of the G2/M DNA damage checkpoint (depicted in Figure 4A). In response to DNA damage, ATM and ATR mediated phosphorylation activates Chk1 [3,4] and Chk2 [5], which then phosphorylates and inhibits Cdc25 [19]. As a result, the N-terminal phosphorylation of Cdk1 cannot be removed by Cdc25, Cdk1/cyclin B1 stays inhibited and cells stay arrested at G2.

During prolonged arrest at G2, these genotoxin-treated cancer cells will attempt DNA damage repair. As a result, they can often delay and/or escape from radio- and chemotherapy-induced cell death. Such phenomena present a great hurdle for the effectiveness of anti-cancer therapies. Various methods to suppress the G2/M DNA damage checkpoint have been proposed and utilized in laboratory research as well as clinical trials [24,25,39-42]. When used together with conventional anti-cancer drugs, these agents abolish the G2 arrest and as a result, tumor cells proceed into mitosis with

broken chromosomes or other forms of severe DNA damages. Such conditions usually cause massive cell death during mitosis. Therefore, co-treatment with agents that suppress the G2/M checkpoint is a promising strategy to enhance the effectiveness of conventional anti-cancer therapies [25].

For example, UCN-01, a chemical inhibitor of Chk1, can be used together with traditional chemotherapy to enhance their killing of cancer cells [43]. Instead of staying at G2 and attempting DNA repair, cancer cells treated with UCN-01 proceed into mitosis with a significant amount of DNA damage. This results in massive cell death during mitosis. Base on this observation, UCN-01 has been used in clinical trials as a co-treatment for chemotherapy and has yielded encouraging results for melanoma and refractory anaplastic large-cell lymphoma [44]. In laboratory studies, caffeine (inhibitor of ATR and ATM) and Wortmannin (inhibitor of ATR) are also used together with genotoxins to achieve similar pro-death effects [39]. More recently, several more inhibitors of Chk1 have been developed and were reported to have anti-cancer effects in *in vitro* studies [42]. Considering this, searching for novel genes that regulate the G2/M DNA damage checkpoint is of particular interest for cancer therapy.

1.4 The M phase and Polo-like kinase 1

During the cell cycle, chromosome segregation and cell division occur in the M phase (M stands for mitosis), a phase equally crucial for genetic stability of cells. The M phase consists of six stages: prophase, prometaphase, metaphase, anaphase, telophase and cytokinesis. These six stages are very complex and dynamic and involve the coordination of multiple cellular components including chromosomes, cytoskeleton,

centrosomes as wells as cytoplasmic and nuclear membranes. Each stage is tightly regulated to ensure the formation of two genetically identical daughter cells.

The cellular events of each stage are depicted in Figure 2A (adapted from Barr *et al* [45]). At the onset of mitosis, mitotic kinase activities lead to chromosome condensation, centrosome separation and mitotic spindle formation at prophase. During prometaphase, nuclear membrane breaks down, chromosomes attach to spindle microtubules and undergo directed movements. At metaphase, bi-polar mitotic spindles function to align chromosomes to the equatorial plate. At anaphase, sister chromatids synchronously separate and are pulled toward spindle poles. During telophase, sister chromatids arrive at the poles of spindles and decondense. Nuclear envelopes begin to assemble around newly formed daughter nuclei. During cytokinesis, the cytoplasm is divided in two and the M phase is complete.

Orderly execution of M phase is critical for normal cellular proliferation, tissue homeostasis, and animal development. Failure to accurately segregate genetic material generates aberrant daughter cells and contributes to the malignancy of human cancers. Like other phases during the cell cycle, faithfulness of M phase events is achieved by coordinated actions of multiple kinases and phosphatases. Among them, Polo-like kinase 1 (Plk1) is an important mitotic kinase that regulates the progression of multiple key mitotic events and is indispensable for mitotic progression (Figure 2A) [45-47]. At the G2/M boundary of the cell cycle, Plk1 phosphorylates Cdc25 [48], Myt1 [49], Wee1 [50] and cyclin B1 [51] to promote the activation of Cdk1/cyclin B1 kinase complex, which subsequently drives cells into mitosis. In early M phase, Plk1 phosphorylates multiple centrosomal and microtubule-associated proteins such as Asp [52,53], Op18 [54], Nlp [55,56] and Katanin [57], which either severs microtubule to enable dynamic
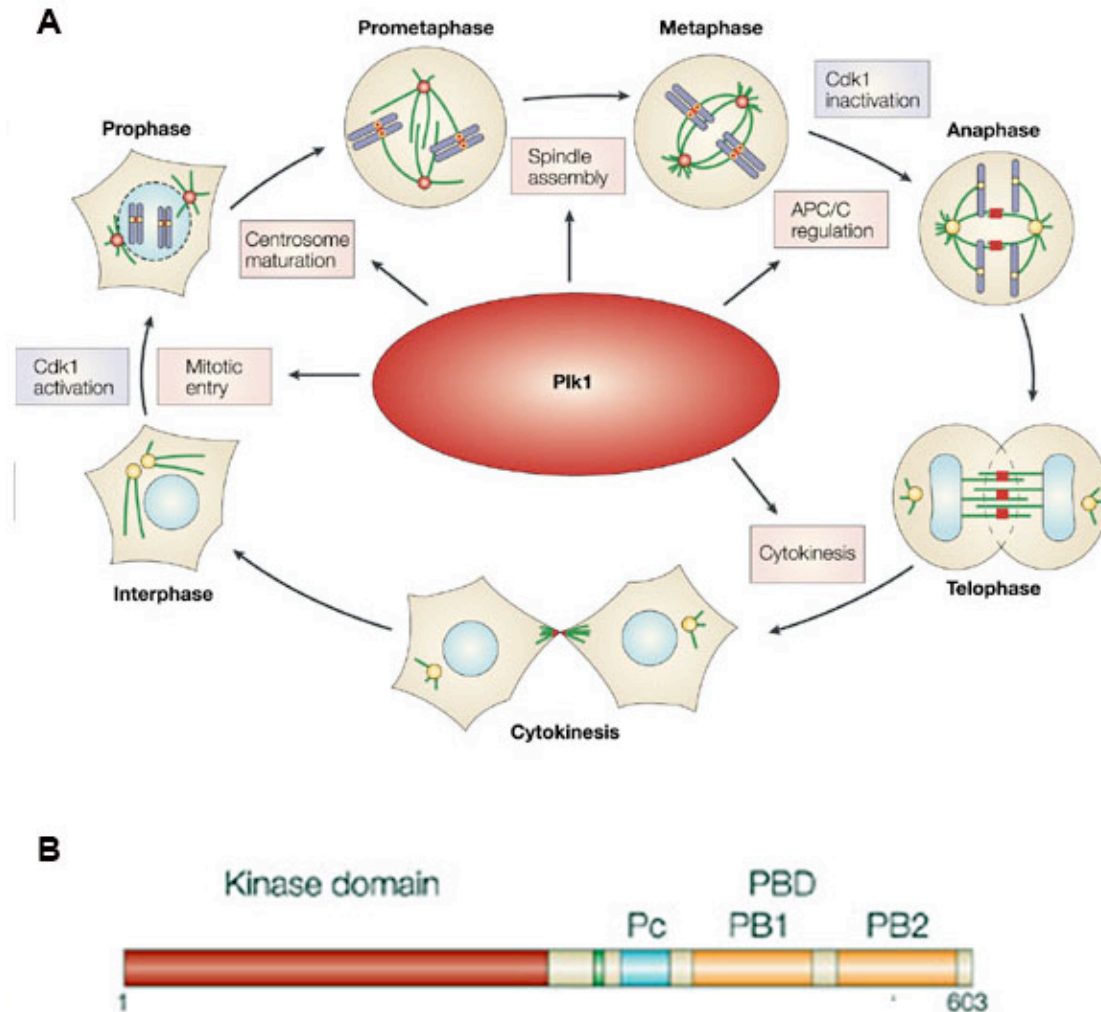
Figure 2 Polo-like kinase 1 and its role in M phase progression

A. Plk1 functions in various stages of M phase to facilitate orderly progression of cell cycle. DNA/chromosomes are marked in blue, microtubules in green and both centrosomes and kinetochores in yellow. Plk1's association with different structures during M phase is indicated in red.

B. Structure of Plk1. Plk1 consists of two parts, the amino-terminal kinase domain and the carboxy-terminal polo-box domain (PBD), which contains two polo boxes (PBs). A linker region (in green) and a small region known as the polo-box cap (Pc) join the two parts. Both A and B are adapted from Barr *et al* [45].

γ- tubulin redistribution important for spindle function [57], or facilitates microtubule nucleation to promote spindle formation [58]. Plk1-mediated phosphorylation of Cohesin and Anaphase-Promoting Complex (APC) promotes chromosome segregation during anaphase [59-63]. Furthermore, Plk1 phosphorylates the microtubule-associated protein NudC, which is necessary for the completion of cytokinesis [64]. Given the high demand for mitotic activities in human cancer cells, Plk1 is often overexpressed in various kinds of human tumors. Examples include gastric, esophageal, prostate, breast, bladder, ovarian, colorectal, lung, endometrial carcinomas, gliomas, squamous cell carcinomas of the head and neck, and many more [65,66]. In some of these studies, overexpression of Plk1 is associated with significantly poor prognosis [67-69]. Therefore, RNA interference and chemical inhibitors of Plk1 have been widely used to treat cancer cells in laboratory studies and clinical trials [70-76]. Compared to conventional anti-cancer drugs, such an approach should incur fewer side effects. Conventional chemotherapeutic agents that target cancer cells' genome sometimes interfere with RNA transcription and other aspects of cellular metabolism in normal cells, thereby causing unwanted side-effects and possibly leading to secondary tumors. Spindle poisons that target the mitotic spindle invariably interfere with microtubule function in neuronal cells, and can cause significant neurotoxicity. Depleting Plk1 activity, in contrast, has fewer such concerns. Recently, it was reported that a chemical inhibitor of Plk1, ON01910, potently inhibits tumor growth in a variety of xenograft nude mouse models [75]. Importantly, it exhibited no hematotoxicity, liver damage, or neurotoxicity. This and other similar studies showed a promising future for combating cancer using Plk1 antagonists.

Plk1 consists of the N-terminal kinase domain and the C-terminal *Polo-box* domain (PBD) (Figure 2B). During cell cycle progression, Plk1 localizes to centrosomes (G2), centrosomes and kinetochores (prometaphase), spindle poles and kinetochores (metaphase), central spindles (telophase) and midbody (cytokinesis) [45]. Because of Plk1's functional importance for cell division, it needs to be tightly regulated to ensure orderly progression of the cell cycle. In fact, both overexpression and depletion of Plk1 are detrimental to cells and cause long-term decrease of viability [70,77]. Cells utilize various mechanisms to control Plk1 activity, most importantly through regulating its abundance and kinase activation. Upon the completion of the previous cell cycle, Plk1 is degraded by the Anaphase-promoting complex/ cyclosome (APC/C) and proteasome [78,79]. During the late S and G2 phases of cell cycle, Plk1 begins to accumulate inside cells. At the G2/M transition point, Plk1 reaches a high level and a T-loop activation is proposed to incur the kinase activation [80]. Briefly, Thr210 in the N-terminal kinase domain (the T-loop) is phosphorylated and Plk1 becomes active [81]. *In vitro* studies using *Xenopus* extracts showed that two upstream kinases, the Plk kinase-1 (Plkk1) [82] and protein kinase A (PKA) [83], are capable of carrying out this Thr210 phosphorylation. However, whether such phosphorylation occurs *in vivo* and in mammalian cells remains unclear. Nonetheless, Plk1 with Thr210E mutation mimicking the T-loop phosphorylation have substantially higher kinase activity [84,85], demonstrating the importance of T210 phosphorylation. Of note, mutation of Ser137 in Plk1 also confers high kinase activity, although whether this site is phosphorylated *in vivo* is not known [84].

Aside from the T-loop phosphorylation within its N-terminal kinase domain, the Plk1's C-terminal *polo-box* domain (PBD) also functions to regulate Plk1 activity [77,80].

Using overexpression studies and kinase assays, Jang *et al* showed that PBD interacts

with the kinase domain and inhibits its activity [86]. It is proposed that such interaction

may prevent kinase activation and/or substrate binding [45]. Structural and biochemical

analyses showed that the PBD is a phosphopeptide-binding domain [87]. Pre-existing

phosphorylation signals on Plk1 substrates recruit the PBD and create docking sites for

Plk1, which then phosphorylates these substrates [88]. It is proposed the occupancy of

PBD by phosphorylated ligands releases the Plk1 kinase domain and may then enable

the T-loop activation [88]. However, to date there is still no direct evidence

demonstrating such a temporal sequence, and how T-loop activation of Plk1 occurs is

still unknown. It remains interesting to see whether alternative mechanism of T-loop

activation exists.

Given the important functions of Plk1 during mitosis, it is not surprising that Plk1

depletion leads to multiple mitotic defects. As mentioned above, Plk1 first functions

during the G2/M transition in the cell cycle. However, this function of Plk1 is not

absolutely required for G2/M transition. As a result, Plk1 depletion or inhibition induces

a moderate delay of mitotic entry, but cells can still proceed into mitosis [71,89]. Once in

mitosis, however, phosphorylation of various centrosomal and microtubule associated

proteins by Plk1 is essential for mitotic progression. Therefore, the majority of Plk1

depleted cells stay arrested in prometaphase with chromosomes moving aimlessly [70].

Another prominent phenomenon is that, in Plk1 depleted cells, centrosomes cannot split

and migrate, and as a result, only mono-polar spindles can be formed. Under such

conditions, chromosome arrangement adopts a rosette-like configuration [70,90]. In

either case, Plk1-depleted cells arrest in mitosis, a state that ultimately leads to cell

death [70,91]. Although such a phenomenon has been widely utilized to cause cancer

cell death, the exact trigger and execution of such mitotic cell death have not been investigated and remain unclear.

Aside from mitotic arrest and subsequent cell death, there are also other mitotic defects associated with Plk1 down-regulation. In most studies of Plk1 depletion, Plk1 is knocked down using RNAi-based technology. Because of the limitation of RNAi efficiency, it is not expected that every cell has 100% Plk1 knockdown. In some cells that have residual activities of Plk1, cell cycle is able to pass the aforementioned prometaphase/ metaphase arrest, and proceeds into later mitotic stages. Defects such as chromosome lagging in anaphase and incomplete cytokinesis have also been reported. Recently, Liu *et al* used a lentivirus-based Plk1 RNAi approach to generate a series of Plk1 hypomorphs, and showed that chromosome lagging and incomplete cytokinesis can indeed result from moderate level of Plk1 knockdown [71]. However, although these Plk1 knockdown cells were able to exit mitosis and give rise to viable daughter cells, the daughter cells, as progeny of aberrant mitosis, often showed severe nuclear shape defects such as "dumbbell" (poly-lobed) or fragmented nuclei, multinuclei and micronuclei [70,71]. Such nuclear shape defects are often observed in various forms of human cancers [92], and it remains to be examined whether Plk1 or its associated proteins are deregulated in such cases.

1.5 The C53 gene and thesis research summary

C53 protein was originally isolated as a binding partner of p35, the activator of Cyclin-dependent kinase 5 (Cdk5) [93]. Subsequently, Dr. Honglin Li identified it as a caspase substrate. The human C53 gene is located in human chromosome 17q21.31, a region often mutated or deleted in human cancers. Overall, the C53 gene is highly

conserved, with homologues found in the genomes of vertebrate, invertebrate and plant, but not yeast or bacteria. Multiple sequence alignment suggests that both amino-(N-) and carboxyl-(C-) terminal portions of the protein are more conserved than the middle part (Figure 3). The C53 gene is ubiquitously expressed as a 66 kDa protein in most human tissues, and is aberrantly expressed in hepatocellular carcinoma (our personal communication with Dr. Y P Ching at Hongkong University).

Recently, two isoforms of C53 (IC53 and IC53-2, respectively) were identified, each derived from alternative splicing [94,95]. Human C53 cDNA is 1.8 kb long, and encodes 506 amino acids. Human IC53 cDNA is 2.5 kb long, and encodes 419 amino acids. Human IC53-2 cDNA is 2.2 kb, and encodes 281 amino acids. Both C53 and IC53 are ubiquitously expressed [94]. In contrast, The IC53-2 transcript is highly expressed in kidney, liver, skeletal muscle and placenta [95]. IC53 is up-regulated in the rat model of sub-acute heart failure and chronic heart failure, and ectopic expression of C53 isoforms stimulates proliferation of endothelial ECV304 cells and hepatocellular carcinoma SMMC-7721 cells [94,95]. These data indicate C53 may be involved in regulation of cellular proliferation.

In this dissertation, I describe my research on C53, which plays multiple roles in regulation of cell cycle and cell death.

First, C53 inhibits the activation and/or activity of Chk1 and Chk2, thereby suppressing the G2/M DNA damage checkpoint. Overexpression of C53 sensitizes cancer cells to multiple genotoxins, while depletion of C53 confers partial resistance to etoposide and X-Ray irradiation. Such a finding has potential implications for chemotherapy. Moreover, C53 is a centrosome-associated protein and also regulates mitotic entry during unperturbed cell cycle.

```
hC53     1 MEDHQHVPIDIQTSKLLDWLVDRRHCSLKWQSLVLTIREKINAAIQDMPESEEIAQLLSGSYIHYFHCLR    70
mC53     1 MQDHQHVPIDIQTSKLLDWLVDRRHCNLKWQSLVLTIREKINTAIQDMPESQEIAQLLSGSYIHYFHCLR    70
rC53     1 MQDHQHVPIDIQTSKLLDWLVDRRHCNLKWQSLVLTIREKINTAIQDMPESQEIAQLLSGSYIHYFHCLR    70
dC53     1  MNESEIPIDIHTLKLQDWLISRRIVPKNVQQELREIHRKISNALQDMPSNEQLIKLLARTNINYYHVKE    69
cC53     1 MSDD--LPIDIHSSKLLDWLVSRRHCNKDWQKSVVAIREKIKHAILDMPESPKIVELLQGAYINYFHCCQ    68
             .****.. ** ***. **      *  .  *. ** *. ***    . ** . *.*.*

hC53    71 ILDLLKGTEASTKNIFGRYSSQRMKDWQEIIALYEKDNTYLVELSSLLVRNVNYEIPSLKKQIAKCQQLQ   140
mC53    71 IVDLLKGTEASTKNIFGRYSSQRMKDWQEIIALYEKDNTYLVELSSLLVRNVNYEIPSLKKQIAKCQQLQ   140
rC53    71 IVDLLKGTEASTKNIFGRYSSQRMKDWQEIISLYEKDNTYLVELSSLLVRNVNYEIPSLKKQIAKCQQLQ   140
dC53    70 IIEILKQTEKDTKSVFGTYGSQRMKDWQEISRLYEKNATYLAETAQIFVRNVNYEIPGVRKQMARLEQQA   139
cC53    69 IIEILRDTEKDTKNFLGFYSSQRMKDWQEIEGMYKKDNVYLAEAAQILQRLAQYEIPALRKQISKMDQSV   138
            *...*. **  **   * * *********** .* *   ** *.. *   **** ..**... *

hC53   141 QEYSRKEEECQAGAAEMREQFYHSCKQYGITGENVRGELLALVKDLPSQLAEIGAAAQQSLGEAIDVYQA   210
mC53   141 QEYSRKEEEGQAGAAEMREQFYHSCKQYGITGDNVRRELLALVKDLPSQLAEIGAGAQS-LGEAIDLYQA   209
rC53   141 QDYSRKEEEGQAGAAEMREQFYHSCKQYGITGDNVRRELLALVKDLPSQLAEIGAGAQS-LGEAIDLYQA   209
dC53   140 DETQKRAHDLNKPESQILADHSALLEQLGVKGDNLHAEFVQVLSGLPELYDKSLVGIAN-IQPGIDLYAE   208
cC53   139 TDAIRKHSEYGKQAEDGRKQFEKEISRMQLKGVHLRKELLELAADLPAFYEKITAEIRK-ISAARDYFQA   207
             .  ..         . .  * ... * . .   **      .  *       .   *

hC53   211 SVGFVCESPT----EQVLPMLRFVQKRG-NSTVYEWRTGTEPSVVERP--HLEELPEQVAE-D----AID   268
mC53   210 CVEFVCDSPT----EQVLPMLRYVQKKG-NSTVYEWRTGTEPSVVERP--QLEEPPEQVQE-D----EID   267
rC53   210 CVEFVCDSPT----EQVLPMLRYVQPKG-NSTVYEWRTGTEPSVVERP--QLEDPPEQVQE-D----EID   267
dC53   209 VS-----GNK----Q-VLPILNHLVEFG-NTTVYQYIHKEAPLAVEEPPIRLNLSEGNASKDDNAVAEID   267
cC53   208 FRDYMSLGAAPKDAAPILPIIGLIGERGLDVTTYEWKYNQKPDKVEKP--NFEMLLTAAEDSD----EID   271
            .**.. .   . *   * *.   * **   *      *      * **

hC53   269 WGDFGVEAVSEGTDSGISAEAAGIDWGIFPESDSKDPGGDGIDWGDDAVAL-------QITVLEAGTQAP   331
mC53   268 WGDFGVEAVSDSG---IVAETPGIDWGISLESEAKDAGADKIDWGDDAAAAS------EITVLETGTEAP   328
rC53   268 WGDFGLEAVSDSGNI-ISAETPGIDWGISLESESKDAGADKIDWGDNAVAS-------EITVLETGTEAP   329
dC53   268 FG------TDDNGGTSSTVSAEIIDYGDFGSGDLPESDGGNIDWGIESAPTDAVEINFDIPVEEYGIVVE   331
cC53   272 FG------GGD----------E-IDFGIAAED----------DAVIDFSAVV------DLVADDTGAVG-   307
              *           ** *      * * *.     *  ** *          .   . *

hC53   332 -----EGVARGPDALTLLEYTETRNQFLDELMELEIFLAQRAVELSEEADVLSVSQFQLA-PAILQGGQTK   395
mC53   329 -----EGVARGSDALTLLEYPETRNQFIDELMELEIFLSQRAVEMSEEADILSVSQFQLA-PAILQGGQTK   392
rC53   330 -----EGVARGSDALTLLEYPETRNQFIDELMELEIFLSQRAVEMSEEADILSVSQFQLA-PAILQGGQTK   393
dC53   332 GTGMDGGTAKGDQAYTLLDSPNYRDRFLDEIYELESFLRMRIYELKQLESSSDIMFSLMD---NIATHDG   398
cC53   308 -----EAIASGQDALHLLENSEAQKAVKHELIELLAFLSMRLDDETRETTADVLIRGAEKRPDGVAAVTE   372
                 * *  ** **.   *. ** ** *    .          .     . . .

hC53   396 EKMVTMVSVLEDLIGKLTSLQLQHLFMILASPRYVDRVTEFLQQKLKQSQLLALKKELMVQKQQEALEEQ   465
mC53   393 EKMLSLVSTLQQLIGRLTSLRMQHLFMILASPRYVDRVTEFLQQKLKQSQLLALKKELMVEKQQEALQEQ   462
rC53   394 EKMLSLVSTLQHLIGQLTSLDLQHLFMILASPRYVDRVTELLQQKLKQSQLLALKKDLMVEKQQEALQEQ   463
dC53   399 ESIWKILVSVEKIIQQTSDKQTQHLFQLKHSPKYANMLATKLQQMTKAVEKLRATREALKQLTIELREQR   468
cC53   373 KRLKTWITEVEGILKELENPQKVHLFKIRGSPQYVEQVVEELEKKRDMEHRYKRLQTLMTENQETARQSV   442
                      *** .  **.*  .  *.                 . . . .   .

hC53   466 AALEPKLDLLLEKTKELQKLIEADISKRYSGRPVNLMGTSL                              506
mC53   463 AALEPKLDLLLEKTRELQKLIEADISKRYSGRPVNLMGTSL                              503
rC53   464 AALEPKLDLLLEKTRELQKLIEADISKRYNGRPVNLMGTSV                              504
dC53   469 QDLNPVLEELIAQTRTLQSHIEKDISKRYKNRVVNLMGGVN                              509
cC53   443 TKSNVELKTIVESTRVLQKQIEAEISKKYNGRRVNLMGGINQALGGN                        489
             *  .. *. ** ** .***.* .* *****
```

Figure 3 Multiple sequence alignment of C53 homologs

Potential C53 homologs include human (AK023722), mouse (BC002318), rat (AF177476), *Drosophila* (AY060743) and *C. elegans* (AL110477). C53 from *Arabidopsis thaliana* (AP002032) is not included.

Second, C53 plays multiple roles in mitosis. C53 depleted cells manifest multiple M phase defects, including inability to separate centrosome, mono-polar spindle, rosette-like chromosome arrangement, chromosome lagging, incomplete cytokinesis, and irregularly shaped daughter nuclei.   Most of these defects have been observed in Plk1 depleted or functionally impaired cells. C53 co-localizes with Plk1 during various stages of M phase. We further demonstrated that C53 interacts with the kinase domain of Plk1 and is a possible Plk1 substrate. Therefore, C53 may be a novel component of Plk1 signaling during M phase.

Lastly, C53 is cleaved by caspases during cell death induced by multiple cell death stimuli. Four forms of cleavage fragments of C53 (N, C1, C2 and C3) are generated by caspase cleavage. The C1 fragment showed enhanced ability to suppress the G2/M checkpoint and is most effective at sensitizing cells to etoposide. The C3 fragment induces nuclear deformation, which resembles the defect caused by C53 depletion, suggesting the C3 fragment may act as a dominant negative inhibitor of full length C53.

Taken together, our research on C53 is the first to characterize its functions in cell cycle and cell death. C53 is important for the G2/M DNA damage checkpoint, and it also plays important roles in mitosis. In addition, such functions of C53 seem to be modulated by caspase cleavage. These results provide important initial clues of C53's function, and may potentially benefit chemotherapy in the future.

Chapter II. Material and Methods

2.1 Materials

2.1.1 Cell lines, Bacteria strains and reagents

Tissue Culture Cells— U-2 OS osteosarcoma cell (from ATCC) were grown in MaCoy's 5A medium supplemented with 10% fetal bovine serum (FBS), while HeLa, MCF7, T47D and HCT116 and HCT116 (p53-/-) cells were cultured in Dulbecco's modified Eagle's medium (DMEM) supplemented with 10% fetal bovine serum and antibiotics. IMR90E1A cell line was a kind gift from Dr. Yuri Lazebnik, Cold Spring Harbor Laboratory. HCT116 and HCT116 (p53-/-) cells were kindly provided by Dr. Bert Vogelstein, Johns Hopkins University.

Bacteria strains— *E.coli* strain XL-1 blue was used for molecular cloning. BL21 was used to express GST-fusion protein. BL21 (DE3) was used to express His-tagged protein.

Reagents— TNFα, α-casein, genotoxic reagents, and chemicals were purchased from Sigma. TRAIL was purchased from Perro Tech. Purified Cdk1-cyclin B1 was purchased from Upstate. UCN-01 was obtained from National Cancer Institute.

2.1.2 antibodies

Various anti-C53 antibodies were generated in the lab. Caspase-2 and -8 antibodies were described before [96]. Caspase-3 and -7, poly (ADP-ribose) polymerase, Cdk1 and phospho-Y15-Cdk1, p-S216-Cdc25C, p-S345-Chk1, p-T68-Chk2 antibodies are from Cell Signaling. Caspase-9, cyclin B1, Hsp90 are from Santa Cruz

Biotechnology. Other antibodies include Bcl-2 (DAKO), Bim and Apaf-1 (Stressgen), iκBα, Myc (Santa Cruz Biotechnology), FADD (FAS-associated death domain protein), XIAP (X-chromosome-linked inhibitor of apoptosis), and CIAP1 (cellular inhibitor of apoptosis 1) (BD Biosciences), Bak and p-S10-Histone H3 (upstate Biotechnology), Cdc25C (Calbiochem), Chk2 (LabVision), p-S139-H2AX (BioLegend), Plk1 (Zymed), p21 and p53 (Oncogene), and FLAG M2, Chk1, actin, γ-tubulin and α-tubulin (Sigma).

2.2 Methods

In vitro Expression Cloning—Construction of mouse spleen cDNA small pool library and *in vitro* expression cloning was performed as described [97].

C53 cDNA Cloning, Construction of Expression Vectors, and Site-specific Mutagenesis—Human C53 cDNA was amplified using primers containing SalI and KpnI sites and EST clone BE336801 as a template. Amplified C53 cDNA was sequenced and subcloned in-frame into pCMV-5a (Sigma), and the resulting construct was used for expression of the C-terminal FLAG-tagged C53 in mammalian cells. Site-specific mutagenesis was performed using the Quick-Change site-specific mutagenesis kit (Stratagene) according to the manufacturer's protocol. Mutations were confirmed by DNA sequencing.

Construction of Other Expression Vectors— Human cDNAs for C53 truncated mutants (C53N and C53C1, C2, C3) were subcloned in-frame into pcDNA-CMV-5a (Sigma), and the resulting constructs were used for expression of C-terminal Flag-tagged C53 in

mammalian cells. Human cDNAs for Chk1 and Chk2 were amplified from their full-length MGC cDNA clones (ATCC), and subcloned in-frame in pcDNA-Myc (Clontech). Centrosome-targeting C53 (C53-GFP-PACT) was constructed by two-step PCR. Specifically, C53-GFP cDNA was amplified using specific primers (primer 1: 5' GCGTCGACATGGAGGACCATCAGCAC3' and primer 2: 5' GGCAATGATGGCTTCAATGTTGGCCTTGTACAGCTCGTCCATGCCGAG3') and pEGFP-N3-C53 as the template, while PACT cDNA was amplified using primers (primer 3: 5' CTCGGCATGGACGAGCTGTACAAGGCCAACATTGAAGCCATCATTGCC3' and primer 4: 5' GGATCGATTTATGCACCTTGATTCAGTCCAAAGCC3') and GFP-Chk1-PACT (a gift from Dr. J. Bartek) as the template. Since primers 2 and 3 were complementary, the second PCR was performed using primer 1 and 4 as primers and purified C53-GFP and PACT cDNAs as templates. The recombinant C53-GFP-PACT cDNA was digested with Sal I and Cla I and subsequently cloned into pLPCX vector (Clontech). All cDNA clones were verified by DNA sequencing. H2B-GFP was a kind gift from Dr. Hongtao Yu, UT southwestern medical center.

Small Interfering RNA (siRNA) Synthesis and Construction of Small Hairpin RNA (shRNA) Expression Vectors—C53 siRNAs were designed according to Elbashir *et al* [98] and synthesized by Qiagen. SiRNA-1 for human C53 is r(GCAGAUUGCCAAGUGCCAGC), whereas siRNA-2 is r(GCUGGCACUUGGCAAUC GGC). To construct shRNA expression vectors, we ligated shRNA oligonucleotide template into linearized pSIREN-RetroQ vector (Clontech) to generate pSIREN-RetroQ-C53 expressing C53 shRNA. Oligonucleotide templates were designed and synthesized according to guidelines provided by Clontech. Plk1 shRNA were designed as described

before [89].

Establishment of C53-deficient Stable Clones—HeLa cells (10^6) were transfected with pSIREN-RetroQ-C53 plasmid or pSIREN-RetroQ-Luc (expressing luciferase siRNA). After a 48-h incubation, cells were treated with puromycin (2 μg/ml) for 3–4 days. Single clones were obtained by serial dilutions, and C53 expression was examined by immunoblotting.

Production and Purification of C53 Antibodies—His-tagged human C53 fusion protein was purified using a nickel column (Novagen) and injected into three rats to generate polyclonal antibodies from rat. Rat polyclonal antibody (used for immunostaining assay) was affinity-purified using His-C53 conjugated affinity column. Two rabbit polyclonal antibodies were generated against two peptides (residues 242–256, KRGNSTVYEWRTGTE, and residues 491–506, SKRYSGRPVNLMGTSL). Sera were further purified using affinity column cross-linked with respective peptides (Pierce). In addition, rat anti-C53 monoclonal antibodies were generated using standard monoclonal antibody protocols.

Co-immunoprecipitation, Immunoblotting, Immunostaining—For co-immunoprecipitation assay, HeLa cells (5×10^7) were harvested and resuspended in the lysis buffer (10 mM HEPES, pH7.4, 150 mM NaCl, 5 mM $MgCl_2$, 1 mM dithiothreitol, 1 mM EDTA, 0.2% Nonidet P-40, 50 mM NaF supplemented with protease inhibitor cocktails). After clearance, respective antibody was incubated with cell lysate for 2 h at 4 °C followed by the addition of 10 μl of protein A/G beads (Pierce). After three washes of lysis buffer, the

bound proteins were eluted with 0.1 M glycine, pH 2.5. The samples were subjected to SDS-PAGE and immunoblotting.

Immunostaining of C53, Plk1, Chk1 and γ-tubulin— Cells were fixed in 100% methanol (-20°C) for 10 min, followed by three washes of phosphate buffered saline (PBS). After incubated with blocking buffer (10% goat serum, 2 % BSA in 1xPBS) for 1 hour at room temperature (RT), cells were stained with specific primary antibodies overnight at 4°C. After three washes (5 min each) in PBS, cells were incubated with specific secondary antibodies for 30 min at RT, and subsequently washed in PBS three times (5 minutes each). Cells were mounted in anti-fade reagent Fluosaver (Calbiochem) and analyzed by fluorescence microscopy. Confocal images were acquired using a Zeiss 510 META confocal microscope, while epifluorescence images were obtained using Leica DMR-HC upright microscope with Openlab software.

Caspase Activity Assay— Caspase activity was analyzed by Apo-one caspase assay kit (Promega) according to the manufacturer's instruction.

Cell Death and Cell Viability Assays—For trypan blue exclusion assay, cells were trypsinized, combined and harvested with floating cells, and subsequently incubated with 0.4% trypan blue solution (Sigma) for 5 min. Blue cells were scored as dead cells. Three independent assays were performed for each experiment, and at least 200 cells were scored. For annexin V assay, $1x10^{6}$ cells were partially trypsinized, harvested, and incubated with annexin V and propidium iodine (Oncogene) in the binding buffer according to the supplier's instruction. The samples were subjected to flow cytometry

analysis. Cell viability was measured by CellTiter-Blue assay (Promega) according to the supplier's instruction.

Cell Cycle Analysis—Cells were trypsinized, washed in phosphate-buffered saline and fixed with 100% ethanol at -20 °C. Cells were then washed in phosphate-buffered saline again and resuspended in phosphate-buffered saline containing RNase A (5 µg/ml) and propidium iodide (10 µg/ml). A total of 10,000 labeled nuclei were analyzed in a FACScan Flow Cytometer (BD Biosciences).

Subcellular Fractionation—Cell pellets collected from individual dishes were resuspended in lysis buffer (20 mM Tris-HCl, pH 7.2, 150 mM NaCl, 2 mM MgCl$_2$, 1 mM dithiothreitol, 0.5% Nonidet P-40, 50 mM NaF) supplemented with protease inhibitor cocktails. After 30 min of incubation on ice, lysates were centrifuged at 1000 x *g* for 10 min at 4 °C. The supernatants were cleared again at 13,000 x *g* for 15 min at 4 °C to harvest the cytosolic fraction. The pellets from the first centrifugation were washed twice with lysis buffer and centrifuged again at 1000 x *g* for 10 min at 4 °C. Pellets from this step contained the nuclear fractions.

Cell Transfection, Cell Synchronization and C53 Depletion by shRNA— HeLa cells were synchronized by double thymidine block. Briefly, HeLa cells were plated at 40% confluency and arrested with 2 mM thymidine. After 19-hr incubation, cells were washed 4 times with fresh medium and transfected with shRNA vectors (C53 and control) using Lipofectamine 2000 (Invitrogen). After incubation with DNA-lipid mixture for 3 hours, cells were washed twice and incubated in fresh medium for additional 6 hrs. Subsequently, cells were cultured in medium containing 2 mM thymidine and 2 mg/ml

puromycin for the second arrest and drug selection. After 19-hr arrest at the G1/S transition, cells were washed and cultured in fresh medium. Cells were collected or fixed at indicated times and subjected to specific analyses.

BrdU Labeling and Mitotic Index— BrdU labeling was used to evaluate DNA synthesis. After releases from the second thymidine arrest at indicated time points, cells grown in 12-well plates were pulse labeled with BrdU (50 mM) for 30 min. After three washes of PBS, cells were fixed with 1 ml of Carnoy's fixative (3 parts methanol: 1 part glacial acetic acid) at -20°C for 20 min, and rinsed three times in PBS. Subsequently, DNA was denatured by incubation of 2M HCl at 37°C for 60 min, followed by three washes in borate buffer (0.1 M borate buffer, pH 8.5). After incubated with the blocking buffer, cells were stained with anti-BrdU antibody (BD Biosciences, 1: 100) overnight at 4°C. After washes in PBS, cells were incubated with Texas Red-conjugated anti-mouse goat IgG for 30 min at RT. Cells were washed and mounted and BrdU positive cells were manually scored under immunofluorescence microscope.

Mitotic events were scored by time-lapse video microscopy. HeLa cells were transfected with control or C53 shRNA and synchronized as described above. At 4 hours after release from the second block, real-time images of cells were captured every half hour with Openlab software. Mitotic events of control and C53-depleted cells were scored by their morphological change. For each experiment, at least 800 cells of control or C53-depleted cells were videotaped, tracked and analyzed. Alternatively, nocodazole (100 ng/ml) was added into the medium after release, cells were collected, fixed and stained with DNA dye (Hoescht dye 33258). Mitotic cells were scored by their nuclear morphology (condensed and fragmented nuclei).

Time-Lapse Video Microscopy—Time-lapse video microscopy was achieved using Open lab automation. Cells were grown on 12 or 24 well plates and kept with adequate O2 and CO2 supply. A hot air blower and digital thermometer were used to ensure a 37C temperature. Pictures were taken every 5, 10 or 30 minutes in different experiments.

Cdk1 Kinase Assay—Cells were detached from dishes with a rubber policeman, harvested by centrifugation, and resuspended in lysis buffer (10 mM HEPES, pH 7.4, 150 mM NaCl, 5 mM $MgCl_2$, 1mM dithiothreitol, 1 mM EDTA, 0.2% Nonidet P-40, 50 mM NaF, supplemented with protease inhibitor cocktails). After 30 min of incubation on ice, lysates were clarified by centrifugation (10,000 x *g* for 20 min at 4 °C). For the histone H1 kinase assay, cell lysates (150 µg) were incubated for 2 h at 4 °C with anti-cyclin B1 polyclonal antibody (Santa Cruz). Protein A/G beads were then added to the lysates and incubated for 1 h. Immunoprecipitates were washed 3 times with lysis buffer, once with HBS (10 mM HEPES, pH 7.4, 150 mM NaCl). The beads were incubated with 5 µg of histone H1 in HBS (20 µl) containing 15 mM $MgCl_2$, 50 µM ATP, 1 mM dithiothreitol, and 1 µCi of $[\gamma\text{-}^{32}P]ATP$. After 10 and 30 min of incubation at 30°C, the reaction products were analyzed by SDS-PAGE and autoradiography.

Chk2 Kinase Assay— GST or GST-C53 were pre-incubated with purified His-Chk2 (50 ng) for 30 min at RT. Assays were performed in 50 µl of kinase reactions buffer containing 50 mM Tris-HCl, pH 7.5, 10 mM MgCl2, 1 mM DTT, 50 µM cold ATP, 5 µCi of γ-32P-ATP (Pekin Elmer) and 2 µg GST-Cdc25C (200-256) for 10 min at 25°C. Phosphorylation of GST-Cdc25C was detected by autoradiography. Chk2 auto-

phosphorylation was indicated by His-Chk2.

Plk1 Kinase Assay— GST-C53 and α-casein were incubated with Plk1 at 30°C for 15 min in 20 μl of kinase buffer (20 mM HEPES, pH 7.4, 50 mM KCl, 10 mM $MgCl_2$, 1 mM DTT, and 1 μM ATP) supplemented with 5 μCi of $[\gamma\text{-}^{32}P]$ATP. The reaction was stopped by addition of protein sample buffer and samples were subjected to SDS-PAGE and phospho-imager analysis.

Chapter III

Results and Discussions

Part I

3.1 C53 regulates the G2/M checkpoint via inhibiting Chk1 and Chk2

3.1.1 the G2/M DNA damage checkpoint and mitotic cell death

The G2/M DNA damage checkpoint functions by inhibiting Cdk1/cyclin B1 to arrest cell cycle at G2 (Figure 4A). While arrested at G2, cells actively attempt DNA damage repair. For normal proliferating cells, such mechanisms help prevent the formation of aberrant daughter cells. However, in the case of chemotherapies, tumor cells also utilize G2/M checkpoint to arrest cell cycle at G2 and attempt DNA repair. As a result, they are able to delay or possibly escape from cell death. This presents a great hurdle for the effectiveness of traditional chemotherapy. Therefore, chemicals that suppress the G2/M DNA damage checkpoint have been used in clinical trials as co-treatment for conventional chemotherapy and yielded encouraging results [41,42].

Human cervical cancer HeLa cells express the E6 protein of human papillomavirus and do not have a functional p53 signaling pathway. When treated with 20uM etoposide, a topoisomerase II inhibitor that induces double-strand DNA breaks (DSBs), HeLa cells do not undergo rapid p53-induced cell death. Instead, they stay arrested at G2 phase (Figure 4B, panel b). To demonstrate the effect of suppressing G2/M checkpoint in these cells, we used 30 mM caffeine to inhibit the upstream ATM and ATR kinases. As shown in Figure 4B panel c, caffeine treatment potently abolished the G2/M arrest induced by etoposide. Cells entered mitosis and underwent massive cell death.
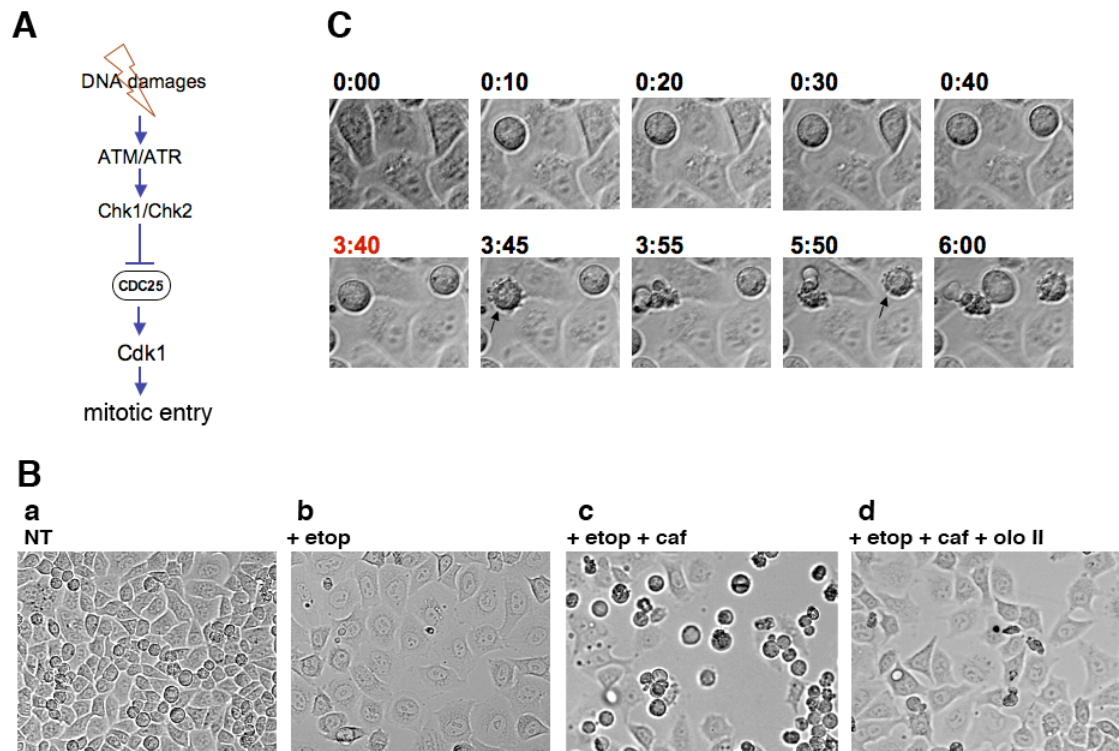
Figure 4 Suppression of G2/M DNA damage checkpoint sensitizes cancer cells to genotoxins

A. A brief illustration of the G2/M DNA damage checkpoint.

B. a, HeLa cells without treatment (NT); b, HeLa cells after 30 hours of etoposide (20 μM) treatment; c, HeLa cells were treated with 20 μM etoposide for 18 hours to establish G2 arrest. 30mM caffeine was then added to abolish G2/M checkpoint. Pictures were taken 12 hours later. d, treatment was similar to c, except 5 μM olomoucine II was added together with caffeine. *Etop*, etoposide. *caf*, caffeine. *olo II*, olomoucine II.

C. Time-lapse video analysis of cell death. HeLa cells were treated with 20 μM etoposide for 18 hours followed by 30 mM caffeine. Time-lapse videotaping starts approximately 2 hours after the addition of caffeine. Pictures were taken every 5 minutes. Representative picture clips were chosen to depict the death process. Arrows indicate sudden cell death after hours of mitotic arrest.

The kinase complex of Cdk1/cyclin B1 is the driving force of mitotic entry. We next used inhibitors of Cdk1 to test the requirement of mitotic entry for etoposide induced cell death. When a Cdk1 specific chemical inhibitor olomoucine II (5 μM) was added to the medium, caffeine and etoposide-treated cells were unable to enter mitosis. Instead, they still arrested at G2 and were largely alive (Figure 4B, panel d). This experiment demonstrates that Cdk1 activity and mitotic entry are prerequisite for etoposide-induced mitotic cell death.

Using time-lapse video microscopy, we documented the process of this kind of cell death. As shown in Figure 4C, when ATM inhibitor caffeine was added to the medium, it rapidly abolished etoposide-induced G2 arrest. Cells entered mitosis and assumed mitotic arrest for 3 to 5 hours, followed by sudden cell death. Together, these experiments demonstrated that, when etoposide-activated G2/M checkpoint is suppressed, HeLa cells no longer stay arrested at the G2 phase. Instead, they enter mitosis, and subsequently die during mitosis.

3.1.2 C53 depletion prolongs G2 arrest induced by etoposide and delays etoposide-induced cell death

C53 is a novel caspase substrate and is the main subject of our lab's research. To investigate its cellular functions, we used RNAi-based technologies to knock down the expression of C53 in HeLa cells and studied the phenotype. As shown in Figure 5A, C53 siRNA-1 potently inhibited the expression of C53-Flag fusion protein in HeLa cells. This siRNA sequence was subsequently used to construct a plasmid-based shRNA vector (pSIREN-RetroQ-C53). HeLa cells were transfected with this construct, and single clones of HeLa cells were isolated under puromycin (2 µg/ml) selection. These HeLa

clones have C53 shRNA plasmid stably inserted to their genome and express extremely

low levels of C53. Morphologically, these clones fall into two categories. About 80% of

single clones showed extensive multi-nucleation and enlarged cell body, and have a very

slow proliferation rate. This suggests C53 plays a role in normal cell proliferation, which

will be discussed later. The other 20% of single clones did not show apparent defects in

their proliferation and cellular morphologies. Three stable cell lines of this kind were

established (Figure 5B, cell line #2,4,6). In these three cell lines, expressions of major

cell death-related proteins such as caspases (casp-2, -3, -7, and -9), Bcl-2 family

members (Bcl-2, Bcl-xL, Bim, Bak, Bax), Apaf-1, inhibitor of apoptosis CIAP1 (cellular

inhibitor of apoptosis 1) and XIAP (X-chromosome-linked inhibitor of apoptosis) and iκBα

were not affected (Figure 5B). Various death-inducing stimuli were used to treat these

cells and their cell death responses were analyzed. C53-depleted cells showed partial

but significant resistance to cell death induced by etoposide (Figure 5C). In control and

parental HeLa cells, 20uM etoposide induced about 60% cell death 48 hours after

treatment, while in three C53-deficient cell lines, the cell death percentages were reduced

to less than 30%.   This suggests C53 deficiency confers a partial resistance to

etoposide.

Using annexin V staining and flow cytometry analysis, we demonstrated that

etoposide-induced cell death was an apoptotic response. C53 depletion significantly

inhibited both early (42.88% in control vs. 23.75% in stable cell line #4) and late (18.66%

in control vs. 12.92% in stable cell line #4) stages of apoptosis induced by etoposide

(Figure 5D).

To prove that the partial resistance to etoposide was not due to clonal variation,

we transiently transfected HeLa cells with C53 shRNA constructs and studied their
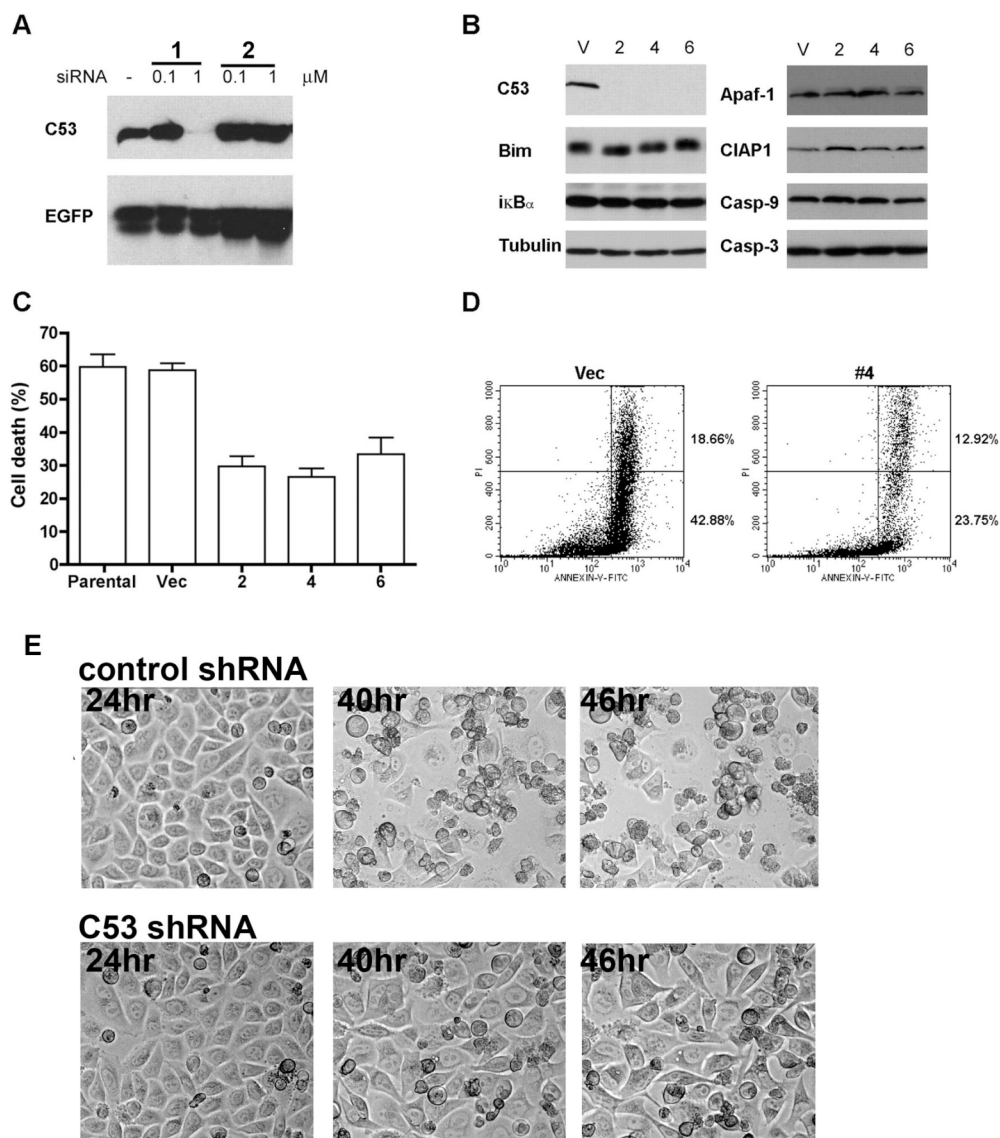
Figure 5 C53 deficiency confers partial resistance to etoposide

A. C53 siRNA inhibited overexpression of C53. Two C53 siRNAs were co-transfected along with C53-Flag construct into HeLa cells, and the expression of C53 was examined by immunoblotting with anti-Flag M2 antibody. SiRNA-1 was able to suppress the expression of C53-Flag, while SiRNA-2 was not.

B. Stable cell lines with loss of C53 expression. One control and three C53-deficient cell lines were established as described under "Materials and Methods." Expression of endogenous C53 and various proteins were examined by immunoblotting. *V*, vector control. 2,4,6, three C53-deficient stable cell lines.

C. Loss of C53 partially inhibited etoposide-induced cell death. Cells were treated with 20 μM etoposide for 48 h, and the percentage of cell death was scored using trypan blue exclusion assay. *Vec*, vector.

D. Loss of C53 partially inhibited both apoptotic and necrotic cell death induced by etoposide. Cells were treated with 20 μM etoposide for 48 h, and cell death was evaluated by annexin V staining and flow cytometry. *FITC*, fluorescein isothiocyanate.

E. Transient knockdown of C53 confers resistance to etoposide. HeLa cells were transfected with control or C53 shRNA for 48 hours, followed by treatment of 20 μM etoposide. 24 hours later, time-lapse video microcopy was used to analyze the death response. 40 hours after etoposide treatment, the majority of control shRNA transfected cells went into mitosis and subsequently died during mitosis. C53 depleted cells maintained G2 arrest and stayed alive.

response to etoposide-induced cell death. After 40 hours of etoposide treatment, the majority of control cells already entered mitosis and subsequently died during mitosis, while C53 shRNA transfected HeLa cells stayed arrested at G2 and were mostly alive (Figure 5E). This experiment strongly demonstrated that C53-depleted cells are more resistant to etoposide-induced cell death.

Using cell viability assay, we attempted to determine whether C53 deficiency confers resistance to other death stimuli. As shown in Figure 6, C53-deficient cell lines were resistant to etoposide, but not to other death stimuli such as cisplatin, camptothecin, doxorubicin, UV, stausporine and TNFα/cycloheximide. The difference between etoposide and these other death stimuli will be compared and discussed later.

We further analyzed the time-course of etoposide-induced HeLa cell death. In a control HeLa cell line, etoposide induced a prolonged G2/M arrest up to 36 hours, followed by a massive cell death response in later hours. As shown in figure 7A, only 25% of cells died during the first 36 hours of etoposide treatment, while about 40% died between 40 and 48 hours. In comparison, C53 depleted cells did not show such a dramatic increase in cell death (Figure 7A). Interestingly, in control cells, the G2/M checkpoint broke down before 40 hours (as evidenced by the decrease of p-Y15-Cdk1, Figure 7B, top panel). Such an event was accompanied by substantial caspase activation (Figure 7C). However, in C53 depleted cells, CDk1 inactivation was slightly stronger in early hours (24 and 32 hours) and was sustained up to 48 hours (Figure 7B), while there was little or no caspase activation (Figure 7C). The differences of caspase activities in control and C53-depleted cell lines were also confirmed using an *in vitro* caspase activity assay (Figure 7D).
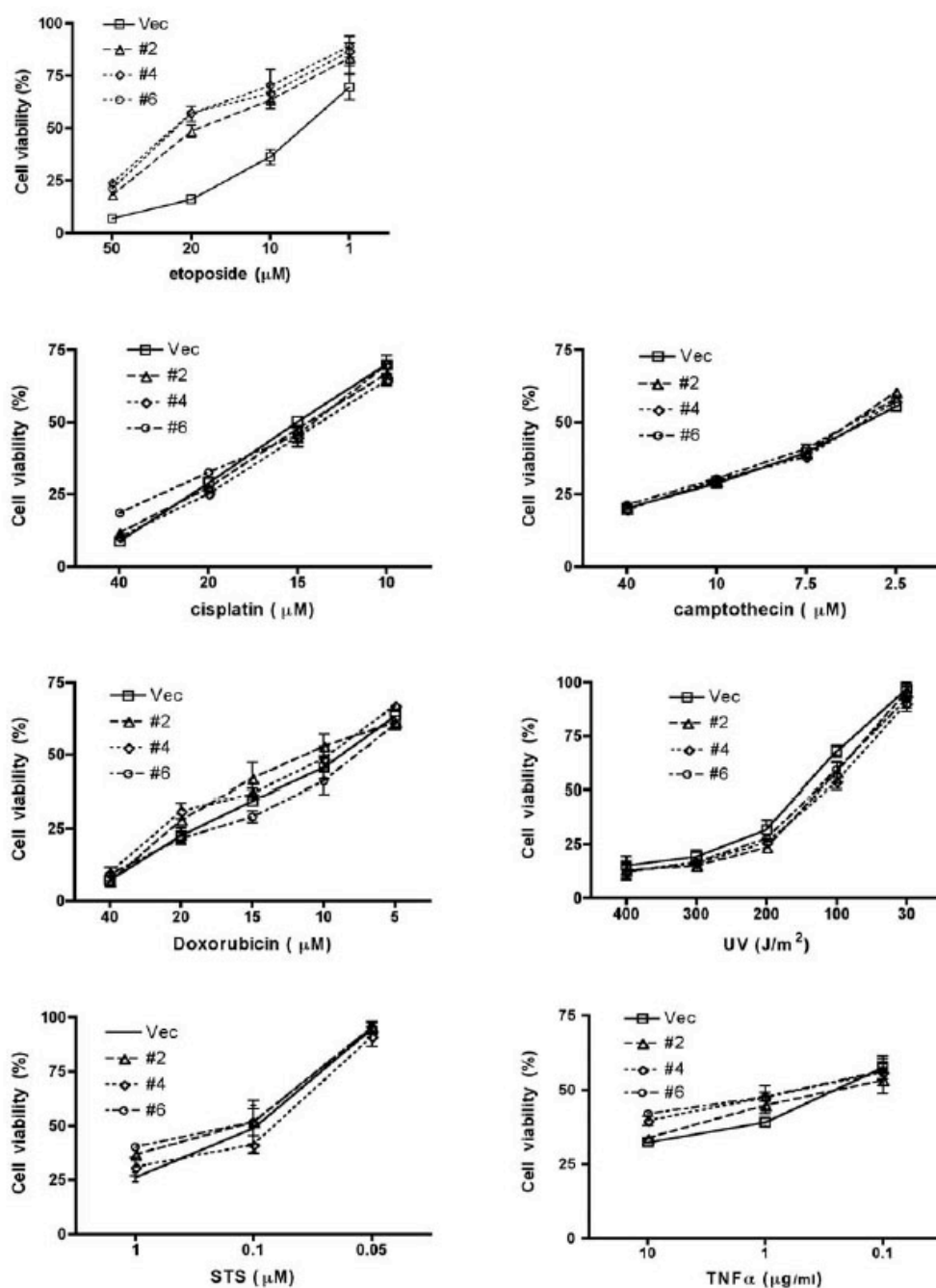
Figure 6 Loss of C53 specifically affects etoposide-induced apoptosis

Cells were treated with various agents as indicated for 24 hours, except for cells that were treated with etoposide for 48 hours. Cell viability was scored using CellTiter-Blue assay (Promega). Results were mean ± SD, with three independent repeats. *STS,* staurosporine.
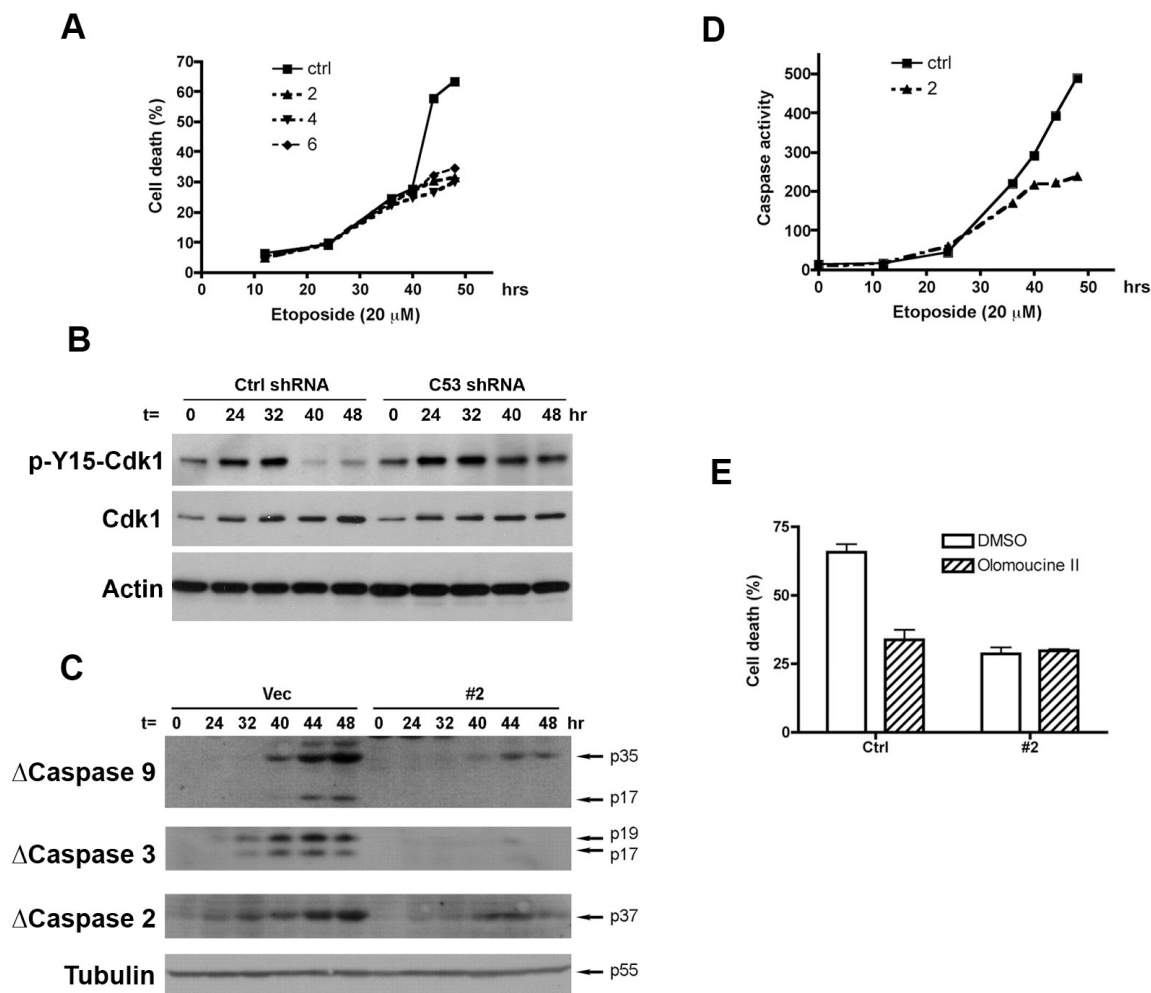
Figure 7 C53 depletion suppresses reactivation of Cdk1 and inhibits caspase activation

A. Time course of etoposide-induced cell death of HeLa cells. The control and C53-deficient cells were treated with etoposide (20 µM) for the indicated periods of time. The percentage of cell death was scored using trypan blue exclusion assay. *ctrl*, control.
B. C53 depletion suppresses reactivation of Cdk1 during DNA damage response. Control and C53 shRNA transfected HeLa cells were treated with 20 µM etoposide for indicated periods of time, and Cdk1 reactivation (panel p-Y15-Cdk1) were detected by immunoblotting.
C. Loss of C53 partially prevents caspase activation. Control and C53-deficient cells were treated with etoposide (20 µM) for the indicated periods of time, and caspase

activation was detected by immunoblotting and marked by the appearance of active forms. *Vec*, vector control.

D. Time course of caspase activation in etoposide-induced cell death. Caspase activity was analyzed by Apo-one caspase assay kit (Promega).

E. Cdk1 inhibitor olomoucine II partially inhibited etoposide-induced cell death of HeLa cells. The control and C53-deficient HeLa cells were treated with 20 µM etoposide for 48 hours in the presence of Me$_2$SO or olomoucine II (2 µM). Cell death was scored by trypan blue exclusion assay. Results were the mean ± S.D., with three independent repeats.

Importantly, the Cdk1 inhibitor olomoucine II was able to reduce etoposide-induce cell death in control cells, but not in the C53-deficient cell line (Figure 7E). This demonstrates the importance of Cdk1 activity and mitotic entry for etoposide-induced cell death. Furthermore, the lack of additive effects of Cdk1 inhibition and C53 depletion indicates in C53 deficient cells, Cdk1 activation was inhibited. Together with our finding that control cells were able to re-activate Cdk1 at later time points (Figure 7B), this experiment indicates that in control cells, endogenously expressed C53 contributes to etoposide killing through Cdk1 activation, while in a C53-deficient cell line, Cdk1 activation was delayed and consequently there was a reduced level of cell death.

In summary, we conclude that when C53 is depleted, breakdown of the G2/M checkpoint and activation of Cdk1 is significantly suppressed. As a consequence, cells stay arrested in G2 and are able to delay etoposide-induced cell death.

3.1.3 C53 overexpression abolishes the G2/M checkpoint and sensitizes cancer cells to multiple genotoxic stress

Since C53 depletion partially inhibited etoposide-induced cell death, we next investigated whether C53 overexpression could sensitize cells to such genotoxic stress. As shown in real-time images (Figure 8A), C53-transfected cells (indicated by fluorescence of EGFP, brighter cells in panel a and b) underwent rapid cell death (as early as 6 hours after etoposide treatment, indicated by cell shrinkage and membrane blebbing). In contrast, untransfected cells were arrested at G2 stage, as evidenced by enlarged cell and nuclear body.

At 24 hours post-treatment, etoposide induced only 20% cell death, whereas in the presence of C53 overexpression, more than 60% of HeLa cells underwent cell death

(Figure 8B). C53-promoted cell death was apoptotic, as indicated by more poly (ADP-ribose) polymerase cleavage and caspase-3 activation (Figure 8C). Moreover, overexpressed C53 also sensitized IMR90E1A cells to etoposide-induced cell death (Figure 8B). These results strongly suggest that overexpression of C53 sensitizes tumor cells to etoposide-induced cell death.

We next investigated whether C53 can sensitize cells to other death stimuli. As shown in Figure 9A, killing by etoposide, camptothecin and doxorubicin, three drugs that induce DSBs and G2 arrest in normal HeLa cells (Figure 9B), was substantially increased by C53 overexpression. In contrast, killing by Cisplatin, TNFα/cycloheximide and UV, which do not induce G2 arrest in HeLa cells, were not affected by C53 overexpression (Figure 9A and B). This result suggested that C53 potentiates killing by drugs that normally induces G2 arrest in HeLa cells. Interestingly, X-ray also induces DSBs and causes G2 arrest in HeLa cells. Consistent with our conclusion, C53 overexpression promoted X-ray induced cell death, and C53 depletion reduced such killing (Figure 9C and D).

To further investigate the mechanism by which C53 promotes etoposide-induced cell death, we analyzed cell cycle distribution of control or C53-transfected HeLa cells after etoposide treatment. While control HeLa cells showed G2/M arrest (Figure 10A, indicated by arrow) upon etoposide treatment, C53-overexpressing HeLa cells escaped from such arrest (Figure 10A), suggesting C53 overexpression suppressed the G2/M DNA damage checkpoint.

A.

a. EGFP+C53   b. t= 0   c. t= 12 hrs   d. t= 24 hrs

B.

Cell death (%)

Ctrl
C53

HeLa   IMR90E1A

C.

Ctrl   C53

PARP cleavage — p116, p89

Casp-3 activation — p19, p17

tubulin
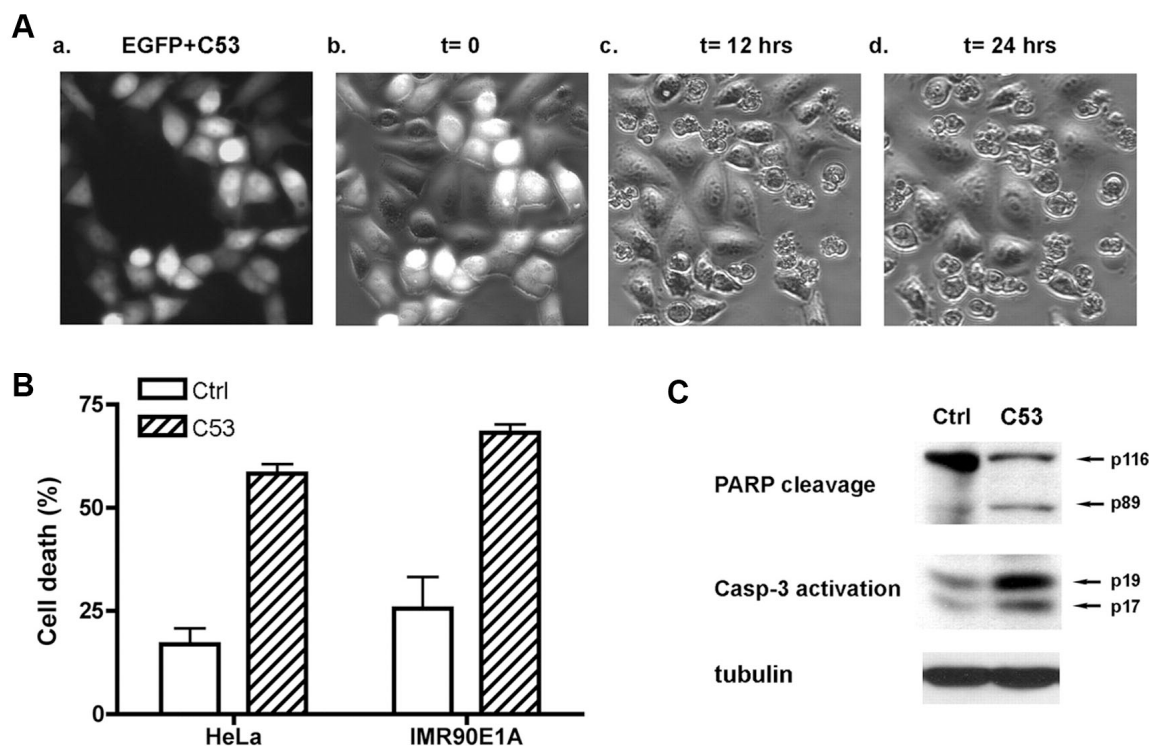
Figure 8 C53 overexpression sensitizes cells to etoposide

A. Real-time images of C53 overexpressing cells after etoposide treatment. HeLa cells were transfected with C53 construct (1.5 µg) along with EGFP (0.2 µg). After a 24-h incubation, cells were treated with etoposide (20 µM). The real-time images were captured by Leica microscope with Openlab software. *Panel a* is the green fluorescence only, whereas *panel b* is the combination of phase contrast and fluorescence images. *Panel c* and *d* are phase contrast only.

B. Ectopic expression of C53 sensitized both HeLa and IMR90E1A cells to etoposide. After transient transfection of C53 for 24 h, HeLa and IMR90E1A cells were treated with 20 and 2 µM etoposide, respectively, for 24 h. The percentage of cell death was scored by DNA staining of GFP-positive cells. Data were the mean ± S.D., with three independent repeats. *Ctrl*, control.

C. More caspase activation in the presence of C53 overexpression after etoposide treatment. Total HeLa cell extracts were subjected to immunoblotting with indicated antibodies. *PARP*, poly(ADP-ribose) polymerase.
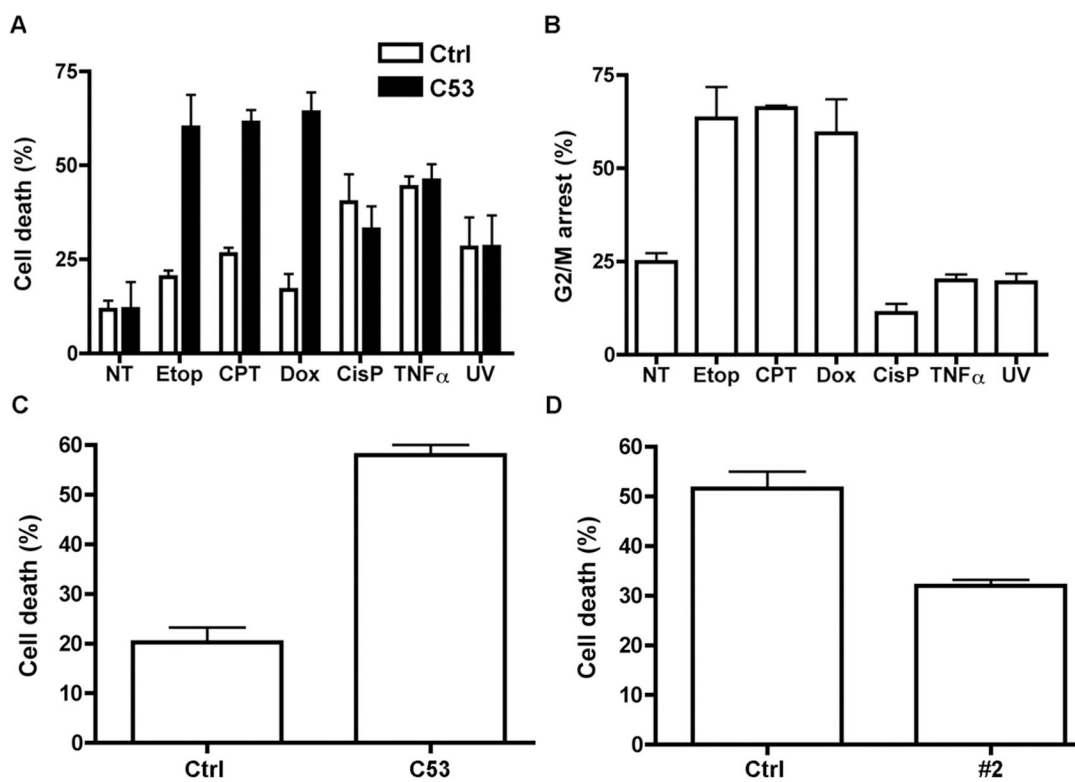
Figure 9 C53 overexpression sensitizes HeLa cells to multiple genotoxic stresses that induces G2 arrest

A. Ectopic expression of C53 renders HeLa cells susceptible to multiple genotoxic agents. HeLa cells were transfected with C53 construct (1.5 µg) along with EGFP (0.2 µg). After 24 h of incubation, cells were treated for 24 h with the following agents: etoposide (ETOP; 20 µM), camptothecin (CPT; 2 µM), doxorubicin (Dox; 5 µM), cisplatin (CisP; 10 µM), TNFα (0.5 ng/ml) plus cycloheximide (1 µg/ml), and UV (60 J/m^2). NT, no treatment. Cell death was scored by trypan blue exclusion assay. Results were the mean ± S.D., with three independent repeats. *Ctrl*, control.
B. G2/M arrest after drug treatment. The percentage of G2/M arrest was evaluated by flow cytometry. Data were mean ± S.D., with two independent repeats.
C. Overexpression of C53-sensitized HeLa cells to x-ray irradiation. *Ctrl*, control.
D. C53 deficiency partially inhibited x-ray irradiation-induced cell death. X-ray irradiation (2.5 Gy/min) was administered by Faxitron RX-650 (130 kilovolt peak and 5 mA) for 30 min (C) or 60 min (D). Cell death was scored by or DNA staining of GFP-positive cells (C) or trypan blue assay (D). C53 was overexpressed for 24 h in (C). Data were mean ± S.D., with three independent repeats. *Ctrl*, control.

At the molecular level, etoposide-treated control cells showed substantial accumulation of inhibitory phosphorylation of Cdk1, a hallmark for G2/M DNA damage checkpoint activation (Figure 10B, panel p-Cdk1). C53 overexpression blocked such accumulation of inhibitory phosphorylation of Cdk1 (Figure 10B). Moreover, in etoposide-treated, C53 overexpressing cells, Cdk1/cyclin B1 was more active compared with control (Figure 10C). Taken together, these results suggest C53 overexpression suppresses the G2/M DNA damage checkpoint and promotes Cdk1 activation, thereby sensitizing cells to multiple genotoxic stress. Importantly, co-expression of a dominant negative form of Cdk1 suppressed C53's ability to sensitize HeLa cells to etoposide (Figure 10D), again demonstrating that C53 contributes to etoposide-induced cell death through elevated Cdk1 activity.

3.1.4 C53 promotes nuclear accumulation of Cdk1/cyclin B1 during DNA damage response

As mentioned before, the function of Cdk1/cyclin B1 is also regulated by its subcellular localization. Active Cdk1/cyclin B1 needs to translocate to the nucleus, where most of its substrates reside, to exert its mitotic functions [99,100]. It has been reported that Polo-like kinase 1 (Plk1) mediated phosphorylation of cyclin B1 facilitates such nuclear accumulation of Cdk1/cyclin B1 [48]. Phosphorylation of four serine residues (Ser-126, -128, -133, and -147) at the N-terminal region of human cyclin B1 disrupts the cytoplasmic retention sequence and nuclear export sequence. As a result, nuclear export is inhibited while nuclear import is increased, resulting in a net accumulation of Xdk1/cyclin B1 in the nucleus [38,101-103]. Plk1, the kinase that carries out one of these phosphorylations (Ser-133) [38], is also a target of the G2/M checkpoint
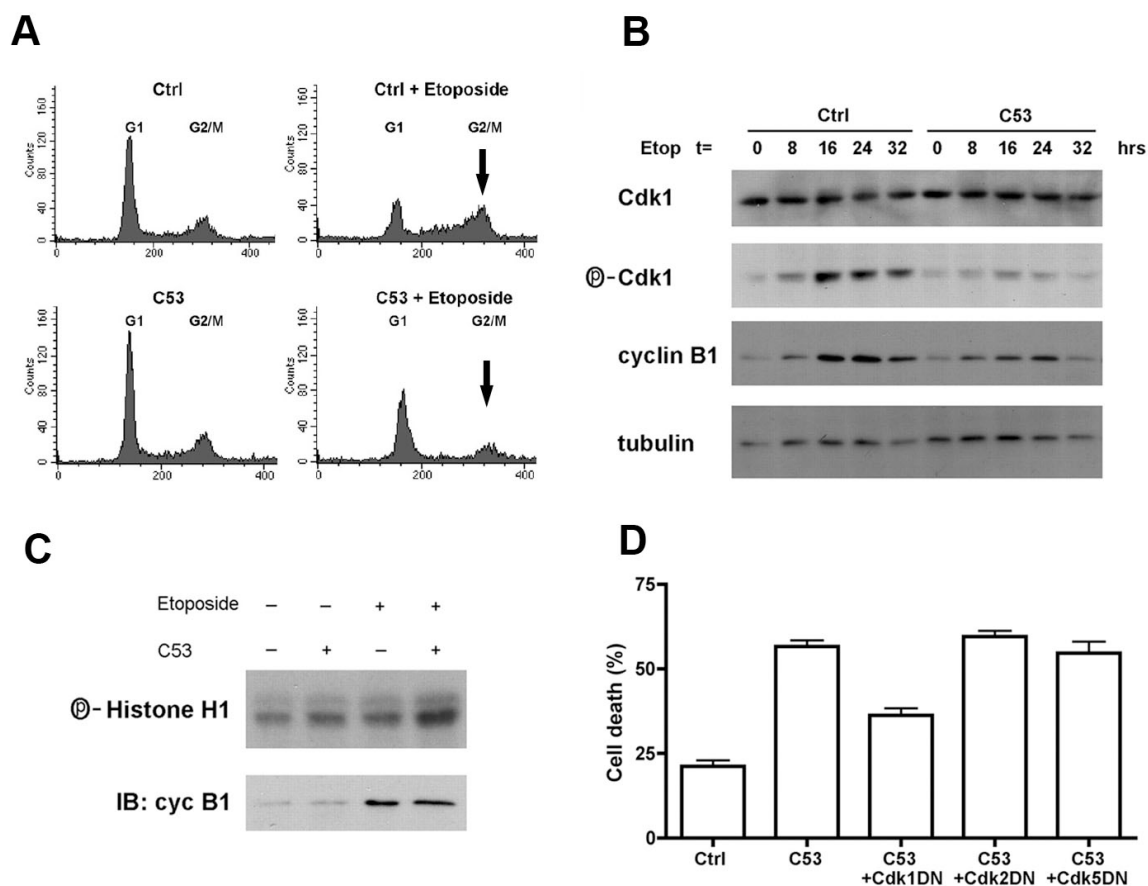
Figure 10 C53 overexpression sensitizes cells to multiple genotoxic stress

A. C53 overexpression suppressed etoposide-induce G2/M arrest. HeLa cells were transfected with control or C53 expressing vectors for 24 hours and treated with 20 µM etoposide and 20 µM zVAD-fmk for 24 hours. DNA content profile was analyzed by flow cytometry.   Arrows indicate G2/M arrest. *Ctrl*, control.

B. C53 overexpression reduced the inhibitory phosphorylation of Cdk1 and cyclin B1 protein levels. HeLa cells were transfected with C53 or control plasmid followed by etoposide (20 µM) treatment for various periods of time as indicated. Total cell lysates were subjected to immunoblotting using indicated antibodies. *Etop*, etoposide.

C. C53 overexpression promoted the Cdk1 kinase activity after etoposide treatment. HeLa cells were transiently transfected with either control plasmid or C53 followed by 18 hours of etoposide treatment. Cdk1 kinase assay was performed as described under "Materials and Methods." *IB*, immunoblot. *Ctrl*, control.

D. Cdk1 dominant negative mutant inhibited C53-mediated chemosensitization of HeLa cells. HeLa cells were co-transfected with C53 construct and various Cdk DN mutants as indicated. After 24-h of etoposide treatment, cell death was scored by DNA staining of GFP-positive cells. Results were the mean ± S.D., with three independent repeats. *Ctrl*, control.

[104,105]. Due to the function of checkpoints, Plk1 is inactivated during DNA damage response [105,106]. As a result, it is expected that cyclin B1 cannot translocate to nucleus, which represents a further inhibition of the Cdk1/cyclin B1 kinase complex by the G2/M checkpoint. Since we found C53 suppresses G2/M DNA damage checkpoints, we next tested whether C53 facilitates the nuclear accumulation of Cdk1/Cyclin B1. As shown in Figure 11A, control-transfected cells retained most of its Cdk1/cyclin B1 in the cytoplasm 24 hours after etoposide treatment, while C53 overexpressing cells showed substantial Cdk1/cyclin B1 nuclear accumulation under the same condition. This indicates C53 overexpression promotes the nuclear accumulation of Cdk1/cyclin B1. We next examined whether C53 depletion inhibits such translocation of Cdk1/cyclin B1. As shown in Figure 11B, after 40 hours of etoposide treatment, cyclin B1 and Cdk1 disappeared from cytoplasm in control cells which have endogenous level of C53. In contrast, in C53 deficient cells, cyclin B1 and Cdk1 was retained in the cytoplasm up to 48 hours after etoposide treatment. Since phosphorylation of cyclin B1 was responsible for nuclear accumulation of Cdk1/cyclin B1, we then examined whether C53 affects cyclin B1 phosphorylation. Shown in Figure 11C, C53 overexpression promoted cyclin B1 phosphorylation, as indicated by more slow-migrating phosphorylated cyclin B1. Taken together, these experiments showed that C53 facilitates cyclin B1 phosphorylation, as well as nuclear accumulation of Cdk1/cyclin B1. This again demonstrates that C53 suppresses the G2/M checkpoint during DNA damage response.
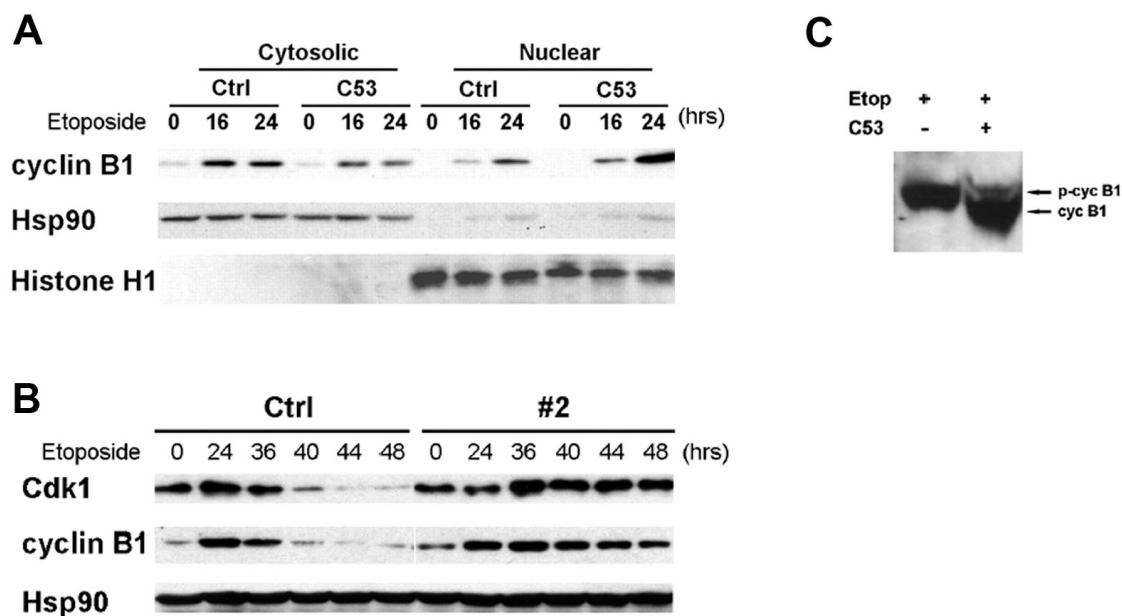
Figure 11 C53 overexpression promotes nuclear accumulation of Cdk1/Cyclin B1 in etoposide-treated cells

A. C53 promoted nuclear accumulation of cyclin B1 after etoposide treatment. Cells were transfected with control or C53 vectors for 24 hours before treatment with etoposide (20 µM), zVAD-fmk (20 µM) and MG132 (10 µM) for indicated periods of time. Cytoplasmic and nuclear fractions were subjected to immunoblotting of indicated antibodies. The proteasome inhibitor MG132 was used to prevent cyclin B1 degradation.*Ctrl*, control.

B. More cytoplasmic retention of Cyclin B1 in C53 deficient cells. Both the control and C53 deficient cells (#2) were treated with etoposide (20 µM), zVAD-fmk (20 µM) and MG132 (10 µM) for the indicated periods of time. Cytoplasmic fractions were subjected to SDS-PAGE and immunoblotting. In control and C53-deficient cells, the total (cytoplasmic and nuclear) level of Cdk1 and cyclin B1 was comparable (data not shown). *Ctrl*, control.

C. C53 overexpression promoted cyclin B1 phosphorylation. Control and transfected cells were treated with etoposide (20 µM), zVAD-fmk (20 µM) and MG132 (10 µM) for 24 hours. Cell lysates were immunoblotted with anti-cyclin B1 antibody. *Etop*, etoposide.

3.1.5 Overexpression of C53 suppresses the G2/M checkpoint and causes uneven chromatin condensation during unperturbed cell cycle

The molecular signaling network of the G2/M DNA damage checkpoint also functions during normal cell cycle. This ensures that cells with unreplicated chromosomes do not enter mitosis prematurely, thereby preventing the generation of genetically aberrant daughter cells. Since our data showed C53 suppresses the G2/M DNA damage checkpoint during DNA damage response, we next asked whether C53 overexpression suppresses the G2/M checkpoint and interferes with cell cycle progression under normal conditions. Interestingly, when C53 was overexpressed in HeLa cells, more than 60% of cells showed increased chromatin condensation around nucleoli (Figure 12A and B). Such a phenomenon is called uneven chromatin condensation (UCC), which is defined by the formation of hypercondensed chromatin aggregates at nucleloar sites [107]. Previous studies suggested UCC is probably accompanied by premature mitosis. Recently, Blank *et al* showed that UCC occurs at high rates when tumor cells with defective G2/M checkpoint are treated with genotoxic stress [107]. It was also concluded that UCC is caused by unscheduled Cdk1 activation. Based on their conclusion, our finding that C53 overexpression induces UCC in untreated HeLa cells suggests C53 inhibits the G2/M checkpoint and causes premature Cdk1 activation. Indeed, C53 overexpression promotes histone H3 phosphorylation (Figure 12C), indicating Cdk1 was prematurely activated in C53 overexpressed cells. Furthermore, olomoucine II, a chemical inhibitor of Cdk1 substantially suppressed C53 overexpression induced UCC (Figure 12B, p<0.01), demonstrating that C53-induced UCC is indeed the consequence of unscheduled Cdk1 activation. In summary, our
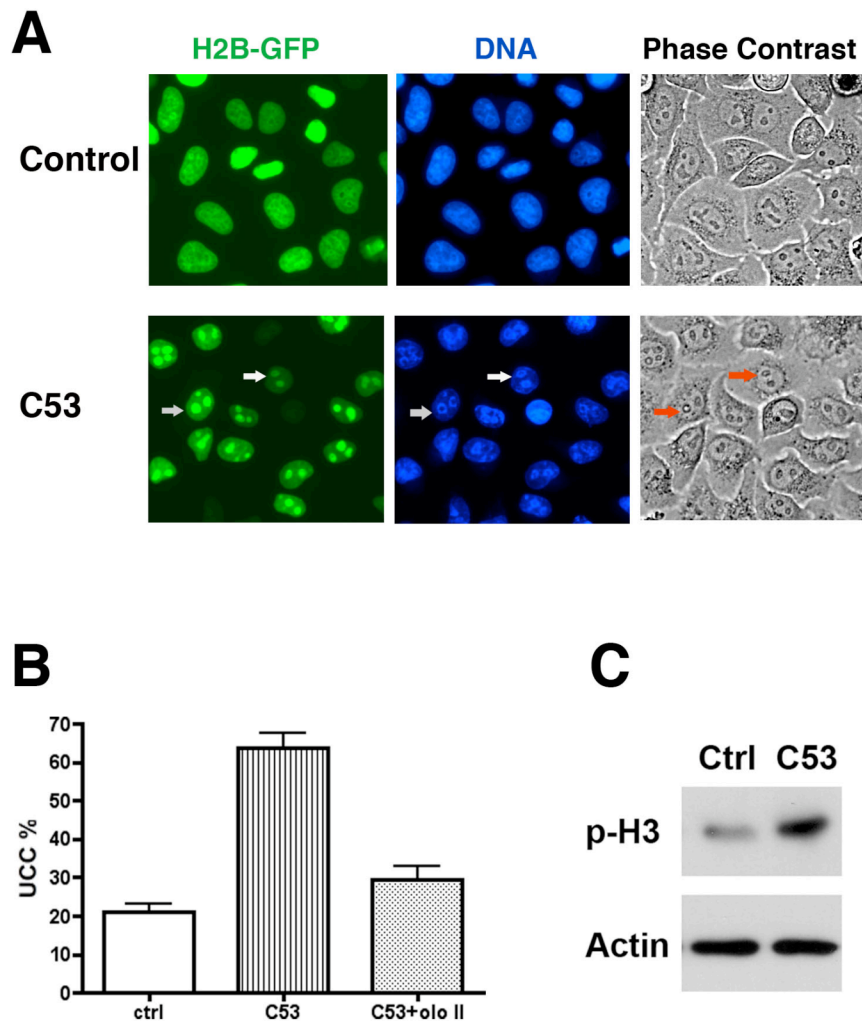
Figure 12 C53 overexpression causes premature Cdk1 activation and uneven chromatin condensation during unperturbed cell cycle

A. C53-expressing HeLa cells displayed uneven chromatin condensation. 1.5×10^5 HeLa cells were transfected with 0.6 µg of control or C53 plasmids together with 1.2 µg of H2B-GFP. 24 hours later, pictures of cells were taken using Openlab software. Arrows indicate the co-localization of H2B-GFP signals, chromatin and nucleoli. *Ctrl*, control.
B. Quantitative results of cells displaying UCC. HeLa cells were transfected as described in (A). For olomoucine II treatment, 5 µM olomoucine II was added to medium 4 hours after transfection. Results were mean ± S.D., with three independent repeats. *Ctrl*, control.
C. Phosphorylation of Histone H3 at Ser10 was elevated in C53-overexpressing cells. Cells were transfected as described in (A), and cell lysates were subjected to immunoblotting using the indicated antibodies. *Ctrl*, control.

results suggest that C53 suppresses the function of G2/M checkpoint during unperturbed cell cycle, which leads to unscheduled Cdk1 activation and causes UCC.

3.1.6 C53 depletion causes delays in Cdk1 activation and mitotic entry

We next examined whether C53 depletion affects Cdk1 activation and mitotic entry under normal conditions. Using the protocol depicted in Figure 13A, we synchronized control and C53-depleted cells at the G1/S transition using a double thymidine block. Because the time line of double thymidine block relies on normal cell cycle progression, there is a possibility that if C53 is depleted too early, alteration of cell cycle may potentially interfere with the effectiveness of double thymidine block. In an attempt to avoid this, transfection of control and C53 shRNA were performed during the first release. By the time of release from thymidine block, endogenous C53 was knocked down by about 50% (data not shown).

After being released into fresh medium, cells undergo G1/S transition and S phase DNA synthesis before the G2/M transition. We used BrdU incorporation assay to monitor the G1/S transition and S phase progression. As shown in Figure 13B, incorporation of BrdU did not differ significantly between control and C53-depleted cells, suggesting that the G1/S transition and S phase progression were not affected by C53 depletion. Upon examining the mitotic entry, we found C53 depleted cells were slower in entering mitosis (Figure 13C). For example, at 14 hours after release from Thymidine block, only 36.5±0.7% of C53 depleted cells entered mitosis, while 53.6%± 2.7% of control cells were mitotic. A Similar observation was also obtained in T47D breast cancer cells (Figure 13C). At the molecular level, C53 depletion prevented Cdk1
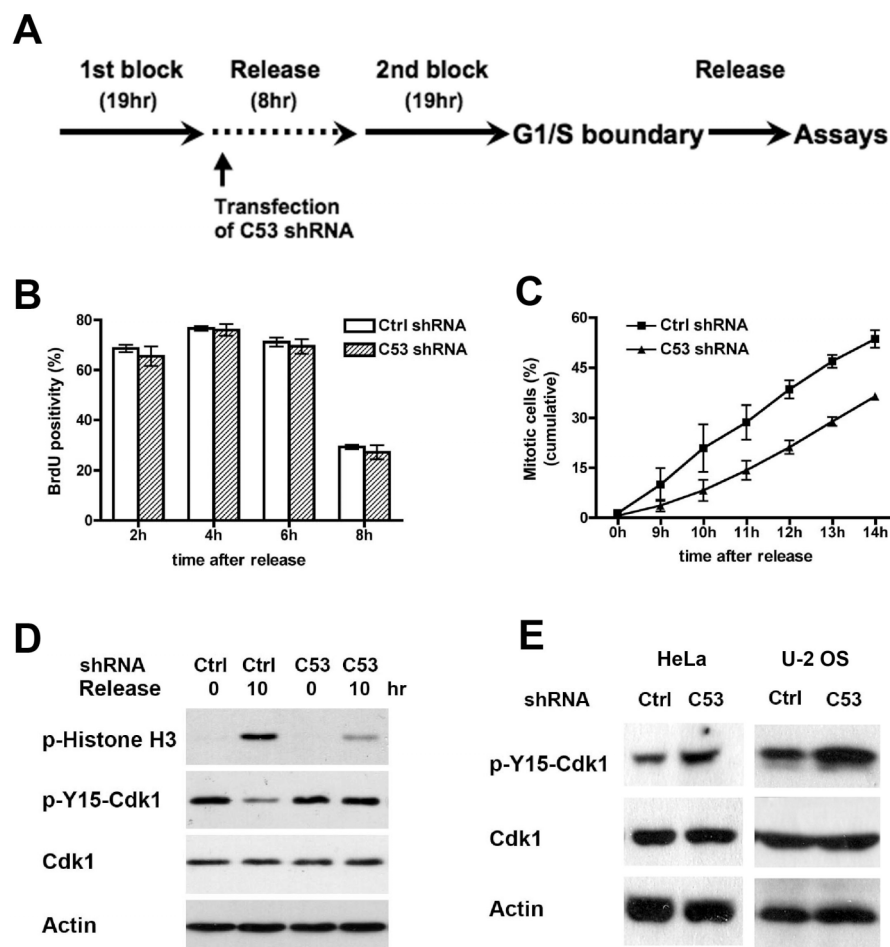
Figure 13 C53 depletion causes delays in Cdk1 activation and mitotic entry

A. Protocols of C53 depletion and synchronization.
B. C53 depletion did not affect DNA synthesis. Synchronized cells were pulse labeled with BrdU (50 mM) for 30 min at indicated time points after release from the second thymidine block. BrdU positive cells were detected by immunostaining and scored manually. More than 500 cells were counted in each of three independent experiments. Data are represented as mean ± SEM. Done in collaboration with Dr. Jianchun Wu. *Ctrl*, control.
C. C53 depletion delayed mitotic entry. Cell cycle progression of more than 1,000 cells were recorded by time-lapse videomicroscopy. The number of mitotic cells was scored by examination of individual cells. Similar results were obtained using DNA staining. Data are represented as mean ± SEM. Done in collaboration with Dr. Jianchun Wu. *Ctrl*, control.
D. C53 depletion delayed Cdk1 activation. Cell lysates were collected at indicated times after release from the second block, and subjected to immunoblotting using indicated antibodies. *Ctrl*, control.
E. C53 depletion caused increased inhibition of Cdk1 in unsynchronized cells.

activation (indicated by the sustained inhibitory phosphorylation of Cdk1, p-Y15-Cdk1 panel in Figure 13D). In addition, phosphorylation of histone H3, a marker for mitosis, was also inhibited by C53 depletion (panel p-histone H3, Figure 13D). Moreover, in unsynchronized HeLa and U-2 OS cells, elevated levels of Cdk1 inhibition were also observed in C53 depleted cells (Figure 13E). Together, these data strongly indicate that C53 depletion causes delays in Cdk1 activation and mitotic entry.

3.1.7 C53 suppresses activation of Chk1 and Chk2 in G2/M DNA damage checkpoint.

In the aforementioned experiments, using both overexpression and RNAi-mediated knock-down, we demonstrated that C53 affects the G2/M DNA checkpoint and Cdk1 activation during both normal cell cycle progression and DNA damage response. These data strongly suggest a regulatory role for C53 in G2/M checkpoint. We next asked what kinase(s) or phosphatases(s) of the G2/M checkpoint signaling pathway is the potential target of C53.

The G2/M DNA damage checkpoint can be briefly described as the ATM/ATR→ Chk1/Chk2→ Cdc25 B→ Cdk1 signaling pathway (Figure14A, left panel). To investigate how C53 functions in G2/M DNA damage checkpoint, we examined the activation state of these molecules in genotoxin-treated, control or C53-overexpressing cells. As shown in Figure 14A, the activities of ATM/ATR did not seem to be affected by C53 overexpression, as the ATM/ATR-mediated phosphorylation of H2AX did not differ in control and C53-overexpressing cells (panel p-H2AX). However, phosphorylation of Chk1 at Ser345 and Chk2 at Thr68, two phosphorylations important for their activation,

A

DNA damage

↓

ATM/ATR (p-H2AX)

↓

Chk1/Chk2 ├── C53

⊥

Cdc25C

↓

Cdk1

	Mock		Etop		Dox		HU		
C53	−	+	−	+	−	+	−	+	

p-S139-H2AX

p-S345-Chk1

Chk1

p-T68-Chk2

Chk2

p-S216-Cdc25C

Cdc25C

p-Y15-Cdk1

Cdk1

Actin

B

		Ctrl shRNA					C53 shRNA				
t=	0	24	32	40	48	0	24	32	40	48 hr

p-Y15-Cdk1

Cdk1

p-S345-Chk1

Chk1

p-T68-Chk2

Chk2

Actin
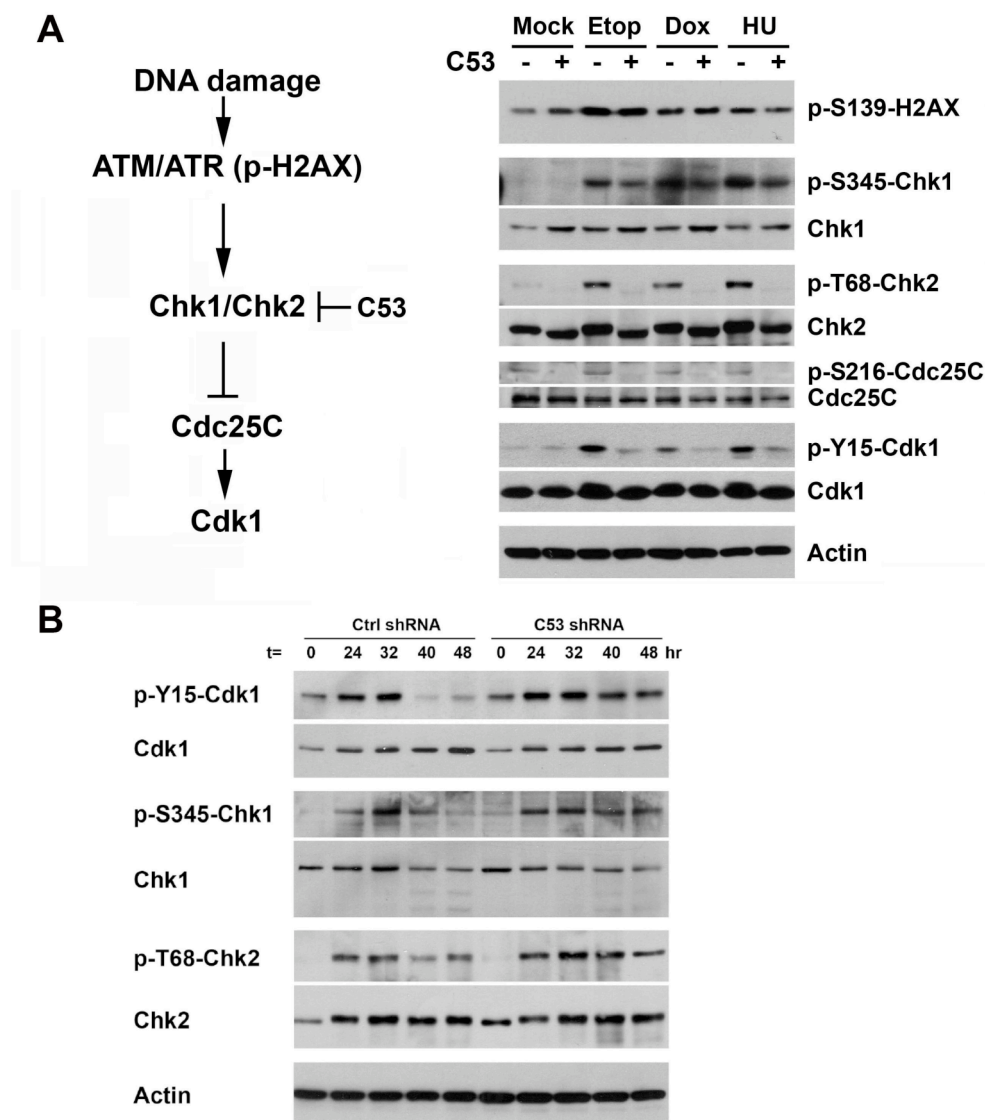
Figure 14 C53 suppresses activation of Chk1 and Chk2 in G2/M DNA damage checkpoint

A. C53 overexpression inhibited the checkpoint response. HeLa cells were transfected with the C53 or control vectors. At 24 hours after treatment, the cells were treated with etoposide (Etop, 20 μM, 18 hours), doxorubicin (Dox, 1 μM, 5 hours), hydroxyurea (HU, 4 mM, 18 hours). Cell lysates were subjected to SDS-PAGE and immunoblotting using indicated antibodies. Done in collaboration with Dr. Jianchun Wu.

B. C53 depletion affects the kinetics of activation/inactivation of checkpoint kinases in DNA damage response. HeLa cells were transfected with control shRNA and C53 shRNA construct, and then treated with puromycin (2 μg/ml) for selection. After three-day selection, cells were treated with etoposide (20 μM) for indicated time points. Cell lysates were subjected to immunoblotting using indicated antibodies.

were partially reduced by C53-overexpression (panel p-S345-Chk1 and p-T68-Chk2), suggesting C53 modulates G2/M DNA damage checkpoint at the Chk1/Chk2 level. Further down the signaling pathway, phosphorylation of Cdc25B and Cdk1 was also reduced (panel p-Cdc25B and p-Y15-Cdk1), which is expected since Chk1 and Chk2 were not active in C53-overexpressing cells. Interestingly, the protein level of Chk1 was consistently higher in C53-overexpressing cells (panel Chk1). Such a phenomenon may be explained by C53's suppression of Chk1 Ser345 phosphorylation. Phosphorylation of Chk1 leads to its degradation by the ubiquitin proteasome system [14]. Therefore, the elevated Chk1 level is probably due to reduction of Chk1 phosphorylation conferred by overexpressed C53.

We also examined the activation status of Chk1 and Chk2 in C53 depleted cells. In etoposide-treated control cells, phosphorylation of both Chk1 and Chk2 diminished before 40 hours (Figure 14B). In contrast, when C53 was depleted by shRNA, phosphorylation of Chk1 and Chk2 was largely sustained up to 48 hours (Figure 14B). This experiment indicates that endogenously expressed C53 is necessary for the decrease of Chk1/Chk2 activity at later hours of DNA damage response. In addition, such phosphorylation of Chk1 and Chk2 was slightly stronger in C53 depleted cells during earlier hours (panel p-S345-Chk1 and p-T68-Chk2, 24 and 32 hours, compare with control). Taken together, these experiments showed C53 depletion enhances and sustains Chk1 and Chk2 activation in genotoxin-treated cells.

3.1.8 C53 interacts with Chk1 and Chk2 and inhibits their kinase activity

To investigate the mechanism by which C53 overexpression suppresses Chk1/Chk2 function, we performed co-immunoprecipitation experiment to see whether
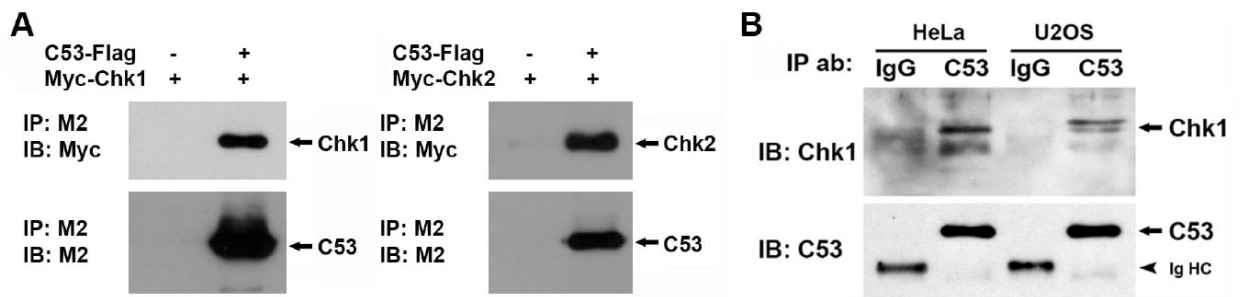
Figure 15 C53 interacts with Chk1 and Chk2

A. Co-immunoprecipitation of C53 with Chk1/Chk2. 1×10^{6} HeLa cells were transfected with 2 μg of C53-Flag and 2μg of Myc-Chk1 (or Myc-Chk2) for 24 hours. Cell lysates were collected and subjected to immunoprecipitation. C53-Flag was immunoprecipitated down with M2 antibody, and Chk1/Chk2 was detected with anti-Myc antibody.
B. C53 interacts with endogenous Chk1. Endogenous C53 was pulled down with anti-C53 antibody, and Chk1 was detected by immunoblotting using Chk1 antibody. IgG HC was IgG heavy chain. Done by Dr. Jianchun Wu.

C53 and Chk1/Chk2 interact with each other. As shown in Figure 15A, overexpressed

Myc-Chk1 and Myc-Chk2 were present in the immunoprecipitates of C53-Flag fusion

protein, suggesting overexpressed Chk1 and Chk2 interact with C53.   Using antibodies

against C53, we further demonstrated endogenous Chk1 co-immunoprecipitated with

endogenous C53 in HeLa and U-2 OS cells (Figure 15B). A doublet of Chk1 was

observed, suggesting C53 may interact with different forms of phosphorylated Chk1.

However, under similar conditions, we were not able to co-immunoprecipitate

endogenous Chk2 with C53 (data not shown). This may be due to possible disruption of

C53-Chk2 interaction by C53 antibody. Alternatively, Chk2-C53 interaction may be

dependent on other modifications, such as Chk2 phosphorylation.

We next used affinity purified anti-C53 antibody to study the subcellular

localization of C53. As shown in Figure 16A, anti-C53 antibody recognizes only one

band corresponding to C53 on Western Blot. When we used GST-C53 beads to deplete

the antibody, or C53 ShRNA to deplete endogenous C53 protein, the immunostaining

signal was significantly reduced (Figure 16B). These experiments demonstrated the

specificity of our anti-C53 antibody.

The endogenous C53 protein is mostly cytoplasmic, with a strong staining of

perinuclear region (Figure 16B). Interestingly, a portion of C53 localizes to the

centrosome (Figure 16B, enlarged insert), as indicated by its co-localization with the

centrosomal marker γ-tubulin at the centrosomes. Kramer *et al* reported that Chk1 is

recruited to centrosome during interphase [108]. We next asked whether C53 and Chk1

co-localize with each other on centrosomes. As shown in Figure 16C, both C53 and

Chk1 displayed a "U"-shaped distribution around the centriole (Figure 16C, high-

magnification pictures in the inserts). Such a pattern was described by Ou *et al* as the
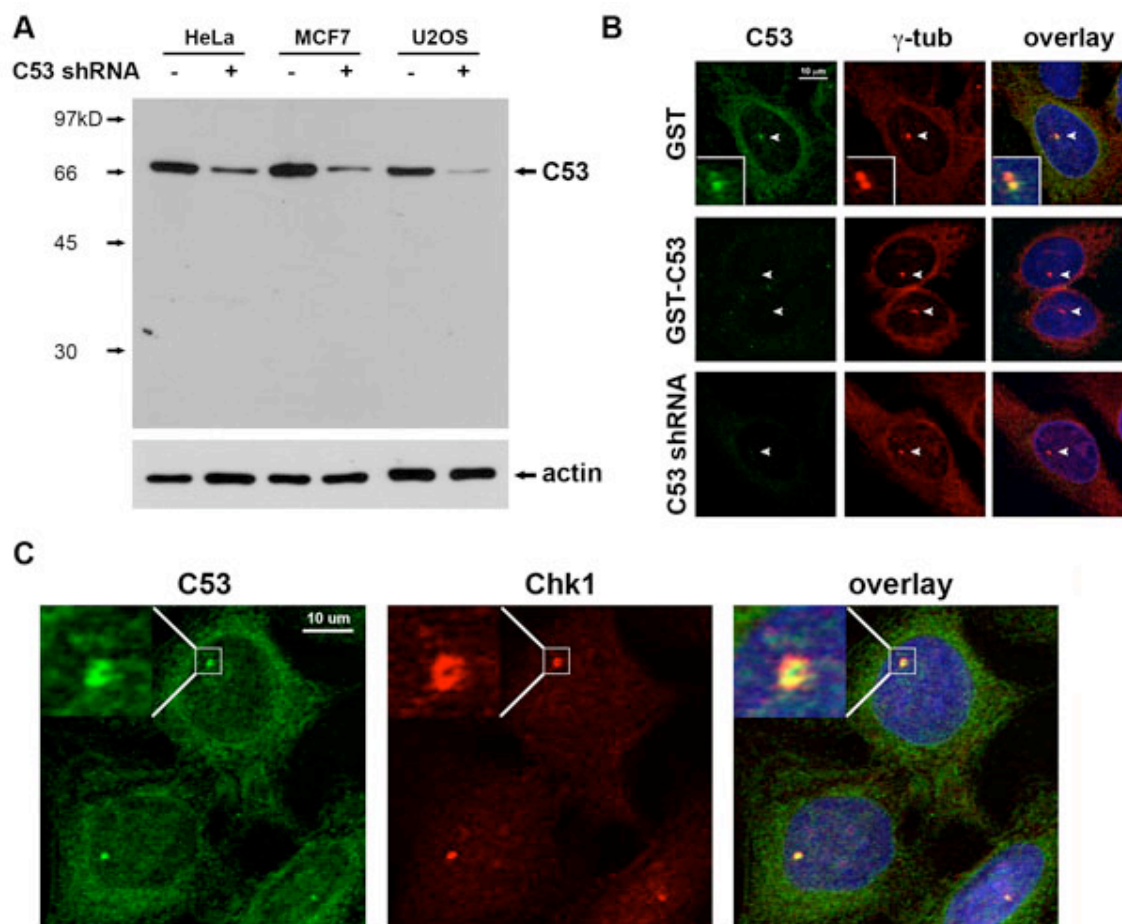
Figure 16 C53 and Chk1 co-localize on the centrosome

A. Immunoblotting of cell lysates with or without C53 depletion using purified C53 rat polyclonal antibody.

B. Immunostaining of endogenous C53. U-2 OS cells were stained with C53 polyclonal rat antibody and γ-tubulin monoclonal antibody (GTU-88, Sigma). For depletion, the primary antibodies were incubated with immobilized GST or GST-C53 fusion proteins. For shRNA knockdown, U-2 OS cells were transfected with C53 shRNA. After 4-day puromycin selection, the cells were subjected to immunostaining.

C. Co-localization of C53 and Chk1 at the centrosome. U-2 OS cells were fixed with methanol (- 20°C) for 5 min, and then immunostained with C53 and Chk1 antibodies. Confocal images were acquired with a Zeiss 510 Meta confocal microscope. At higher magnification (insets), both C53 and Chk1 displayed a "U"-shaped distribution that was described as the PCM tube {Ou, 2003 #28}. All three Experiments were performed by Dr. Jianchun Wu.

PCM (pericentriolar material) tube, and is common for centrosome-associated proteins such as Cdk1 and Ninein [109].

3.1.9 C53 counteracts Chk1 to promote G2/M transition during normal cell cycle progression.

Since we have demonstrated that C53 suppresses activation of Chk1 and Chk2 during the G2/M DNA damage response, we next examined whether C53 depletion delays normal G2/M transition by elevating Chk1 activity. As shown in Figure 17A, C53 depleted cells showed delays in Cdk1 activation (panel p-Y15-Cdk1, compare lane 1 and 4). When a chemical inhibitor of Chk1 UCN-01 was added to the medium, it abolished such a mitotic delay, as evidenced by diminished p-Y15-Cdk1 and increased p-Histone H3 (compare lane 4 and lane 8, Figure 17A). This suggests that the delay of mitotic entry caused by C53 depletion involves Chk1.

We further tested whether C53 antagonizes the kinase activity of Chk1 and Chk2. As shown in Figure 17B, ectopic expression of Myc-Chk1 in HeLa cells leads to increased Cdk1 inhibition (Figure 17B, panels of Cdk1 and p-Y15-Cdk1, lanes 1 and 2), which is in agreement with previous observations by Kramer *et al* [108]. Co-expression of full-length C53 with Myc-Chk1 increased expression of Chk1 (Figure 17B, panel of Myc-Chk1), indicating that C53-Chk1 interaction may stabilize Chk1 (also see Figure 14A, panel of Chk1). Importantly, co-transfection of C53 reverted Chk1-induced inactivation of Cdk1 (Figure 17B, panel of p-Y15-Cdk1, lane 3). This result indicates that C53 may be able to directly inhibit Chk1 activity. We also tested the effect of C53 on Chk2 activity *in vitro*. As shown in Figure 17C, purified C53 clearly inhibited the Chk2-

A

UCN-01	-	-	-	-	+	+	+	+
shRNA	Ctrl	Ctrl	C53	C53	Ctrl	Ctrl	C53	C53
Res. time	0	10	0	10	0	10	0	10 hr

p-Y15-Cdk1

Cdk1

p-Histone H3

Actin

1   2   3   4   5   6   7   8

B

C
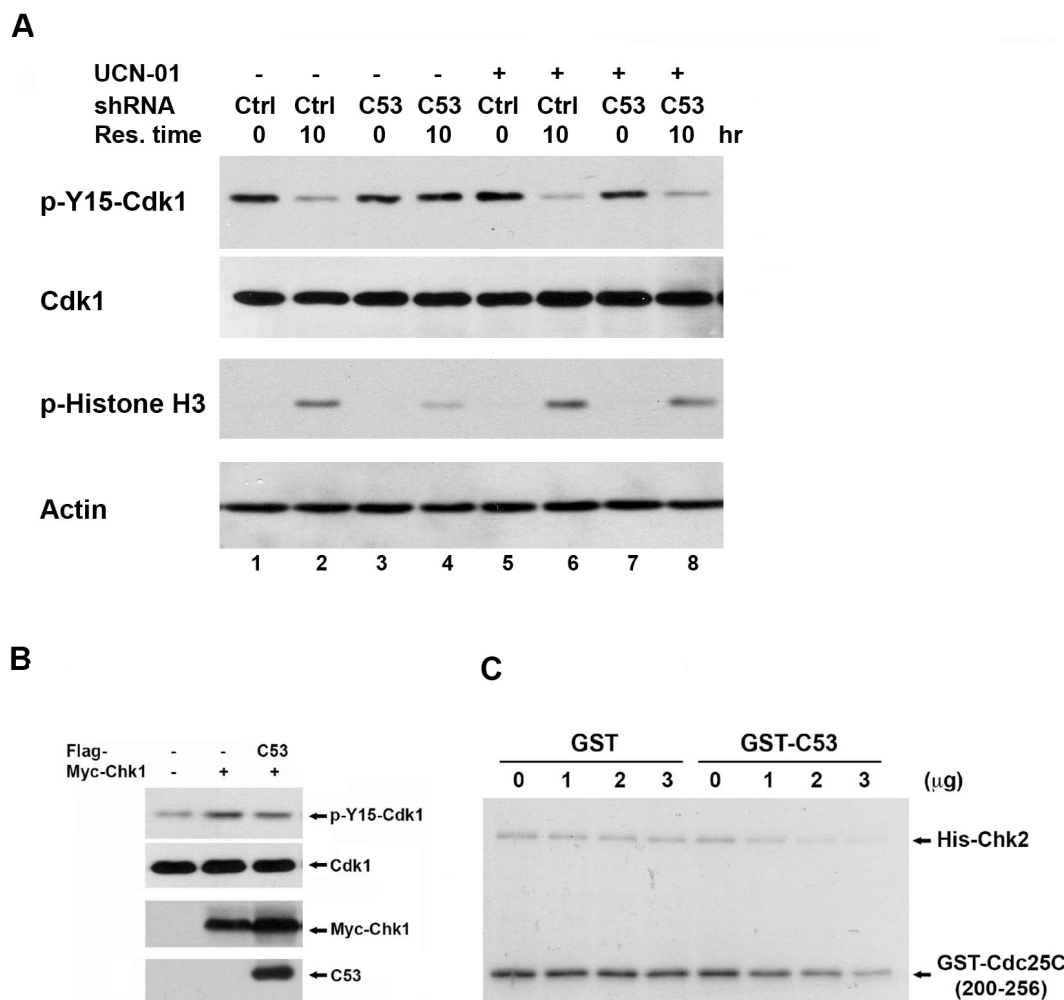
Figure 17 C53 counteracts Chk1 to promote G2/M transition during normal cell cycle progression

A. Chk1 inhibitor UCN-01 prevented delayed Cdk1 activation induced by C53 depletion. HeLa cells were synchronized by double thymidine block. UCN-01 (300 nM) was added into the medium at 5 hours after release from the second block. Cells were collected at 10 hours after release, and the total cell lysates were subjected to SDS-PAGE and immunoblotting using indicated antibodies.
B. C53 antagonizes Chk1-mediated Cdk1 inactivation. HeLa cells were transiently transfected with Myc-Chk1 and C53 constructs. Total cell lysates were subjected to immunoblotting using indicated antibodies.
C. C53 inhibits Chk2 kinase activity. Indicated amounts of GST or GST-C53 were pre-incubated with purified His-Chk2 (50 ng) for 30 min at RT. The assays were performed in 50 μl of kinase reactions buffer containing 50 mM Tris-HCl, pH 7.5, 10 mM MgCl2, 1 mM DTT, 50 μM ATP, 5 μCi of [γ-32P] ATP (Pekin Elmer) and 2 μg GST-Cdc25C (200-256) for 10 min at 30oC. Phosphorylation of GST-Cdc25C was detected by autoradiography. Chk2 auto-phosphorylation was indicated by His-Chk2.

mediated phosphorylation of GST-Cdc25C (200-256), as well as auto-phosphorylation of Chk2. This *in vitro* assay strongly suggests that C53 may be a novel Chk2 inhibitor.

3.1.10 C53 is important for the initial activation of Cdk1/Cyclin B1 at the centrosome

As mentioned before, both C53 and Chk1 localized at the centrosome (Figure 16C). Recently it was shown that the initial activation of Cdk1/cyclin B1 occurs at the centrosome [110]. Chk1 constantly phosphorylates and inhibits Cdc25B [111], and centrosome-associated Chk1 shields Cdk1/cyclin B1 from Cdc25B, thereby preventing its premature activation [108]. Since our results demonstrated that C53 is localized at the centrosome and antagonizes Chk1 during mitotic entry, we wondered whether C53 affects the initial activation of Cdk1/cyclin B1 at the centrosome. γ-tubulin staining was used to indicate centrosome, and p-Y15-Cdk1 staining was used to indicate inactive Cdk1. In any particular cell, the presence of p-Y15-Cdk1 at the centrosome indicates Cdk1 is not yet active (Figure 18A, the two lower arrows). Using this assay, we analyzed whether C53 affects the initial activation of Cdk1/cyclin B1 at the centrosome.

As shown in Figure 18B, when C53 was depleted, more p-Y-15 Cdk1 was found at the centrosomes, suggesting C53 depletion suppresses the initial activation of Cdk1/Cyclin B1 at the centrosome. We also used a centrosome-targeted C53 construct to overexpress C53 specifically at the centrosome. As shown in Figure 18C, increased local C53 concentration greatly reduced the presence of p-Y-15 Cdk1 at the centrosomes, suggesting that locally-concentrated C53 facilitates the initial activation of Cdk1/Cyclin B1 at the centrosome. Of note, centrosomal-associated C53 was more

potent at promoting Cdk1 activation (Figure 18D), suggesting C53's centrosomal localization is important for its role in promoting Cdk1 activation.

Conclusion and Discussion

In this section, we investigated the role of C53 in regulation of G2/M checkpoint, both during unperturbed cell cycle and DNA damage response. We found C53 deficiency confers partial resistance to etoposide and X-ray, while C53 overexpression renders cells susceptible to multiple genotoxic stress. These phenomena can be explained by C53's ability to regulate the G2/M DNA checkpoint. In C53 deficient cells, G2/M checkpoint lasts longer, which prevents Cdk1 activation, mitotic entry and subsequent mitotic cell death. In C53 overexpressing cells, the G2/M checkpoint is suppressed, which allows mitotic entry and leads to mitotic cell death. Moreover, C53's regulation of the G2/M checkpoint also affects cell cycle progression in unperturbed conditions. C53 overexpression leads to premature Cdk1 activation and uneven chromatin condensation, a marker for premature mitotic entry. In contrast, C53 depletion caused delays in Cdk1 activation and mitotic entry.

We further identified C53's target in the G2/M checkpoint signaling pathway. We found C53 overexpression inhibits ATM/ATR-mediated phosphorylation of Chk1 and Chk2, thereby preventing their activation. In addition, C53 directly inhibits the kinase activity of Chk2 and Chk1. Such a dual mechanism of inhibition leads to the potent suppression of the G2/M checkpoint by C53 overexpression. We also found C53 deficiency delays the breakdown of the G2/M checkpoint during DNA damage response. Furthermore, a portion of C53 co-localizes with Chk1 at the centrosome, and is
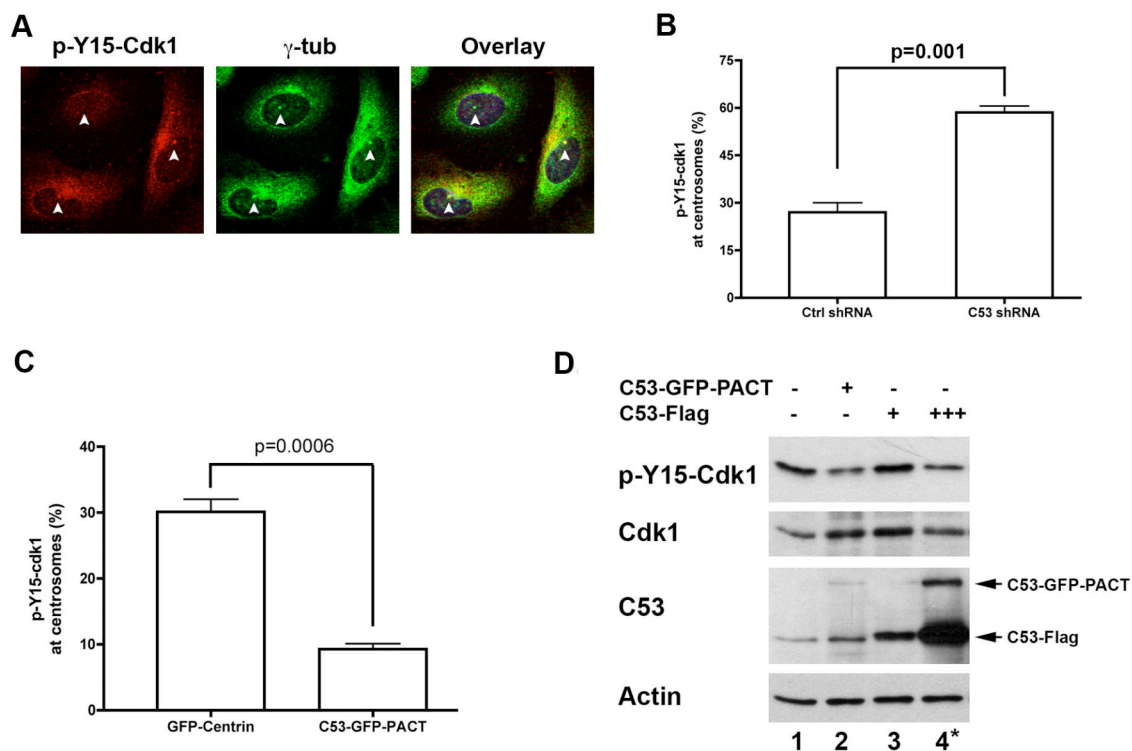
Figure 18 C53 is important for the initial activation of Cdk1/Cyclin B1 at the centrosome

A. Inactive Cdk1 (p-Y15-Cdk1) decorated centrosomes in C53-depleted U-2 OS cells. U-2 OS cells were infected with retroviruses expressing either control shRNA or C53 shRNA. After 4-days of puromycin (2 μg/ml) selection, U-2 OS cells were immunostained with p-Y15-Cdk1 and γ-tubulin antibodies. Centrosomes were marked by arrowheads.

B. More centrosomes were decorated by inactive Cdk1 in C53-depleted cells. The numbers of cells containing inactive Cdk1-decorated centrosomes were scored manually. Data were mean ± S.D., with three independent repeats. More than 200 cells were examined in each of three independent experiments.

C. Centrosome-targeting C53 reduced the number of inactive Cdk1-decorated centrosomes in U-2 OS cells. C53-GF-PACT or GFP-centrin constructs were transfected into U-2 OS cells. After 24 hours, cells were fixed and immunostained with p-Y15-Cdk1 antibody. p-Y15-Cdk1-decorated centrosomes were scored as described above. Data were mean ± S.D., with three independent repeats. More than 200 cells were examined in each of three independent experiments.

D. Total p-Y15-Cdk1 was evaluated by immunoblotting. U-2 OS cells were infected with retroviruses expressing control shRNA or C53 shRNA. After 4-day drug selection (puromycin 2 μg/ml), cells were collected and subjected to immunoblotting using the indicated antibodies.

important for the initial activation of Cdk1/cyclin B1 at the centrosome. Together, these experiments showed C53 is an important regulator of the G2/M checkpoint, and has potential implications for cancer therapy.

Several interesting questions arose from these experiments. First, C53 depletion confers no resistance to camptothecin and doxorubicin, while overexpression of C53 sensitizes cells to these two drugs. This may be explained by different mechanisms of drug action. Like etoposide, camptothecin and doxorubicin are also topoisomerase inhibitors and induce DNA double strand breaks (DSBs). However, their actions are not limited to this. Camptothecin blocks ribosome formation and inhibits RNA synthesis [112,113], while Doxorubicin can form DNA adducts and has been reported to act directly on mitochondria and cause mitochondrial damage [114]. Therefore, these two drugs may cause cell death by action in addition to inducing DSBs. Since we propose C53 depletion prolongs DSBs-induced G2 arrest and therefore delays mitotic cell death, it is possible that C53 depletion cannot rescue cells from other pro-death effects of Camptothecin and Doxorubicin. Nonetheless, when C53 is overexpressed, it suppresses the G2/M checkpoint, therefore it can still sensitize cells to camptothecin and doxorubicin-induced cell death.

Second, how does C53 inhibit Chk1 and Chk2? Our data suggest that C53 inhibits the function of Chk1 and Chk2 at two levels. First, overexpression of C53 suppressed activation of Chk1 and Chk2, as evidenced by reduced phosphorylation of Ser345 of Chk1 and Thr68 of Chk2 (Figure 14A). There are two possible mechanisms. By binding with Chk1 and Chk2, C53 may act to block ATM/ATR mediated phosphorylation and activation of these two proteins. Alternatively, it may facilitate dephosphorylation of these two checkpoint kinases. Our finding that C53 interacts with

phosphorylated Chk1 (Figure 15B) seems to support such a hypothesis. Recently, more focus has been brought to the dephosphorylation of Chk1 and Chk2. It was reported the phosphatase PPM1D dephosphorylates Chk1, Chk2 and p53, thereby abrogating the checkpoints [115-117]. In addition, phosphatase PP2A dephosphorylates both Chk1 and Chk2 [111,118]. By interacting with Chk1 and Chk2, C53 may promote their dephosphorylation by these phosphatases.

We also showed C53 directly inhibits Chk2 activity *in vitro*. C53 interacts with Chk2 and therefore may block substrate binding and phosphorylation of Chk2 substrates. In the case of Chk1, due to its low expression and degradation, we could not purify active His-tagged Chk1. When we used GST-Chk1 in *in vitro* kinase assay, we did not observe C53's inhibitory effects on Chk1 phosphorylation of GST-Cdc25B (200-256) (data not shown). One possible explanation is that GST-tagged proteins tend to form dimers, which may lead to intermolecular association between GST-Chk1 and GST-Cdc25B through GST-dimers. Under such conditions, C53 may not be able to block the binding of Cdc25B to Chk1, and therefore is not able to inhibit the phosphorylation. Alternatively, GST-Chk1 may adopt a conformation that is uninhibitable by C53 *in vitro*. Nonetheless, *in vivo* experiments showed C53 indeed antagonizes Chk1's activity inside cells (Figure 17B), which demonstrates C53's potent effects in inhibiting Chk1.

Third, our data further support a role for the centrosome during mitotic entry. The centrosome is the major microtubule-organizing center (MTOC) that contributes to the regulation of cell shape, polarity, adhesion and motility [119]. A growing body of evidence indicates that centrosomes serve as integral platforms for a multitude of signaling networks, especially cell cycle control and checkpoint signaling [120]. During

the G2 phase, Cdk1 and cyclin B1 begin to accumulate at the centrosome, where initial activation of the Cdk1/cyclin B1 complex occurs in late prophase [110]. Active Cdk1 in turn promotes nuclear membrane breakdown and mitotic spindle assembly [30,121]. Both positive and negative pathways that regulate Cdk1 activation integrate at the centrosome [122]. Mitotic kinases such as Polo-like kinase 1 (Plk1) and aurora-A kinase localize at the centrosome [110]. Plk1 phosphorylates Ser 133 of cyclin B1 at the centrosome. Aurora-A kinase is first activated in late G2 phase at the centrosomes, which in turn phosphorylates Cdc25B at residue Ser353 to activate its phosphatase activity [123]. Active Cdc25B further activates Cdk1 at the centrosomes [123,124]. Meanwhile, the negative regulators of mitotic entry such as Chk1 and Chk2 also localize at the centrosomes [122,125]. At interphase, the centrosome-associated checkpoint kinase Chk1 acts as a negative regulator to shield centrosomal Cdk1 from unscheduled activation by Cdc25B, thereby preventing premature mitotic entry [108]. At the onset of mitosis, Chk1 dissociates from the centrosome, thereby allowing Cdc25B to activate Cdk1. In the same study, the authors observed that Chk2 (phosphorylated at Thr387) is recruited to centrosomes after γ-irradiation-induced DNA damage [108]. Our data suggest that centrosome-associated C53 can counteract Chk1 to promote initial activation of Cdk1/cyclin B1 at the centrosome. Together with the aforementioned studies, our results further support the notion that the centrosome is crucial for Cdk1 activation and mitotic entry. Whether the centrosome plays a role in the DNA damage response remains unclear and is an interesting topic for further investigation.

Part II

3.2 C53 is a Polo-like kinase 1-associated protein and plays multiple roles during M phase

3.2.1 Depletion of C53 causes multiple mitotic defects

The centrosome is the major microtubule-organizing center (MTOC) inside mammalian cells. During the cell cycle, the centrosome undergoes its own centrosome cycle. It duplicates itself in the S phase. In prophase, duplicated centrosomes split and migrate, which is important for the formation of bi-polar spindle poles [119]. Such events are critical for the orderly progression of mitosis. We found that a portion of C53 is localized at centrosomes (Figure 16B). In an attempt to elucidate C53's role in mitosis, we first analyzed the impact of C53 depletion on centrosome dynamics during cell cycle progression. Control and C53-depleted cells were synchronized by double thymidine block, and then released into fresh medium. Using γ-tubulin as a centrosomal marker, we followed centrosome duplication and separation at different time point. As shown in Figure 19A, centrosome duplication was largely unaffected by C53 depletion in synchronized HeLa cells, which is consistent with our observation that C53 depletion did not influence S phase progression in HeLa cells. Interestingly, centrosome separation was inhibited by C53 depletion (Figure 19B). Because centrosomes need to split and migrate to the opposite ends of nucleus to enable the formation of bi-polar spindles, it is not surprising that when C53 is depleted and centrosomes are tethered together, HeLa cells have increased incidence of mono-polar spindles. Such spindles lead to the rosette-like chromosome arrangement (Figure 19C) [89]. Re-introduction of shRNA-
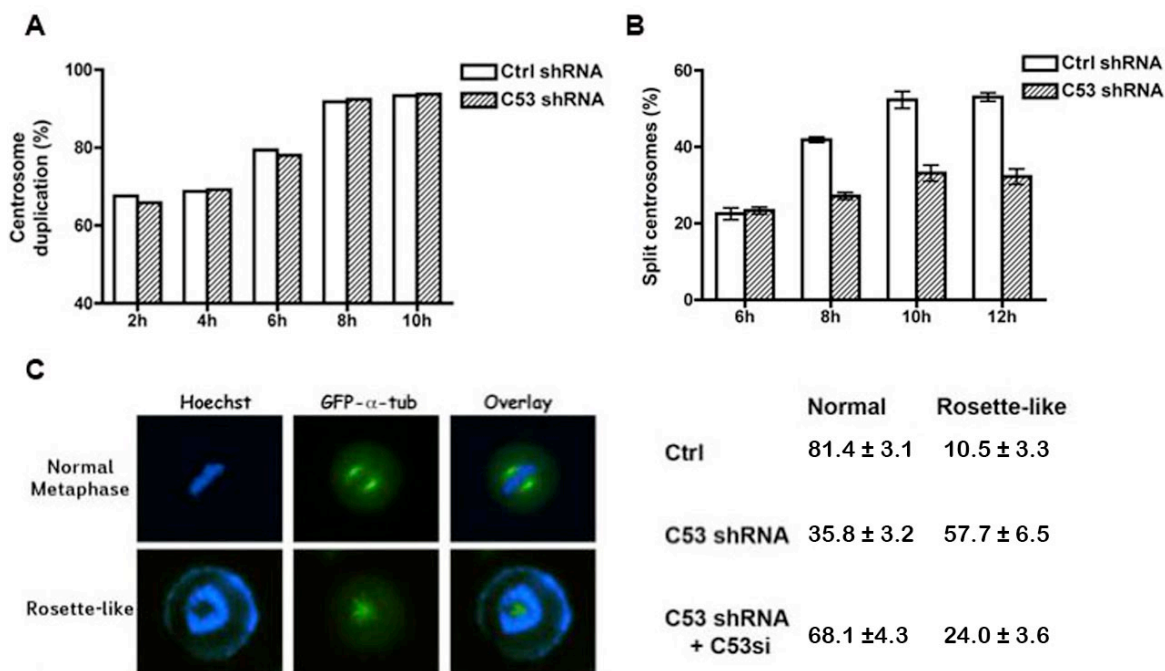
Figure 19 Depletion of C53 causes unspilt centrosome, mono-polar spindle and rosette-like chromosome arrangement

A. HeLa cells were transfected with control or C53 shRNA and synchronized as described in "Material and Methods". Centrosomes were marked by γ-tubulin staining. Centrosome duplication was scored by counting cells with a pair of centrosomes. Done in collaboration with Dr. Jianchun Wu. *Ctrl*, control.

B. C53 depletion delayed centrosome separation. Centrosome separation was scored by centrosomes separated by > 2 μm (the distance was calculated by Openlab software). Centrosome duplication was scored by examining cells with two centrosomes. Data were mean ± S.D., with three independent repeats. More than 200 cells were examined in each of three independent experiments. Done in collaboration with Dr. Jianchun Wu. *Ctrl*, control.

C. C53 depletion leads to monopolar spindle and rosette-like chromosome arrangement during mitosis. Control and C53 shRNA were co-transfected with GFP-α-tubulin into HeLa cells. After 72 hours of puromycin (2 μg/ml) selection, chromosomes were stained with Hochest Dye. Metaphase cells were pictured and scored. While counting, cells were kept at 37°C with adequate O_2 and CO_2 supply. In control cells, spindles were bi-polar (green) and chromosomes aligned to the metaphase plate (purple). In C53 depleted cells, nearly 60% of Metaphase cells showed mono-polar spindles and rosette-like chromosome arrangement. Re-expression of C53 (C53 si) rescued such phenotype. Data were mean ± SEM, from at least three independent experiments, each counting about 200 metaphase cells. *Ctrl*, control.

resistant C53 construct reduced the incidence of rosette-like chromosome arrangement (Figure 19C).

Using time-lapse video microscopy, we observed mitosis in C53 depleted cells. Surprisingly, these C53-depleted, mono-polar cells were able to undergo chromosome segregation. As shown in Figure 20A, chromosomes in C53-depleted HeLa cells stayed in rosette-like arrangement, then suddenly separated into two "clouds" of chromosomes, without a stage of metaphase alignment at the equatorial plate observed in normal mitosis. About 20% of C53 depleted cells exhibited mitosis of this kind.

In addition to aberrant mitosis described above, other cells managed to align chromosomes at the equatorial plate. However, there is increased incidence (30% in C53 depleted cells) of chromosome lagging during anaphase (Figure 20B). Additionally, the separated chromosomes were often less compact, and in many cases non-linear comparing to those observed in control cells (data not shown). This suggests C53 may also function during anaphase.

Both rosette-like chromosome arrangement and chromosome lagging are aberrant forms of mitosis, and as a result, the daughter cells may be genetically unstable, manifesting severe defects in nuclear shape and structure. In Figure 21 panel A, a C53 depleted cell adopted a rosette-like chromosome arrangement, struggled at metaphase for almost 5 hours, then suddenly decondensed its chromosomes and formed an ill-shaped nucleus with 4N DNA. In panel B, a cell adopted a rosette-like chromosome arrangement, and then separated into two "clouds" of chromosomes. In the end, however, a bi-nucleated cell was formed. In panel C, the cell showed chromosome lagging at anaphase. The cell was able to complete mitosis but the
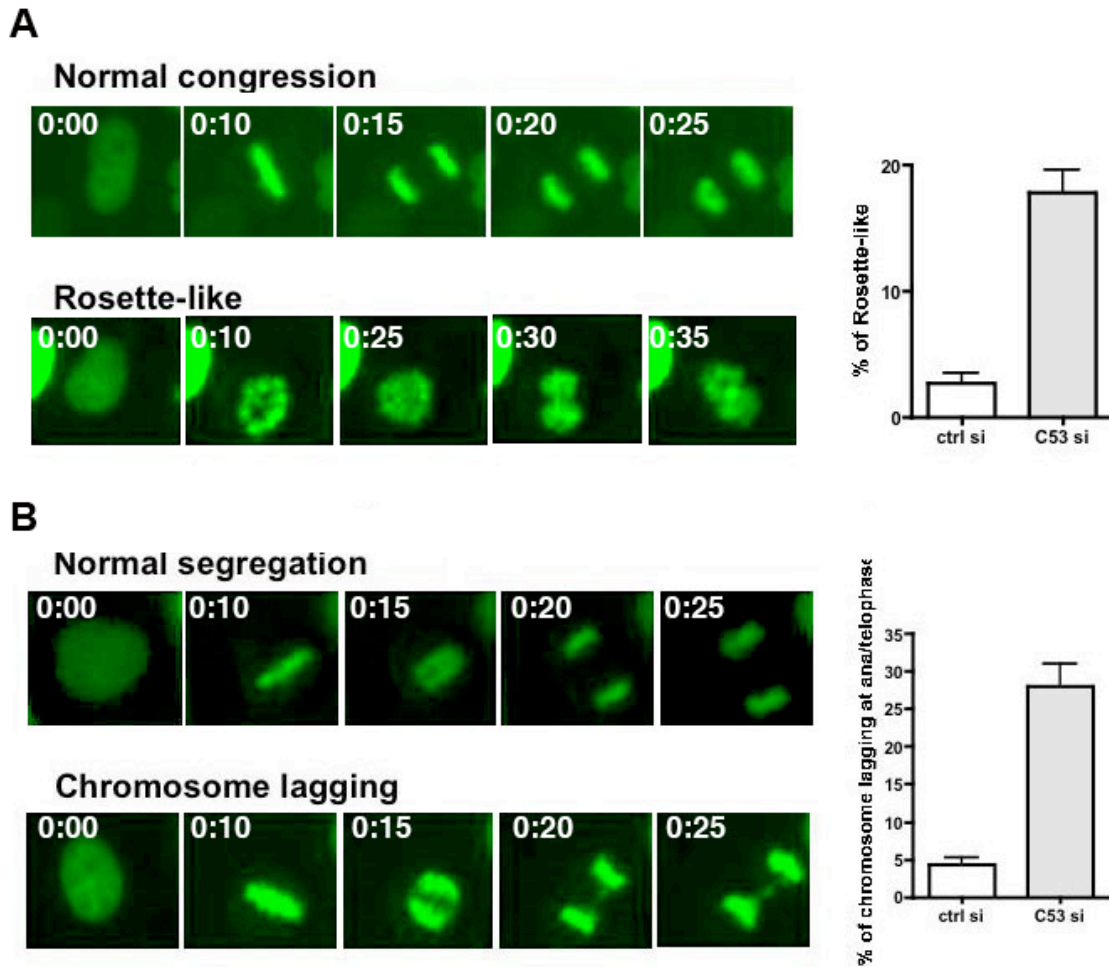
Figure 20 Aberrant mitosis in C53-depleted cells

A. Aberrant Mitosis following rosette-like chromosome arrangement. HeLa cells were transfected with control or C53 shRNA and H2B-GFP for 24 hours and observed in time-lapse video microscopy.   Top row, images of mitosis with normal chromosome congression. Bottom row, images of mitosis with rosette-like chromosome arrangement. Right panel, quantitative results of mitotic events. Data were mean ± S.D., with three independent repeats, each counting more than 100 mitotic events. *Ctrl*, control.
B. C53-depleted cells showed chromosome lagging during anaphase. Images were acquired from the same experiment as (A). An increased percentage of C53-depleted cells showed chromosome lagging at Anaphase. Right panel, quantitative results of mitotic events. Data were mean ± S.D., with three independent repeats, each counting more than 100 mitotic events. *Ctrl*, control.
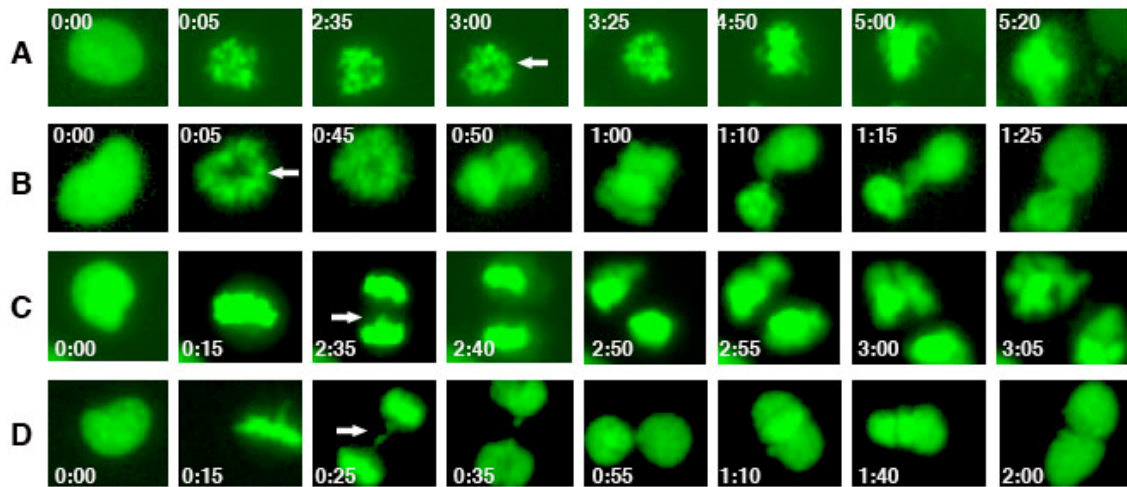
Figure 21 Rosette-like chromosome arrangement and chromosome lagging lead to nuclear deformation in C53-depleted HeLa cells

HeLa cells were transfected with control or C53 shRNA and H2B-GFP for 24 hours and observed in time-lapse video microscopy.   Images were from the same experiment as Figure 20. H2B-GFP signals illustrate both chromosome movements during mitosis and shape of daughter nuclei after mitosis. Arrows indicate rosette-like chromosome arrangement or chromosome lagging during mitosis. Panel A, B, C, D, four examples of aberrant mitosis caused by C53 depletion, each leading to the formation of deformed nuclei.

daughter cells underwent drastic changes of nuclear shape. In 30 minutes, the nucleus was visibly fragmented. Such a phenomenon was not the result of apoptosis as the cells lived on for hours before the videotaping was finished. In panel D, chromosome lagging led to the formation of a bi-nucleated cell.

Together, these various forms of aberrant mitosis lead to the accumulation of deformed nuclei in C53-depleted HeLa cells (Figure 22A). Another C53 shRNA was able to induce the similar phenotype (data not shown), and re-introduction of shRNA-resistant C53 rescued such nuclear deformation (Figure 22B). These results demonstrated that these defects are specifically caused by C53 depletion. In addition, when C53 was depleted in colon cancer line HCT116 p53-/- cells, we also observed such nuclear irregularity (Figure 22C).

We grouped these deformed nuclei into four major categories: poly-lobed, fragmented, multi-nucleated and enlarged nuclei (Figure 23). In each category, there was an increased percentage of deformed nuclei in C53 depleted cells. Interestingly, deformities in nuclear shape such as poly-lobulation, fragmentation (grooves and long clefs), multi-nucleation and enlarged nuclei are often observed in various forms of human cancers [92].   To date, the mechanisms underlying such deformations are still largely unknown [92]. Our findings may provide insight on the underlying mechanism of such a prominent but poorly understood phenomenon in human cancers.

Using phase-contrast time-lapse video microscopy, we also observed a cytokinesis defect associated with C53 depletion. At 48 hours post-transfection and selection, cells appeared relatively normal (Figure 24A, panel **a**). Cell #1 entered mitosis but failed to separate during cytokinesis, and became a bi-nucleated cell, followed by
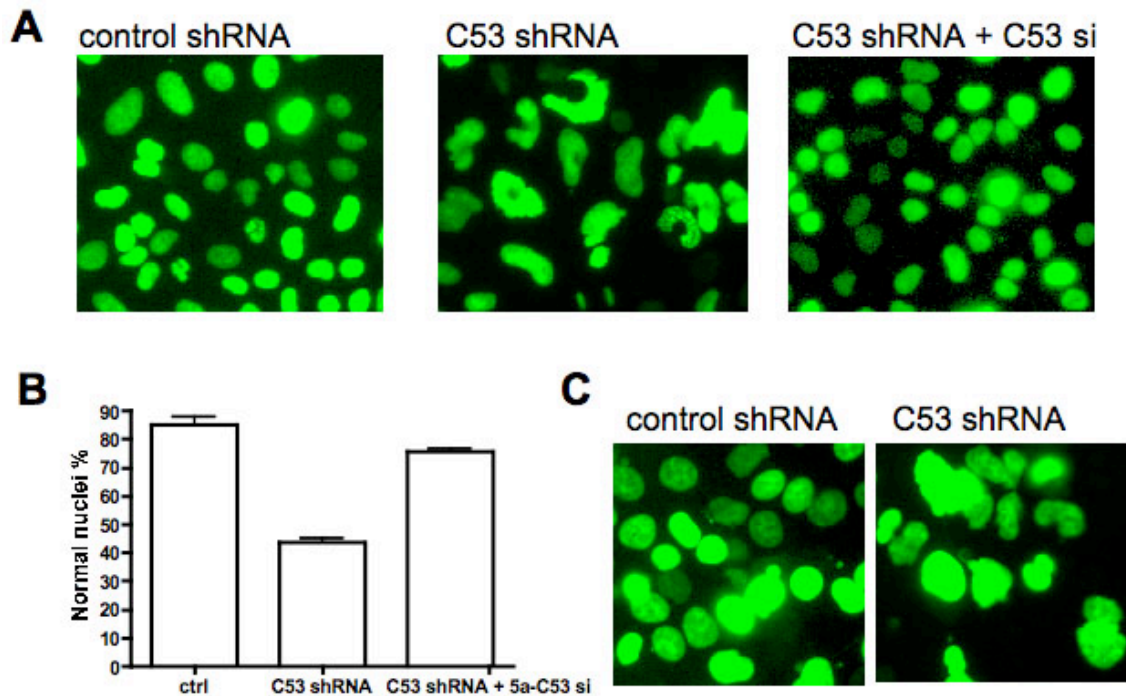
Figure 22 C53 depletion leads to the formation of deformed nuclei

A. HeLa cells were transfected with control or C53 shRNA. A C53 si construct was co-transfected to re-express C53. After 72 hours of puromycin selection, the shape of nuclei was imaged via H2B-GFP. C53 depleted cells showed extensive nuclear deformation. Re-expression of C53 in these cells restored wild type phenotype.
B. Quantitative result of C53-depletion induced nuclear deformity. Oval, smooth nuclei were scored as normal nuclei. Three independent experiments were performed. In each experiment, more than 600 cells were counted. Results were mean ± S.D., with three independent repeats. *Ctrl*, control.
C. In HCT 116 p53-/- cells, C53 depletion also caused nuclear deformity. HCT 116 p53-/- cells were transfected with control or C53 shRNA. Co-transfection of H2B-GFP were used to mark the shape of nucleus. After 4 days of puromycin (2 μg/ml) selection, cells were examined and photographed.

	Normal	Poly-lobed	Fragmented	Multi-nucleated	Enlarged
Ctrl (%)	90.0	6.1	0.8	2.1	1.2
C53 shRNA (%)	41.9	38.0	11.5	4.8	7.3
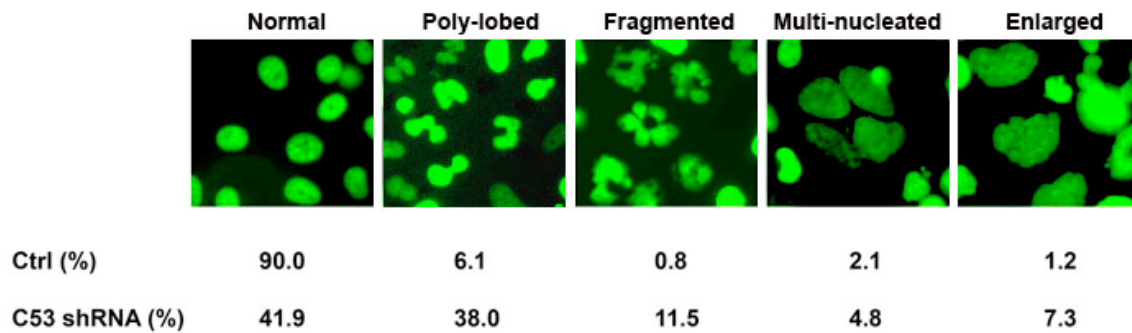
Figure 23 C53 depletion causes multiple forms of nuclear deformities

HeLa cells were transfected with H2B-GFP and control or C53 shRNA. After 72 hours of puromycin (2 μg/ml) seletion, nuclei were imaged. The number of poly-lobed, fragmented, multinucleated and grossly enlarged nuclei was scored. Data are from three independent experiments, each counting more than 600 cells. In four categories of nuclear deformities, there was statistically significant increase in C53-depleted cells ($p<0.01$ for poly-lobed, fragmented, enlarged, and $p<0.05$ for muti-nucleated).

cell death (panels **a** to panel **g**). Cell #2 divided but failed to separate, resulting in a bi-nucleated cell (panels **a** to panel **g**). This bi-nucleated cell underwent a second division (panel **h**) and a failed cytokinesis, thereby leading to the formation of a hexa-nucleated cell (panels **g** to **l**, 6 nuclei). This time-lapse analysis clearly demonstrated that C53 deficiency leads to defective cytokinesis.

Furthermore, long term C53 depletion results in decreased proliferation and survival. We transfected cells with either control or C53-shRNA plasmids, and replated them at dilute concentration. After puromycin selection, we observed their ability to form clones after 7-day incubation. The majority of C53-depleted cells (> 80%) displayed cell cycle defects. As shown in Figure 24B, the average size of C53-depleted HeLa cell clones (average 6 cells per clone) was much smaller than that of control clones (average 80 cells per clone), indicating that C53 deficiency caused decrease in proliferation and/or viability. The difference on the clone size was not due to different transfection efficiency because co-transfection of GFP marker indicated comparable transfection efficiency (data not shown). Importantly, HeLa cells that were co-transfected with shRNA-resistant C53 construct (C53si) gave an average size of 27 cells per clone, indicating a partial rescue of cellular phenotypes caused by C53 depletion (Figure 24C). Similar cell proliferation defects have been observed for C53-depleted T47D, MCF-7 (Figure 22D and E), HCT116 (wild-type and p53-/-), and U-2 OS cells (data not shown).

3.2.2 C53 interacts with Plk1 and is a possible Plk1 substrate

Interestingly, nearly all the mitotic defects we observed in C53-depleted cells have been reported in Plk1 depletion or mutation studies. The list includes failure of centrosome separation, formation of mono-polar spindles, rosette-like chromosome

A

B

C

D

E
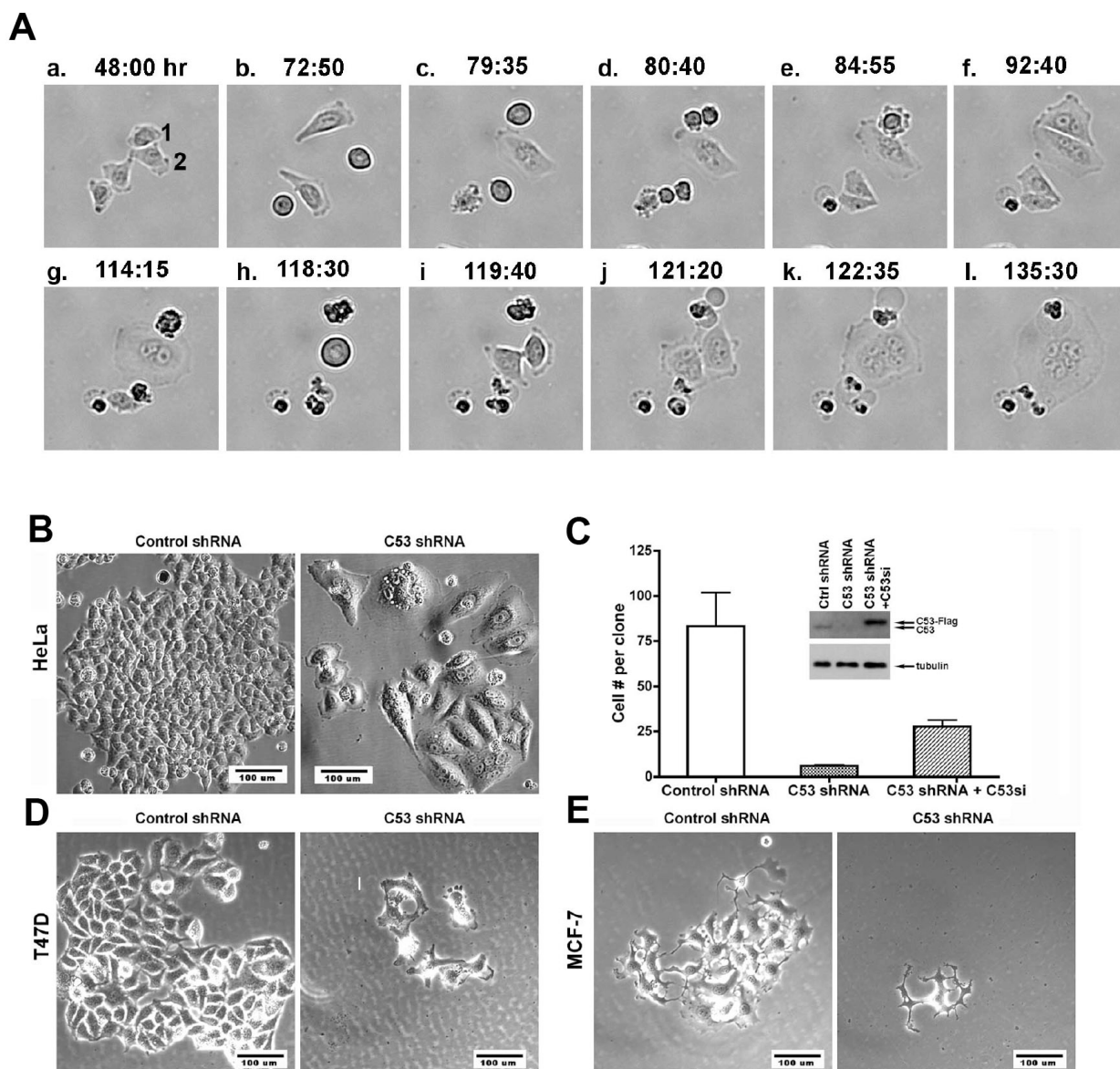
Figure 24 C53 depletion causes defect in cytokinesis and reduced cellular proliferation and survival

A. HeLa cells were transfected with C53 shRNA vector, and followed by selection with puromycin (2 μg/ml). Time-lapse images were taken every 5 minutes. The time points indicate the time after transfection.

B. C53 depleted HeLa cells. HeLa cells were transfected with control shRNA, C53 shRNA construct, or C53 shRNA and C53si (resistant to C53 shRNA inhibition) together, and then treated with puromycin (2 μg/ml) for selection. Pictures were taken at 7 days after initial transfection using Openlab software.

C. Average cell number per clone of HeLa cells after 7-day selection. The top panel showed expression of C53 protein. **D.** C53-depleted T47D cells. **E.** C53-depleted MCF-7 cells. Cells were transfected with C53 shRNA, and selected by puromycin (1.5 μg/ml) for 5 days before counting.

arrangement, chromosome lagging during anaphase, incomplete cytokinesis, decreased survival and/or proliferation [64,70,71,90]. Such observations prompted us to investigate the functional relationship between C53 and Plk1 signaling. Using co-immunoprecipitation assays, we found overexpressed C53 interacts with endogenous Plk1 in both normal and genotoxin-treated HeLa cells (Figure 25A). We further confirmed interaction between endogenous C53 and Plk1 proteins (Figure 25B). Moreover, purified His-tagged Plk1 can be pulled down by GST-C53 conjugated-agarose beads, indicating direct binding between these two proteins (Figure 25C).

In earlier studies, we found a fraction of C53 localized to the centrosome (Figure 16B). Interestingly, Plk1 is also localized at the centrosome in G2 and M phases. Using affinity-purified anti-C53 antibodies, we then studied the possible subcellular co-localization of Plk1 and C53.   We found these two proteins co-localize with each other in various stages of cell cycle. Except for G1 and early S phases, during which the Plk1 level is low, C53 and Plk1 are constantly found together on the centrosome (Figure 26). In addition, C53 and Plk1 co-localize on spindle poles during metaphase and anaphase. They also co-localize on central spindles during anaphase and telophase, as well as midbodies during cytokinesis (Figure 26 and data not shown). The only exception where C53 and Plk1 are not found together on mitotic apparatus is that Plk1 localizes to kinetochores, while C53 does not. Together with our finding that they interact with each other, such close association between C53 and Plk1 during cell cycle suggests they may work together to carry out mitotic functions.

Plk1 phosphorylates many proteins to facilitate mitotic progression. Since we have demonstrated the functional and molecular association of C53 and Plk1, we next asked whether C53 is a Plk1 substrate. As shown in Figure 27A, when incubated with
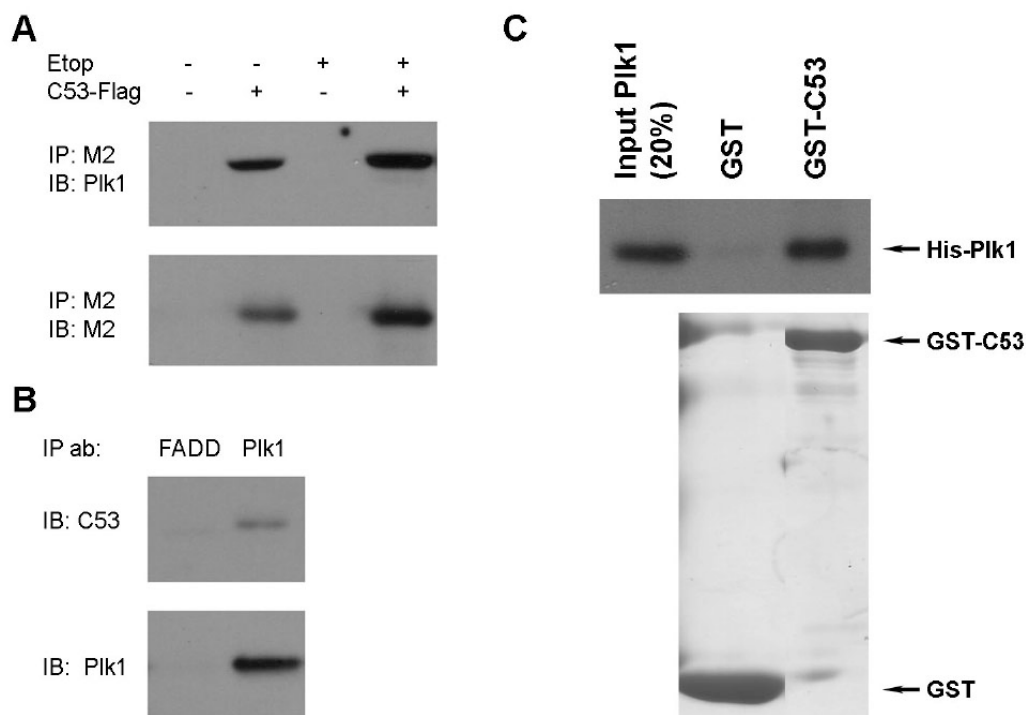
Figure 25 C53 and Plk1 interact with each other

A. Co-immunoprecipitation of C53-Flag and endogenous Plk1. 1×10^{6} HeLa cells were transfected with 4 μg of control or C53-Flag constructs. 24 hours after transfection, cells were treated with etoposide and zVAD-fmk for 24 hours, or left without treatment. Lysates from cells were subjected to immunoprecipitation using anti-Flag (M2) beads. The presence of Plk1 in immuno-complex was examined by immunoblotting using anti-Plk1 antibody.

B. Co-immunoprecipitation of endogenous C53 and Plk1. Lysates from HeLa cells were subjected to immunoprecipitation using anti-Plk1 antibody. Anti-FADD antibody was used as control. The presence of endogenous C53 in immuno-complex was examined by immunoblotting using anti-C53 antibody.

C. *In vitro* interaction between C53 and Plk1. Purified His-Plk1 (0.5 μg) was incubated with purified either GST or GST-C53 (1 μg) in buffer described in immunoprecipitation assay. After three washes, Plk1 was detected by immunoblotting using Plk1 antibody.
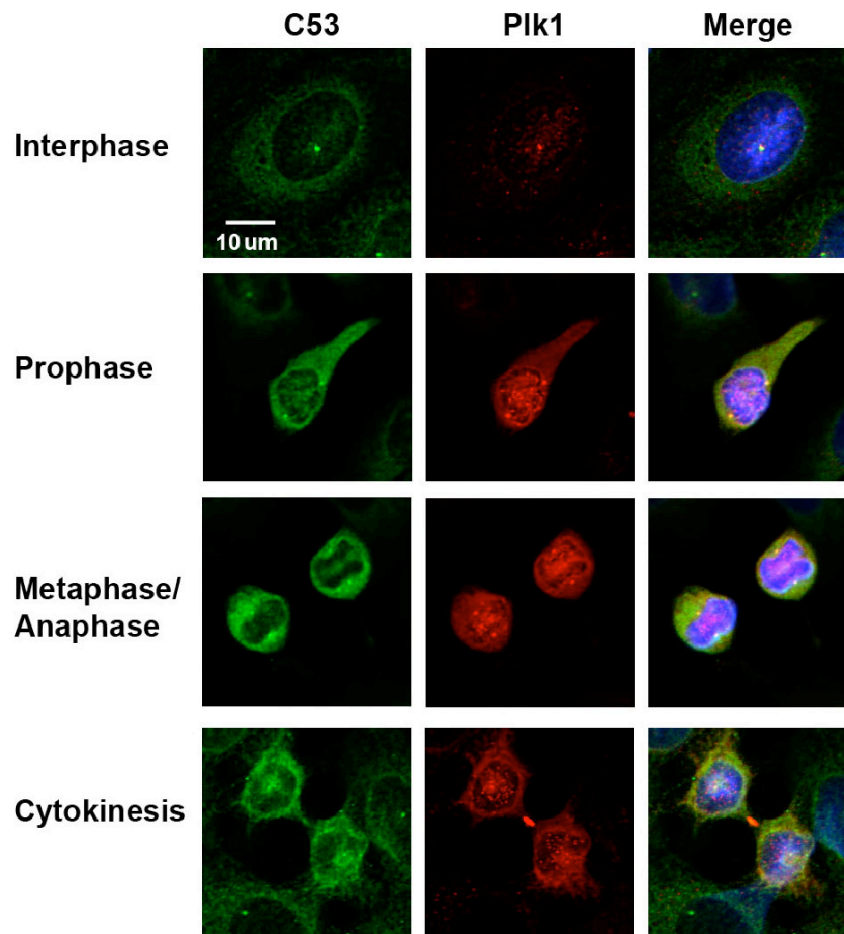
Figure 26 Co-localization of C53 and Plk1 during the cell cycle

U-2 OS cells were immunostained with C53 rat polyclonal antibody and Plk1 monoclonal antibody. Images were acquired by Zeiss META 510 confocal microscope. Purple signals in merged pictures were Hoechst staining of DNA. Experiment was done in collaboration with Dr. Jianchun Wu.

purified Plk1 *in vitro*, C53 was substantially phosphorylated. Plk1's phosphorylation of C53 is comparable to its phosphorylation of α-casein, a substrate commonly used in Plk1 activity assay. Moreover, C53 phosphorylation was reduced in Plk1-depleted cells, and enhanced by Plk1 overexpression (Figure 27B). In addition, sequence analysis indicates that regions around Thr479 (EKT[479]K) and Ser491 (DIS[491]K) on the C-terminus of C53 fit as Plk1 consensus sequences and are possible Plk1 phosphorylation sites. Taken together, these data strongly support C53's role as a Plk1 kinase substrate.

3.2.3 C53 interacts directly with the kinase domain of Plk1

The *Polo-box* domain (PBD) of Plk1 interacts with its kinase domain and is proposed to inhibit kinase activation and substrate binding [84]. Plk1 substrates with priming phosphorylations interact with PBD and release the Plk1 kinase domain [88]. Considering C53's role as a possible Plk1 substrate, we wondered whether C53 interacts with Plk1 through the *polo-box* domain (PBD) like other Plk1-interacting proteins. Surprisingly, when we used PBD and Plk1 kinase domain in co-immunoprecipitation assays, we found C53 interacted directly with the Plk1 kinase domain, with little or no interaction with PBD (Figure 28A). Such kind of interaction is unprecedented for Plk1 associated proteins and its substrates, and it prompted us to examine C53's possible role in Plk1 activation. Interestingly, the presence of PBD on full-length Plk1 did not seem to inhibit C53's interaction with Plk1 kinase domain at all (Figure 28A), suggesting C53's interaction with Plk1 kinase domain could overcome the inhibitory effect of PBD. We designed another co-immunoprecipitation experiment to test this hypothesis. As shown in Figure 28B, when only PBD and Plk1 kinase domain were expressed in cells, anti-PBD antibody was able to pull down Plk1 kinase domain
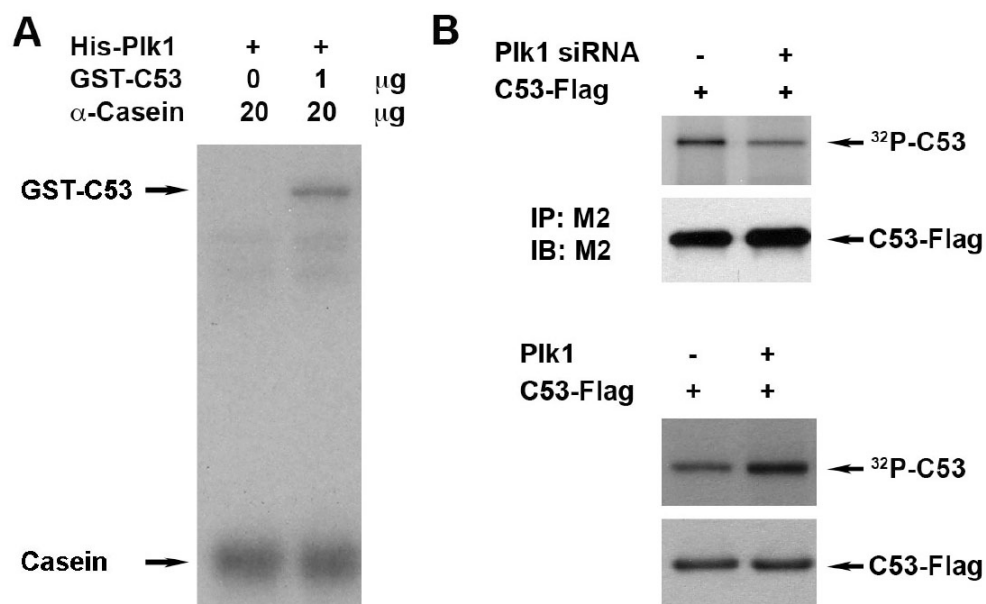
Figure 27 C53 is a Plk1 substrate

A. *In vitro* kinase assay was performed using purified His-Plk1 and dephosphorylated casein as substrate. GST-C53 was pre-incubated with Plk1 for 20 minutes before the start of kinase reaction. Image is autoradiograph.

B. C53 phosphorylation was regulated by Plk1 expression. HeLa cells were transfected with C53-Flag constructs, while Plk1 were either depleted or overexpressed. Cells were subsequently labeled with inorganic ^{32}P-phosphate for 4 hours. C53 was immunoprecipitated with M2 antibody, and C53 phosphorylation was detected by autoradiography.
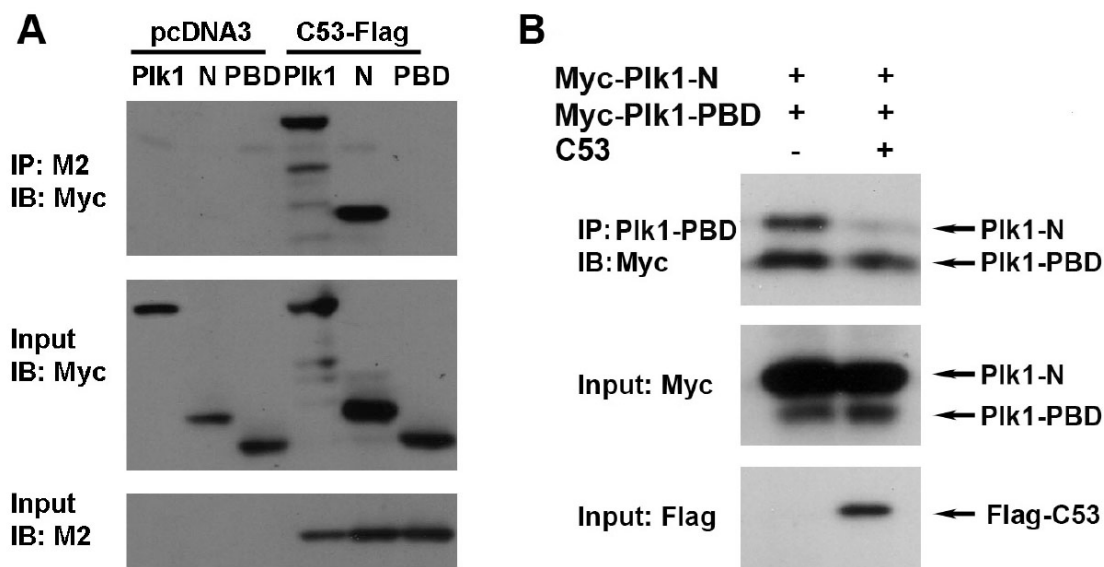
Figure 28 C53 binds to the kinase domain of Plk1

A. Co-immunoprecipitation assay. 2 μg of C53-Flag and 2 μg of Myc-tagged Plk1 or its fragments (N and PBD) were transfected into 1×10^6 HeLa cells. 24 hours after transfection, cell lysates were subjected to immunoprecipitation. C53-Flag was pulled down by M2 beads. The presence of Plk1 or its fragments in the immno-complex was examined by immunoblotting using a Myc antibody.
B. C53 binding disrupts the intramolecular interaction between Plk1 kinase domain and PBD. Myc-tagged Plk1 kinase domain and PBD were overexpressed in the absence or presence of C53 overexpression. PBD was pulled down by Plk1 monoclonal antibody, and the presence of Plk1 kinase domain was detected by Myc antibody. Done in collaboration with Dr. Jianchun Wu.

together with PBD. However, when C53 was co-transfected in such cells, interaction

between PBD and kinase domain was significantly weakened (Figure 28B). This

experiment suggested that C53's interaction with Plk1 kinase domain is exclusive, and

may shield it from inhibitory effect of PBD. This suggests an interesting new model of

Plk1 activation. We propose by disrupting the association between PBD and Plk1

kinase domain, C53 may antagonize the inhibitory effect of PBD binding, and may

facilitate the T-loop activation of Plk1. This model, if confirmed, should further advance

our understanding of Plk1 activation, and could possibly help design new regimens of

anti-cancer treatment using Plk1-related drugs.

Conclusion and Discussion

In this section, we investigated C53's function in M phase and the underlying

molecular mechanisms. C53 depletion leads to multiple defects in M phase, including

inability to separate centrosome, mono-polar spindle, rosette-like chromosome

arrangement, chromosome lagging, incomplete cytokinesis, and irregular shapes of

daughter nuclei. Interestingly, most of these defects resemble those observed in Plk1

depleted or functionally impaired cells. We further find C53 co-localizes with Plk1 during

various stages of M phase. Multiple evidence suggested that C53 is a possible Plk1

substrate. Surprisingly, C53 interacts directly with the kinase domain of Plk1, but not the

polo-box domain. Such an unprecedented pattern of interaction suggests C53 may also

be involved in Plk1 activation.

Plk1 is an important mitotic kinase whose function is crucial for the orderly

progression of M phase [45].   At the onset of mitosis, Plk1 phosphorylates multiple

substrates to promote the G2 to M transition. During early M phase, Plk1-mediated

phosphorylation of various centrosomal and microtubule associated proteins is crucial to the assembly of focused, functional bi-polar spindle [89]. In late M phase, Plk1 activity is needed for the separation of sister chromatids. During cytokinesis, Plk1 phosphorylates NudC, which is important for the completion of cytokinesis [64]. Our data showed C53 is a centrosome-associated protein, and is a possible Plk1 substrate. Depletion of C53 results in multiple M phase defects resembling those caused by Plk1 knockdown. Therefore, Plk1 mediated phosphorylation of C53 may be crucial to its function during M phase.

Interestingly, as a result of recent vigorous research on Plk1, the list of Plk1 kinase substrates with prominent mitotic functions keeps growing. Oshimori *et al* recently reported that a novel Plk1 substrate Kizuna is important for the maintenance of pericentriolar material in prometaphase, and depletion of this protein caused early fragmentation of pericentriolar material, which then led to the formation of fractured and multi-polar spindles [126]. Plk1-mediated phosphorylation of Kizuna is essential for its function [126]. Similar to Kizuna, C53 is also a centrosomal-associated protein and is a possible Plk1 substrate. Interestingly, unlike depletion of Kizuna, which leads to multi-polar (>2) spindles, C53 depletion lead to mono-polar spindles. Such a phenomenon will be further investigated and it will help explain why Plk1 is essential for the formation of functional, bi-polar spindles.

Sequence analysis indicates that regions around Thr479 (EKT^{479}K) and Ser491 (DIS^{491}K) on the C-terminus of C53 fit as Plk1 consensus sequence and are possible Plk1 phosphorylation sites. These two regions are conserved through evolution. The favorable Plk1 consensus sequence is D/E-X-S/T followed by a hydrophobic residue [49]. Both Thr479 and Ser491 of C53 are followed by either Lys or Arg that are charged

residues, which is very similar to another Plk1 substrate NudC [64]. Therefore, we expect both Thr479 and Ser491 to be good Plk1 sites. Our lab plans to use site-directed mutagenesis to test whether these two residues are Plk1 phosphorylation sites.

One of the most interesting phenotypes caused by C53 depletion is the nuclear deformation observed in a majority of C53-depleted cells. Nuclear deformities, such as poly-lobed, fragmented, multi-nucleated and grossly enlarged nuclei have been widely observed in many types of human tumors. Although such observations were made many decades ago, the underlying molecular mechanism is still unknown [92]. *In vitro* knock-down of Plk-1 could result in such nuclear deformities, however, Plk-1 down-regulation is not widely observed in human cancers. There are two possible explanations for this: 1) Cancer cells have a high demand for mitotic kinase activity. Therefore, instead of being down-regulated, Plk-1 is often up-regulated in human tumors. 2) Plk-1 activity is so extensively involved in mitosis, that complete depletion of Plk-1 often arrests cancer cells at mitosis and kill cells via mitotic cell death. Under such circumstances, very few cells will complete mitosis and give rise to daughter cells manifesting deformed nuclei.

However, it is still possible that impairment of Plk-1 function to a certain level or at a specific mitotic stage (e.g., depletion of a certain Plk-1 substrate) could contribute to such phenotypes. Our data indicate C53 depletion leads to severe nuclei deformities. Unlike Plk-1, complete depletion of C53 does not arrest cells in mitosis or causes massive mitotic cell death. Instead, a majority of cells go through mitosis and give rise to daughter cells manifesting deformed nuclei (Figure 21, 22 and data not shown). It is interesting to see whether there is connection between C53 deregulation and nuclear deformities observed in human tumors. Interestingly, 20%-30% of human liver cells are

bi-nucleated, and in comparison to other organs, liver expresses relatively low level of C53. Therefore, differential regulation of C53 may play a role in development as well.

Multiple data suggest human Plk-1 undergoes "T-loop" activation. It is activated by phosphorylation on Thr210 within the kinase domain. Mutation of this threonine residue to asparate mimics T-loop phosphorylation and confers substantial kinase activity. However, the *polo-box* domain of Plk-1 interacts with its N-terminal kinase domain, and is thought to prevent substrate binding or kinase activation [45]. Phosphorylated ligands on Plk-1 substrate are thought to occupy polo-box domain and reverse such inhibition [45,88]. However, whether this event occurs before or after T-loop activation is not known. Also, the critical events leading to T-loop activation are still not well understood.

Our studies of C53 yielded some interesting results. First, C53 interacts directly with the kinase domain of Plk-1. Such an interaction is unprecedented for Plk-1 interacting protein. Interestingly, as shown in Figure 28, C53 binding of full-length Plk-1 is not attenuated by the presence of its polo-box domain. It is possible C53 competes with the *polo-box* domain for the kinase domain, allowing certain kinases to phosphorylate Plk-1 on Thr210 and thus facilitating Plk-1 activation. Indeed, in the presence of overexpressed C53, the *polo-box* domain of Plk-1 was no longer able to interact with the N-terminal kinase domain. These experiments suggest C53 may affect Plk-1 activation. In support of such a hypothesis, we found the phenotypes of C53 depletion much like those conferred by moderate Plk-1 inhibition. Of note, Plk-1 activation leads to cyclin B1 phosphorylation and APC activation, two processes eventually resulting in cyclin B1 nuclear accumulation and degradation. In C53 overexpressing HeLa cells, we observed both cyclin B1 nuclear accumulation and

degradation (Figure 10B and Figure 11A and C). This indicates that overexpressed C53 promotes Plk-1 activation. Taken together, these results suggest that by interacting directly with the kinase-domain of Plk-1, C53 may antagonize the inhibitory effects of polo-box domain and facilitates Plk-1 activation.

Part III

3.3 Caspase cleavage of C53 and its role in G2/M checkpoint and mitosis

3.3.1 C53 is cleaved by caspase during cell death

Caspases are an evolutionarily conserved family of cysteine proteases that catalyze the cleavage of target proteins at sites downstream of specific aspartic acid residues, and play a pivotal role in both initiation and execution of apoptosis [127]. It is generally believed that there are two major apoptotic signaling pathways: the death receptor-mediated pathway (extrinsic) and the mitochondria-mediated pathway (intrinsic) [127]. Crosstalk and synergy between these two pathways have been reported in many experimental systems [128]. Caspases cleave various proteins during cell death [128] [97,129,130]. Many of these cleavage events carry functional importance for cell death. For example, caspase 8 cleavage of Bid couples extrinsic and intrinsic pathways together and propagates death signaling [96]. Caspase cleavage of gelsolin was thought to be responsible for the cellular shrinkage during apoptosis [131]. However, there are examples of caspase cleavage events that do not seem to participate directly in death process [132]. Such cleavages were though to be bystander effects. Nonetheless, identification and characterization of novel caspase substrates should help further advance our understanding of the cell death process.

C53 was first identified by Dr. Honglin Li as a possible caspase substrate using an *in vitro* expression cloning strategy [97]. Briefly, a small pool mouse spleen cDNA library was transcribed and translated in the presence of ^{35}S-methionine. The radioactively labeled protein pools were incubated with bacterial lysates containing either active caspases or control plasmid, and the cleavage reactions were subsequently

analyzed by SDS-PAGE. 1800 cDNA small pools (about 100 clones per pool) were screened, and the individual cDNA clones encoding candidate substrates were isolated and identified. Among them, BID has been demonstrated to be a proximal substrate of caspase-8 in the Fas signaling pathway [96]. In the same screening, C53 was isolated in pool #1790. The human C53 cDNA encodes a putative protein of 506 amino acid residues with predicted molecular weight (MW) 57 kDa, and migrates as a 66 kDa band on SDS-PAGE (Figure 27A). As shown in Figure 29A, full-length C53 protein was fully cleaved by caspase-3 into 4 fragments (33kDa, 32kDa, 29kDa and 25kDa) and partially cleaved into two fragments (38kDa and 32kDa) by caspase-8, but is resistant to caspase-2. Interestingly, C53 was also efficiently cleaved into two fragments (35kDa and 22kDa) by m-calpain, a calcium-activated cysteine protease, indicating that C53 activity may be regulated by multiple proteases.

We next examined whether endogenous C53 is cleaved during cell death. As shown in Figure 29B, anti-C53 antibodies specifically recognized a 66 kDa protein, which was processed to multiple fragments as cells underwent apoptosis. The time course of C53 cleavage was comparable with activation of caspase-7 and –8 (Figure 29B). This result demonstrates that endogenous C53 is indeed cleaved during apoptosis. In TNFα-induced apoptosis of HeLa cells, multiple cleavage fragments (45kDa, 33kDa, 32kDa, 29kDa and 25kDa) were derived from C53 (indicated by stars in Figure 29B). Fragments of 33kDa, 32kDa, 29kDa and 25kDa fragments appeared to be caspase cleavage products, while a 45kDa product appeared in late time points, indicating that it may be generated by other proteolytic events in addition to caspase cleavage. The pattern of *in vivo* cleavage of C53 was similar to that of *in vitro* caspase-3 cleavage (Figure 28B), indicating that C53 may be the substrate of caspase-3 or
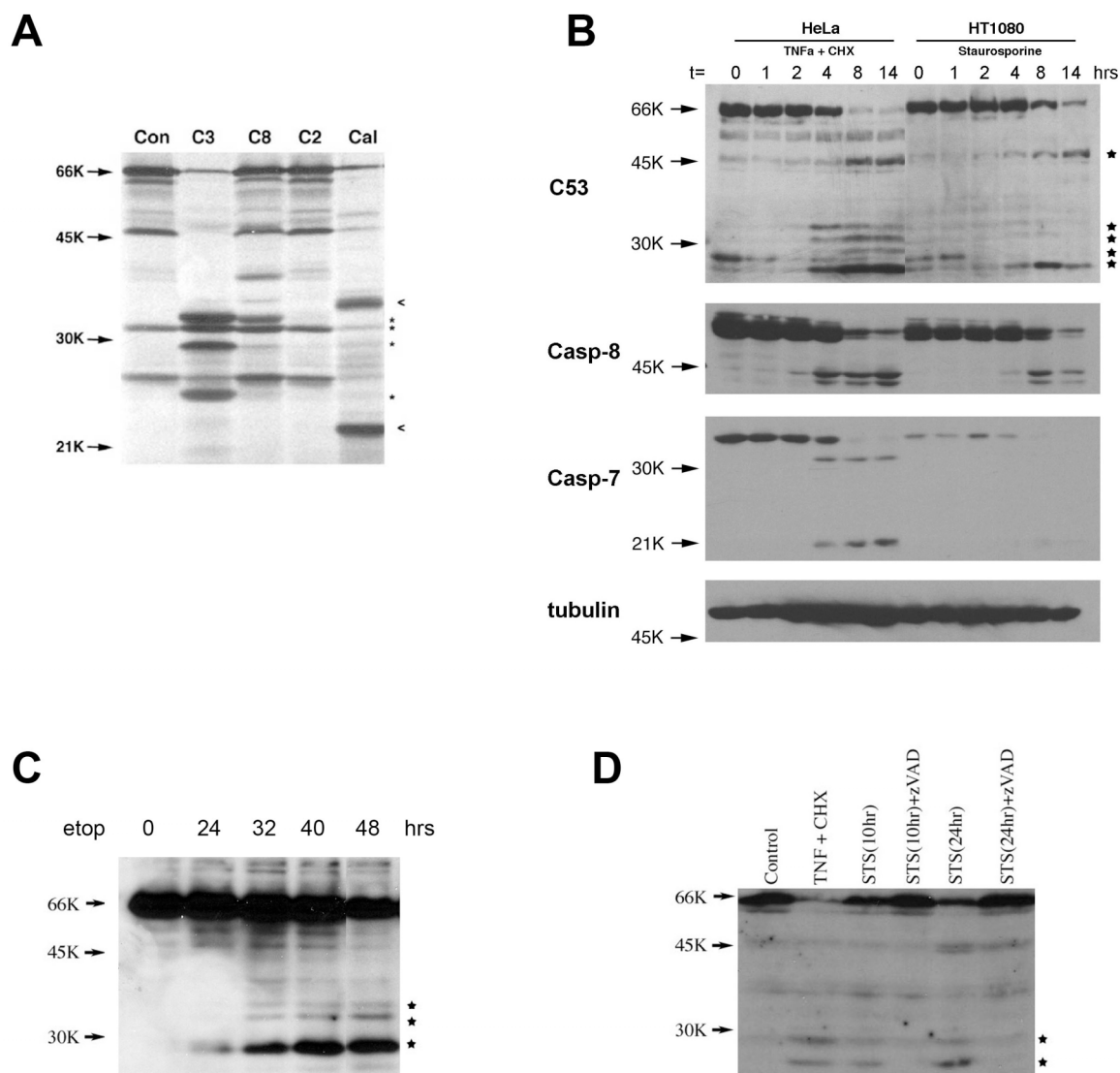
Figure 29 C53 is a caspase substrate

A. *In vitro* cleavage of C53. ^{35}S-labeled C53 was incubated with control bacterial lysate (con.), caspase-3 (C3), caspase-8 (C8), caspase-2 (C2) and m-calpain (Cal) at 30°C for 1 hour. 5 mM Ca^{2+} was present in calpain cleavage. Caspase-3 cleavage products are indicated by stars, while calpain cleavage products are marked by <. Experiment was done by Dr. Honglin Li.

B. Endogenous C53 is cleaved in TNFα and staurosporine-induced apoptosis. HeLa cells were treated with TNFα (10 ng/ml) and cycloheximide (CHX, 10 μg/ml) and HT1080 cells were treated with 1 mM staurosporine for indicated periods of time. The samples were subjected to immunoblotting with various antibodies (C53, caspase-7 and

–8, tubulin). Multiple cleavage fragments (45kDa, 33kDa, 32kDa, 29kDa and 25kDa) of C53 are marked by stars. Experiment was done by Dr. Shouqing Luo.

C. HeLa cells were treated with etoposide (20 μM) for indicated periods of time, and cell lysates were subjected to immunoblotting using anti-C52 monoclonal antibody 2H2.

D. The cleavage of endogenous C53 is inhibited by pan-caspase inhibitor zVAD-fmk. HeLa cells were treated with 1 μM staurosporine for various times in the absence or presence of zVAD-fmk (100 μM). C53 cleavage products are marked by stars. Done by Dr. Shouqing Luo.

 caspase-3 like caspases. The cleavage pattern of C53 was slightly different in staurosporine-induced apoptosis of HT1080 cells (Figure 29B), in which 25 kDa fragment was the major cleavage product. Moreover, during etoposide and taxol-induced cell death, we were also able to observe the 33kDa, 29kDa and 25kDa fragments (Figure 29C and data not shown). To further confirm that C53 was indeed cleaved by caspases, we tested whether zVAD-fmk, a pan-caspase inhibitor, could inhibit C53 cleavage *in vivo*. As shown in Figure 27D, 100µM zVAD-fmk effectively blocked C53 cleavage in staurosporine-induced apoptosis of HeLa cells. The cleavage of C53 was also fully inhibited by zVAD-fmk in etoposide-induced apoptosis of HeLa cells (data not shown). These results strongly suggest that C53 is a novel caspase substrate and is likely cleaved by caspase-3 or caspase-3-like caspases during apoptosis.

To elucidate the function of C53 cleavage fragments, we next mapped the caspase cleavage sites using two standard methods: terminal tagged fusion proteins and site-specific mutagenesis. C-terminal Flag-tagged C53 generated three fragments (33kDa, 29kDa and 25kDa) recognized by anti-Flag M2 antibody during apoptosis, suggesting that these fragments contain the C-terminal portion of C53 (data not shown). Furthermore, we generated a polyclonal peptide antibody against N-terminal peptides of C53, as well as monoclonal antibody against C-terminus of C53, and used them to map the C53 cleavage *in vivo*. As shown in Figure 30A and B, the peptide antibody against the N-terminus specifically recognized a 32kDa cleavage product (designated as C53-N), while C-terminal monoclonal antibody recognized 33kDa, 29kDa and 25kDa cleavage products (designated as C53-C1, C2, and C3, respectively). This result demonstrates that both N and C-terminal cleavage products exist in dying cells, and

Figure 30 Sequential cleavage of C53 by caspase-3

A and B. HeLa cells were treated with TNFα (10 ng/ml) and cycloheximide (CHX, 10 μg/ml) for periods of time as indicated, and the samples were immunoblotted with anti-N-terminal peptide antibody (A) and anti-C-terminal C53 monoclonal antibody 2H2 (B). The arrowheads indicate C53 and its cleavage products, while the asterisk marks non-specific bands recognized by the anti-N-terminal peptide antibody. Arrow in (B) indicates a slower migratory form of C53-C3.

C. Determination of caspase-3 cleavage sites. Specific aspartic acid residues were mutated to glutamate, respectively. Mutations were confirmed by DNA sequencing. ^{35}S-labeled wild-type C53 and its mutants were incubated with caspase-3, and the cleavage products were analyzed by SDS-PAGE and autoradiography.

D. Time courses of *in vitro* cleavage of C53 and C53-C1. ^{35}S-labeled C53 and C53-C1 (residues 269-506) were incubated with caspase-3 at 30°C for various periods of time as indicated. Identities of the cleavage products are indicated. Experiments in (C) and (D) were done by Dr. Shouqing Luo.

E. Sequential cleavage model of C53 and the names of constructs that were used in this study.

there are multiple cleavage sites on the C-terminal part of C53. Based upon the sizes of the cleavage fragments, we postulated that possible cleavage sites were in the middle region of C53 protein. Sequence analysis indicated that there are 5 potential caspase cleavage sites in the middle region of C53. As shown in Figure 30C, triple mutations at residues $D^{268}/D^{282}/D^{311}$ completely blocked multiple caspase-3 cleavage events, suggesting that these three sites are caspase cleavage sites (Figure 30D). The triple mutant was also resistant to proteolysis *in vivo* when cells underwent apoptosis (data not shown).

Interestingly, during TNFα-induced HeLa cell death, the C1 fragment was the major caspase cleavage product in early time points (Figure 30B). Later on, the C1 fragment diminished, while C2 and C3 fragments increased. This pattern suggests C53 is sequentially cleaved during TNFα-induced cell death. The time course of *in vitro* cleavage of full-length C53 by caspase-3 also indicates that C53 is cleaved in a sequential manner. This model of sequential cleavage was further supported by the observation that cleavage of C53-C1 by caspase-3 generated C53-C2 and C3 (Figure 30D, right). Therefore, we proposed a model of C53 cleavage during TNFα-induced apoptosis. Illustrated in Figure 30E, C53 is first cleaved at D268, which generates C53-N and C53-C1. C53-C1 was then cleaved at D282 and D311 to generate C53-C2 and C53-C3. In late apoptosis, C53-N and C53-C3 are the major forms of cleavage products.

3.3.2 Caspase cleavage of C53 enhances its ability to promote etoposide-induced cell death

Since C53 sensitizes cells to etoposide, we next asked whether caspase cleavage of C53 affects its ability to promote etoposide-induced cell death. We cloned D^{268} E /D^{282} E /D^{311} E triple mutant C53 (mt C53) and various C53 cleavage fragments into pCMV-5a vectors, transfected them into HeLa cells, and tested whether they could promote etoposide-induced cell death. As shown in Figure 31A, less than 10% of

control transfected cells were apoptotic after 24 hours of etoposide treatment. When cells were transfected with mt C53 that could not be cleaved by caspases, we saw slightly higher percentage of cell death (19%). Transfection of wt C53 further enhanced the killing to about 30%. This suggests caspase cleavage of C53 may enhance its ability to promote etoposide-induced cell death. Indeed, one of the C-terminal cleavage products, C53-C1, was most potent in promoting etoposide-induced cell death (47%, Figure 31A). Of note, C53-C2 was similar to wt C53 in its ability to promote etoposide-induced cell death, while C53-N and C53-C3 could not promote such killing at all (Figure 31A). These observations prompted us to propose that, during etoposide-induced cell death, caspase cleavage of C53 generates C53-C1, which may carry enhanced ability to promote etoposide-induced cell death.

We then compared the interaction between Myc-Chk1 and different C53 fragments. As shown in Figure 31B, C53-N and C53-C3 did not interact with Myc-Chk1. Full length C53 and C53-C2 interacted with Myc-Chk1 at similar strength. C53-C1 showed the strongest interaction with Myc-Chk1. Interestingly, the ability of different fragments to interact with Chk1 correlates with their ability to promote etoposide-induced cell death. For example, C53-N and C53-C3 does not interact with Chk1, and they cannot sensitize HeLa cells to etoposide (Figure 31A). This demonstrates the functional importance of C53-Chk1 interaction. We also mapped the C53-Chk2 interaction (Figure 31C). Similarly, C53-N and C53-C3 did not interact with Myc-Chk2, while full-length C53 and C53-C2 interacted with Myc-Chk2 with similar avidity. C53-C1 still interacted with Myc-Chk2, although this interaction was not stronger than that of full-length C53 and Myc-chk2. As mentioned before, Chk1 and Chk2 are very different in their structures. This may explain the difference of C1-Chk1 and C1-Chk2 interactions.
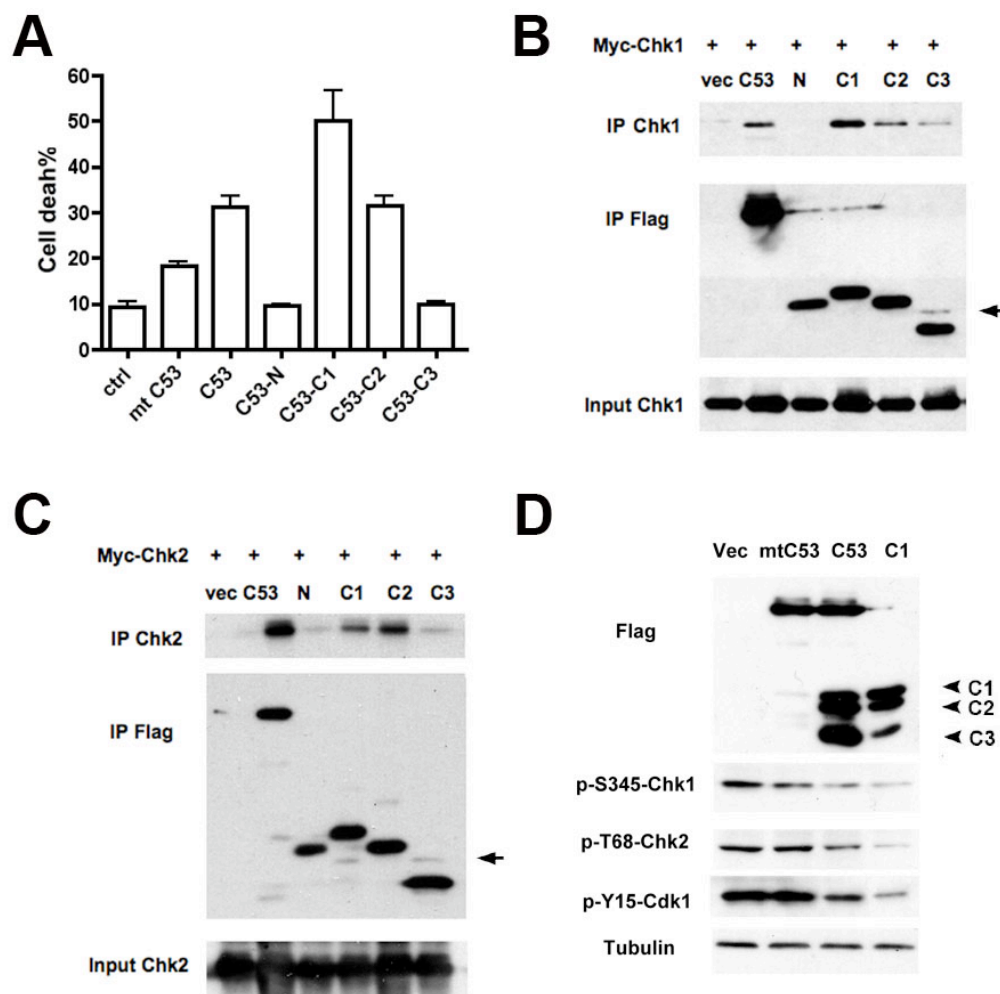
Figure 31 C53-C1 shows enhanced ability to suppress G2/M checkpoint

A. Ability of C53 fragments to sensitize HeLa cells to etoposide. 1.5×10^5 HeLa cells were transfected with 1.2 μg of H2B-GFP together with 0.6 μg of control or indicated Flag-tagged C53 constructs. Cells were then treated with 20 μM etoposide for 24 hours and percentage of cell death was analyzed using trypan blue exclusion assay. Results were mean ± S.D., with three independent repeats. *Ctrl*, control.

B and C. Mapping of C53-Chk1/Chk2 interactions. 1×10^6 HeLa cells were transfected with 3 μg of control or indicated Flag-tagged C53 constructs, together with 3 μg of Myc-Chk1 (B) or Myc-Chk2 (C). 24 hours later, cells lysates were subjected to immunoprecipitation using anti-Flag Beads. The presence of Myc-Chk1 or Myc-Chk2 was examined using immunoblotting of Myc. Arrows indicate a slower migratory form of C53-C3. *Vec*, vector control.

D. C53-C1 is more potent in suppressing G2/M checkpoint. 1.5×10^5 HeLa cells were transfected with 1.2 μg of H2B-GFP together with 0.6 μg of control or Flag-tagged mt, wt C53 or C53-C1. Cells were then treated with 20 μM etoposide for 24 hours and cell lysates were subjected to immunoblotting of indicated antibodies. During etoposide-induced cell death, wt C53 was cleaved into C1, C2 and C3 (indicated by arrowhead), while C1 was cleaved into C2 and C3. mt C53, which has all three caspase cleavage sites mutated, were not cleaved. *Vec*, vector control.

We further examined whether C53-C1 confers stronger suppression of G2/M DNA damage checkpoint than full-length C53. As shown in Figure 31D, when expressed in HeLa cells, C53-C1 was more potent in inhibiting G2/M checkpoint than full-length C53 and mt C53. This explains why C53-C1 is the most effective in promoting etoposide-induced HeLa cell death.

It has been previously reported that the death receptor pathways, in particular those induced by TRAIL(TNFα-related apoptosis inducing ligand), are essential for etoposide-induced cell death in several studies [133,134]. Etoposide treatment causes upregulation of DR4 and DR5 (death receptor 4 and 5), two death receptors for the TRAIL ligand, which were thought to elicit the TRAIL-induced death receptor pathway, and contributed to etoposide-induced cell death [133]. Several more lines of evidence suggest that the TRAIL pathway is important for etoposide-induced cell death. In the studies by Gibson *et al*, when a soluble decoy receptor for TRAIL was added to inhibit the TRAIL pathway, etoposide-induced mitotic cell death was significantly reduced [133]. Various inhibitors of the death pathway, such as dominant negative FADD and chemical inhibitors of caspase 8, were also shown to inhibit etoposide-induced cell death [133,135]. Based on this evidence, we then examined whether the TRAIL pathway participated in the breakdown of the G2/M checkpoint during etoposide-induced cell death. Shown in Figure 32A, cells were pre-treated with etoposide for 18 hours to establish a G2 arrest. Addition of TRAIL rapidly abolished etoposide-induced G2 arrest. Cells went into mitosis and subsequently died during mitosis. This experiment suggests TRAIL induced caspase activation leads to cleavage of certain protein, which then contribute to the G2/M checkpoint breakdown and mitotic entry. One such interesting candidate is C53, since we've demonstrated that caspase cleavage product C53-C1 is
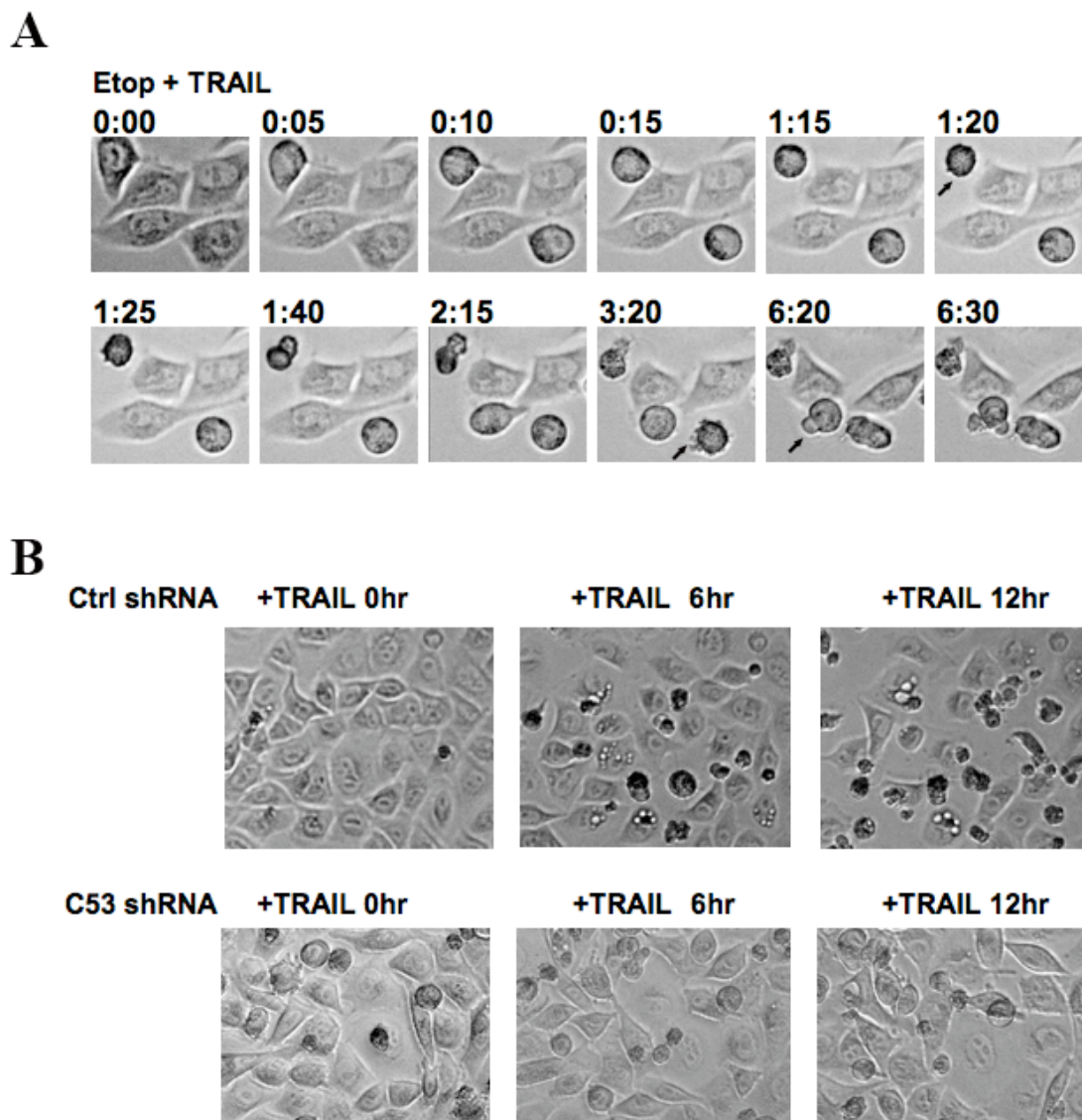
Figure 32 C53 depletion inhibits TRAIL induced mitotic cell death in etoposide-treated HeLa cells

A. TRAIL promotes mitotic cell death in etoposide-treated cells. HeLa cells were treated with etoposide (20 μM) for 18 hours to establish G2 arrest. 25 ng/ml TRAIL was added to the medium. Time-lapse videotaping starts approximately 4 hours after the addition of TRAIL. Arrows indicate sudden cell death after several hours of mitotic arrest. *Etop,* etoposide.

B. TRAIL cannot promote mitotic cell death in C53 depleted cells. HeLa cells were transfected with control or C53 shRNA vectors and selected with puromycin (2 μm/ml). 48 hours later, cells were treated as described in (A), and time-lapse video microscopy was used to examine cell death response. *Ctrl,* control.

more potent in promoting etoposide-induced cell death. To test this possibility, we

depleted C53 from HeLa cells, pre-treated them with etoposide, and examined their

response to TRAIL. As shown in Figure 32B, control transfected cells rapidly entered

mitosis and died after the addition of TRAIL. However, when C53 was depleted, TRAIL

could no longer abolish etoposide-induced G2 arrest in HeLa cells. This suggests

TRAIL induced C53 cleavage may be important for G2/M checkpoint breakdown and

subsequent cell death. Upon etoposide treatment, chromosome breaks are induced and

G2 arrest is established. Meanwhile, DR4 and DR5 are upregulated. Eventually, this

will activate the TRAIL pathway. Active caspases cleave C53 into C53-C1, which then

participates in the G2/M checkpoint breakdown. Cells proceed into mitosis and

subsequently die during mitosis. More experiments are needed to support this model

and will be discussed later.

3.3.3 C53-C3 fragment interferes with mitosis and causes nuclear deformation

In previously described experiments, we showed C53 plays important roles

during M phase. We next examined how caspase cleavage might affect C53's function

during mitosis. Interestingly, when we overexpressed the major C-terminal cleavage

fragment C53-C3, there was an increased percentage of cells manifesting poly-lobed or

fragmented nuclei (Figure 33A). C53-C1 and C53-C2 did not cause similar defects (data

not shown). The poly-lobed and fragmented nuclei conferred by C53-C3 overexpression

resembled those caused by C53 depletion (Figure 23). This suggests 1) like C53

depletion, C53-C3 may interfere with mitosis; and 2) C53-C3 may act as a dominant

negative inhibitor of endogenous C53. Interestingly, when expressed in HeLa cells,

C53-C3, but not other truncated forms of C53, constantly showed an extra slower
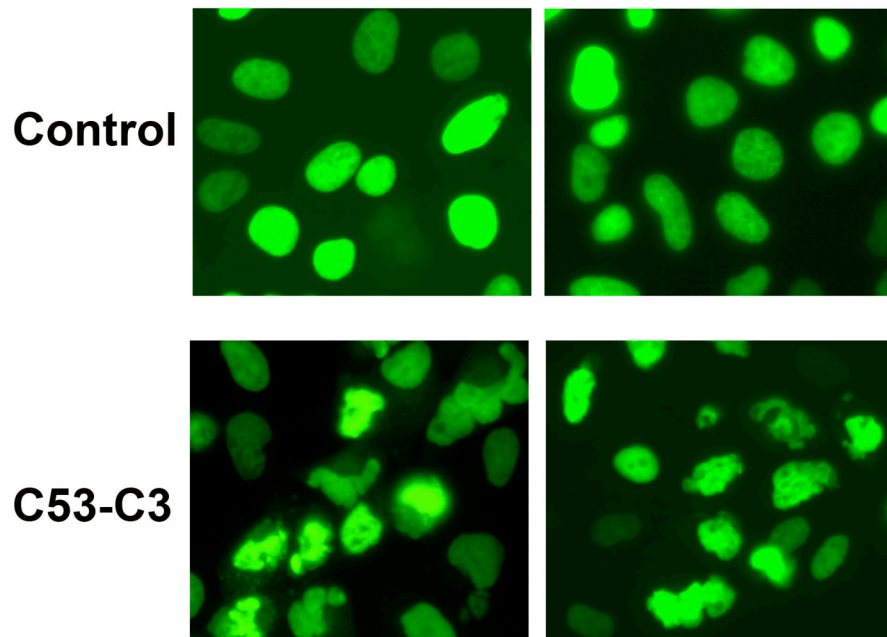
Figure 33 Overexpression of C53-C3 causes nuclear deformities

1.5×10^{5} HeLa cells were transfected with 0.6 μg of control or C53-C3 constructs together with 1.2 μg of H2B-GFP. 24 hours later, cells were analyzed. Pictures were taken using Openlab software. Green signals (H2B-GFP) show the shapes of nuclei.

migratory form on Western Blot (Figure 31B and C, arrow). This indicates post-translational modification of C53-C3, possibly phosphorylation. Of note, the putative Plk1 consensus sites (EKT^{479}K and DIS^{491}K) locate within this C3 fragment. It is possible that truncation of C53 into C3 fragment makes these consensus sites more accessible to Plk1 phosphorylation. Therefore, overexpressed C53-C3 fragment may compete with endogenous C53 for Plk1 phosphorylation. As a result, endogenous C53 could not function properly, and aberrant mitosis follows.

Conclusion and Discussion

In this section we described caspase cleavage of C53 and its possible impact on mitosis and cell death. Human C53 has three caspase cleavage sites, which are cleaved by caspase during cell death. In TNFα-induced HeLa cell death, we observed sequential cleavage of these three caspase sites. In taxol and etoposide-induced HeLa cell death, we did not observe such apparent sequential cleavage. Nonetheless, all three caspase sites were processed and all three C-terminal cleavage fragments were observed. Cleavage of C53 into C53-C1 may enhance its ability to suppress the G2/M DNA damage checkpoint. Such cleavage may help further abolish the G2 arrest and promote mitotic cell death. Interestingly, two other proteins involved in G2/M checkpoint, wee1 kinase and claspin, have also been reported to be cleaved by caspase during cell death [136,137]. Wee1 is the kinase that phosphorylates and inhibits Cdk1. Zhou *et al* showed wee1 is cleaved by caspase during cell death [136]. Claspin is needed for ATR-mediated phosphorylation of Chk1 at Ser345. Recently Clarke *et al* reported that claspin is cleaved by caspase 7 during etoposide-induced cell death [137]. Similar to caspase cleavage of C53, both these two cleavage events seem to promote the breakdown of

G2/M checkpoint. This suggests a common theme for G2/M checkpoint breakdown during cell death. Cleavage of C53 and claspin suppresses the function of Chk1 and Chk2, while cleavage of wee1 reduces the inhibitory phosphorylation on Cdk1. Together, these cleavage events should cause a rapid release from G2 arrest and cells may utilize such a mechanism to ensure mitotic cell death.

Our data show C53-N and C53-C3 are the major cleavage fragments during late time points of cell death. So far, we have not identified the functions associated with C53-N. When overexpressed, C53-C3 caused nuclear deformities similar to those induced by C53 depletion. This suggests: 1) like C53 depletion, overexpression of C53-C3 may cause defects during M phase; 2) C53-C3 may act as dominant negative inhibitor of endogenous C53. Both of the potential Plk1 phosphorylation sites, Thr479 and Ser491 locate within the C53-C3 fragments. When C53-C3 is overexpressed, we consistently observed a slower migratory form (Figure 31B and C, arrow), indicating post-translational modifications, possibly phosphorylation. Interestingly, such a slower migratory form was also observed during cell death (Figure 30B, arrow). It is possible that when C53 is cleaved into C53-C3, the Plk1 phosphorylation sites are made more accessible to Plk1. C53-C3 may compete with C53 for Plk1 phosphorylation and thereby suppress C53's function during M phase. Under normal conditions, C53-C3 may cause aberrant mitosis and nuclear deformity. During mitotic cell death, the cleavage of C53 into C53-C3 may then further ensure cells cannot achieve a successful mitosis and escape from mitotic cell death. Further experiments will be done to test this hypothesis.

Summary

In this dissertation I describe our lab's initial characterization of C53's function in cell cycle and cell death. First, C53 suppresses the G2/M checkpoint via antagonizing Chk1 and Chk2. In DNA damage response, C53 overexpression promotes cell death, while C53 depletion reduces the cell death response [138]. During unperturbed cell cycle, C53 overexpression causes uneven chromatin condensation, while C53 depletion delays mitotic entry. Second, C53 interacts with Plk1 and also plays important roles during mitosis. Depletion of C53 results in multiple mitotic defects, leading to the formation of irregularly shaped daughter nuclei. C53's localization at centrosomes may serve as a converging point for these two major functions of C53. The centrosome is a signaling platform where many regulators of cell cycle reside, and several centrosome-associated proteins are known to play roles in both G2/M transition and M phase. For example, Aurora A, a centrosome-associated kinase, is important for both mitotic entry and spindle bi-polarity [123,124]. Likewise, Plk1, the key mitotic kinase orchestrating multiple M phase events, also promotes mitotic entry by regulating cyclin B1, Cdc25, Wee1 and Myt1 [45]. Furthermore, centrosome-associated Chk1 was shown to prevent premature mitotic entry, and recently Tang *et al* showed Chk1 may play some role in M phase as well [139]. In their study, Chk1 depleted cells exhibited kinetochores defects and chromosomes were misaligned during mitosis. Similar to these molecules, C53 is a centrosome-associated protein, and regulates both mitotic entry and M phase progression. At the G2/M boundary, C53 antagonizes checkpoint kinases to facilitate the initial activation of Cdk1/cyclin B1 at the centrosome. Immediately following this,

C53 may cooperate with Plk1 to promote centrosome separation, which is crucial for orderly progress of various M phase events. One interesting thought is whether Plk1-mediated phosphorylation of C53 affects the C53-Chk1/2 interaction and contributes to mitotic entry. Once we identify Plk1's phosphorylation site(s) on C53, we can use the corresponding mutation constructs to test such hypothesis. Taken together, our study of C53 contributes to an emerging view of centrosome as a cellular organelle important for both mitotic entry and M phase progression.

The functions of C53 during G2/M transition and mitosis seem to be regulated by caspase cleavage. One of the intermediate caspase cleavage products, C53-C1, exhibited enhanced ability to suppress the G2/M checkpoint and promote etoposide-induced cell death. Moreover, overexpression of C53-C3 induced nuclear deformities, indicative of aberrant mitosis. Taken together, these two observations fit into an interesting model of caspase modulation of C53's function. We propose that during DNA damage response, basal caspase activity cleaves C53 into C53-C1, which promotes G2/M checkpoint breakdown and mitotic entry. While these cells are arrested at mitosis, C53-C1 is further cleaved into C53-C3, a fragment capable of interfering with normal mitosis, and such an event will further ensure that cells will not have a successful outcome of mitosis and escape cell death.

Our initial study of C53 found it to promote genotoxin-induced cancer cell death. However, further work is needed to test whether C53 is an oncogene or a tumor suppressor gene. Depending on the genetic context, a given gene can either sensitize or desensitize cancer cells to anti-cancer drugs. For example, Chk2 is an established tumor suppressor gene. In p53 +/+ cancer cells, an RNAi screening identified Chk2 as a chemo-sensitizer, while in p53-/- cells, Chk2 was identified as a chemo-desensitizer

(personal communication with Dr. Michael Hemann at Massachusetts Institute of

Technology). These data demonstrate the difficulty of predicting a gene's role in

tumorigenesis based on their ability to promote genotoxin-induced cell death.

Nonetheless, other arguments can be made on this question. For example, Chk1 and

Chk2 are established tumor suppressors, and since C53 can antagonize Chk1 and

Chk2, it may act as an oncogene. However, C53's function during mitosis further

complicates this question. When C53 was depleted, aberrant mitosis was observed,

which led to the formation of deformed (and probably aneuploid) nuclei. This suggests

that loss of C53 may contribute to genetic instability, which may then facilitate

tumorigenesis. Considering this, C53 may act as tumor suppressor gene as well. In

summary, our data so far cannot help us predict C53's role in tumorigenesis. Such a

question will have to be answered by analyzing real tumor samples, and by studying the

phenotypes of C53-knockout mice. We have obtained necessary tools (e.g., monoclonal

antibodies, ES cell lines) for these projects and will be able to answer this question in the

future.

Finally, our studies of C53 bring some interesting thoughts on C53's function in

post-mitotic cells. As mentioned earlier, C53 is a ubiquitously expressed gene, and

many tissues expressing C53 are post-mitotic. One such example is the brain, which

expresses very high levels of C53. Of note, C53 was originally identified as an

interacting protein for p35, which is the activator of Cdk5, a neuronal Cdk1-like kinase.

Hyperactivity of Cdk5/p35 has been implicated in the pathogenesis of neurodegenerative

diseases such as Alzheimer's disease. In addition, re-activation of cell cycle-associated

cyclin dependent kinases has been shown to precede the formation of degenerative

lesions in Alzheimer's disease [140]. Our findings that 1) C53 promotes Cdk1 activity

and 2) caspase cleavage of C53 enhances its ability to promote Cdk1 activation during DNA damage response give rise to several interesting questions.

First, is C53 upregulation or cleavage involved in Cdk1 reactivation in Alzheimer's disease? Recently we have obtained several monoclonal antibodies that work well in immunostaining and can distinguish between full-length C53, C53-C1 and C53-C3. These antibodies will serve as valuable tools to analyze potential C53 upregulation/cleavage in Alzheimer's disease samples. Interestingly through our collaboration with Dr. Francis Szele's lab, it was found C53 may be upregulated around cortical aspiration lesions. Immunostaining of Alzheimer's disease samples using our anti-C53 antibodies should address whether upregulation/cleavage of C53 is involved in Alzheimer's disease and may bring some interesting results.

Second, does caspase/calpain cleavage of C53 affect Cdk5/p35 activity? We showed that C53 is cleaved by caspase and calpain *in vitro*. Both caspase and calpain are implicated in the pathogenesis of Alzheimer's disease. It remains interesting to see how caspase/calpain cleavage of C53 affects its binding with p35, and whether such cleavage affects the kinase activity of Cdk5/p35.

Third, are caspase cleavage fragments of C53 incorporated in neurofibrillary tangles (NFTs)? During apoptosis, C53-N and C53-C3 are the major cleavage products of C53. Interestingly using both GFP-fusion protein approach and electromicroscopy, we found that overexpressed C53-N and C53-C3 formed protein aggregates around nuclei in HeLa cells (data not shown). A prominent pathological feature of Alzheimer's disease is the neurofibrillary tangles, which consist of insoluble fibers formed by pathological protein aggregates. The microtubule-associated protein, tau, is a major component of neurofibrillary tangles. Cdk5-mediated hyperphosphorylation of tau

deregulates its function and may contribute to the formation of neurofibrillary tangles [141, 142]. It is tempting to see whether caspase cleavage fragments of C53 are also incorporated into these neurofibrillary tangles.

In summary, our studies demonstrated C53's functions during G2/M transition and M phase, both of which seem to be modulated by caspase cleavage of C53. After further analysis of C53's function in both mitotic and post-mitotic cells, we will be able to have more knowledge of this novel gene's potential roles in tumorigenesis and degenerative diseases, which will lead to a better understanding of this interesting new gene.

References

1. Parrilla-Castellar ER, Arlander SJ, Karnitz L: **Dial 9-1-1 for DNA damage: the Rad9-Hus1-Rad1 (9-1-1) clamp complex**. *DNA Repair (Amst)* 2004, **3**:1009-1014.

2. Stracker TH, Theunissen JW, Morales M, Petrini JH: **The Mre11 complex and the metabolism of chromosome breaks: the importance of communicating and holding things together**. *DNA Repair (Amst)* 2004, **3**:845-854.

3. Gatei M, Sloper K, Sorensen C, Syljuasen R, Falck J, Hobson K, Savage K, Lukas J, Zhou BB, Bartek J, *et al*.: **Ataxia-telangiectasia-mutated (ATM) and NBS1-dependent phosphorylation of Chk1 on Ser-317 in response to ionizing radiation**. *J Biol Chem* 2003, **278**:14806-14811.

4. Liu Q, Guntuku S, Cui XS, Matsuoka S, Cortez D, Tamai K, Luo G, Carattini-Rivera S, DeMayo F, Bradley A, *et al*.: **Chk1 is an essential kinase that is regulated by Atr and required for the G(2)/M DNA damage checkpoint**. *Genes Dev* 2000, **14**:1448-1459.

5. Matsuoka S, Huang M, Elledge SJ: **Linkage of ATM to cell cycle regulation by the Chk2 protein kinase**. *Science* 1998, **282**:1893-1897.

6. Banin S, Moyal L, Shieh S, Taya Y, Anderson CW, Chessa L, Smorodinsky NI, Prives C, Reiss Y, Shiloh Y, *et al*.: **Enhanced phosphorylation of p53 by ATM in response to DNA damage**. *Science* 1998, **281**:1674-1677.

7. Canman CE, Lim DS, Cimprich KA, Taya Y, Tamai K, Sakaguchi K, Appella E, Kastan MB, Siliciano JD: **Activation of the ATM kinase by ionizing radiation and phosphorylation of p53**. *Science* 1998, **281**:1677-1679.

8. Cortez D, Wang Y, Qin J, Elledge SJ: **Requirement of ATM-dependent phosphorylation of brca1 in the DNA damage response to double-strand breaks**. *Science* 1999, **286**:1162-1166.

9. Chen J: **Ataxia telangiectasia-related protein is involved in the phosphorylation of BRCA1 following deoxyribonucleic acid damage**. *Cancer Res* 2000, **60**:5037-5039.

10. Ward IM, Chen J: **Histone H2AX is phosphorylated in an ATR-dependent manner in response to replicational stress**. *J Biol Chem* 2001, **276**:47759-47762.

11. Rappold I, Iwabuchi K, Date T, Chen J: **Tumor suppressor p53 binding protein 1 (53BP1) is involved in DNA damage-signaling pathways**. *J Cell Biol* 2001, **153**:613-620.

12. Xia Z, Morales JC, Dunphy WG, Carpenter PB: **Negative cell cycle regulation and DNA damage-inducible phosphorylation of the BRCT protein 53BP1**. *J Biol Chem* 2001, **276**:2708-2718.

13. Bartek J, Lukas J: **Chk1 and Chk2 kinases in checkpoint control and cancer**. *Cancer Cell* 2003, **3**:421-429.

14. Zhang YW, Otterness DM, Chiang GG, Xie W, Liu YC, Mercurio F, Abraham RT: **Genotoxic stress targets human Chk1 for degradation by the ubiquitin-proteasome pathway**. *Mol Cell* 2005, **19**:607-618.

15. Shieh SY, Ahn J, Tamai K, Taya Y, Prives C: **The human homologs of checkpoint kinases Chk1 and Cds1 (Chk2) phosphorylate p53 at multiple DNA damage-inducible sites**. *Genes Dev* 2000, **14**:289-300.

16. Sheikh MS, Li XS, Chen JC, Shao ZM, Ordonez JV, Fontana JA: **Mechanisms of regulation of WAF1/Cip1 gene expression in human breast carcinoma: role of p53-dependent and independent signal transduction pathways**. *Oncogene* 1994, **9**:3407-3415.

17. Nakano K, Vousden KH: **PUMA, a novel proapoptotic gene, is induced by p53**. *Mol Cell* 2001, **7**:683-694.

18. Oda E, Ohki R, Murasawa H, Nemoto J, Shibue T, Yamashita T, Tokino T, Taniguchi T, Tanaka N: **Noxa, a BH3-only member of the Bcl-2 family and candidate mediator of p53-induced apoptosis**. *Science* 2000, **288**:1053-1058.

19. Furnari B, Rhind N, Russell P: **Cdc25 mitotic inducer targeted by chk1 DNA damage checkpoint kinase**. *Science* 1997, **277**:1495-1497.

20. Zhou BB, Elledge SJ: **The DNA damage response: putting checkpoints in perspective**. *Nature* 2000, **408**:433-439.

21. Nojima H: **G1 and S-phase checkpoints, chromosome instability, and cancer**. *Methods Mol Biol* 2004, **280**:3-49.

22. Bartkova J, Horejsi Z, Koed K, Kramer A, Tort F, Zieger K, Guldberg P, Sehested M, Nesland JM, Lukas C, *et al.*: **DNA damage response as a candidate anti-cancer barrier in early human tumorigenesis**. *Nature* 2005, **434**:864-870.

23. Gorgoulis VG, Vassiliou LV, Karakaidos P, Zacharatos P, Kotsinas A, Liloglou T, Venere M, Ditullio RA, Jr., Kastrinakis NG, Levy B, *et al.*: **Activation of the DNA damage checkpoint and genomic instability in human precancerous lesions**. *Nature* 2005, **434**:907-913.

24. Shiloh Y: **Ataxia-telangiectasia and the Nijmegen breakage syndrome: related disorders but genes apart**. *Annu Rev Genet* 1997, **31**:635-662.

25. Zhou BB, Bartek J: **Targeting the checkpoint kinases: chemosensitization versus chemoprotection**. *Nat Rev Cancer* 2004, **4**:216-225.

26. Murray AW, Solomon MJ, Kirschner MW: **The role of cyclin synthesis and degradation in the control of maturation promoting factor activity**. *Nature* 1989, **339**:280-286.

27. Draetta G, Luca F, Westendorf J, Brizuela L, Ruderman J, Beach D: **Cdc2 protein kinase is complexed with both cyclin A and B: evidence for proteolytic inactivation of MPF**. *Cell* 1989, **56**:829-838.

28. Pines J, Hunter T: **Isolation of a human cyclin cDNA: evidence for cyclin mRNA and protein regulation in the cell cycle and for interaction with p34cdc2**. *Cell* 1989, **58**:833-846.

29. Kimura K, Hirano M, Kobayashi R, Hirano T: **Phosphorylation and activation of 13S condensin by Cdc2 *in vitro***. *Science* 1998, **282**:487-490.

30. Peter M, Nakagawa J, Doree M, Labbe JC, Nigg EA: ***In vitro* disassembly of the nuclear lamina and M phase-specific phosphorylation of lamins by cdc2 kinase**. *Cell* 1990, **61**:591-602.

31. Parker LL, Piwnica-Worms H: **Inactivation of the p34cdc2-cyclin B complex by the human WEE1 tyrosine kinase**. *Science* 1992, **257**:1955-1957.

32. Liu F, Stanton JJ, Wu Z, Piwnica-Worms H: **The human Myt1 kinase preferentially phosphorylates Cdc2 on threonine 14 and localizes to the endoplasmic reticulum and Golgi complex**. *Mol Cell Biol* 1997, **17**:571-583.

33. Mueller PR, Coleman TR, Kumagai A, Dunphy WG: **Myt1: a membrane-associated inhibitory kinase that phosphorylates Cdc2 on both threonine-14 and tyrosine-15**. *Science* 1995, **270**:86-90.

34. Millar JB, Blevitt J, Gerace L, Sadhu K, Featherstone C, Russell P: **p55CDC25 is a nuclear protein required for the initiation of mitosis in human cells**. *Proc Natl Acad Sci U S A* 1991, **88**:10500-10504.

35. Nigg EA: **Cyclin-dependent kinase 7: at the cross-roads of transcription, DNA repair and cell cycle control?** *Curr Opin Cell Biol* 1996, **8**:312-317.

36. Adamczewski JP, Rossignol M, Tassan JP, Nigg EA, Moncollin V, Egly JM: **MAT1, cdk7 and cyclin H form a kinase complex which is UV light-sensitive upon association with TFIIH**. *Embo J* 1996, **15**:1877-1884.

37. Clute P, Pines J: **Temporal and spatial control of cyclin B1 destruction in metaphase**. *Nat Cell Biol* 1999, **1**:82-87.

38. Hagting A, Jackman M, Simpson K, Pines J: **Translocation of cyclin B1 to the nucleus at prophase requires a phosphorylation-dependent nuclear import signal**. *Curr Biol* 1999, **9**:680-689.

39. Blasina A, Price BD, Turenne GA, McGowan CH: **Caffeine inhibits the checkpoint kinase ATM**. *Curr Biol* 1999, **9**:1135-1138.

40. Wang JL, Wang X, Wang H, Iliakis G, Wang Y: **CHK1-regulated S-phase checkpoint response reduces camptothecin cytotoxicity**. *Cell Cycle* 2002, **1**:267-272.

41. Koniaras K, Cuddihy AR, Christopoulos H, Hogg A, O'Connell MJ: **Inhibition of Chk1-dependent G2 DNA damage checkpoint radiosensitizes p53 mutant human cells**. *Oncogene* 2001, **20**:7453-7463.

42. Chen Z, Xiao Z, Gu WZ, Xue J, Bui MH, Kovar P, Li G, Wang G, Tao ZF, Tong Y, *et al.*: **Selective Chk1 inhibitors differentially sensitize p53-deficient cancer cells to cancer therapeutics**. *Int J Cancer* 2006.

43. Senderowicz AM: **The cell cycle as a target for cancer therapy: basic and clinical findings with the small molecule inhibitors flavopiridol and UCN-01**. *Oncologist* 2002, **7 Suppl 3**:12-19.

44. Senderowicz AM: **Novel direct and indirect cyclin-dependent kinase modulators for the prevention and treatment of human neoplasms**. *Cancer Chemother Pharmacol* 2003, **52 Suppl 1**:S61-73.

45. Barr FA, Sillje HH, Nigg EA: **Polo-like kinases and the orchestration of cell division**. *Nat Rev Mol Cell Biol* 2004, **5**:429-440.

46. Fenton B, Glover DM: **A conserved mitotic kinase active at late anaphase-telophase in syncytial Drosophila embryos**. *Nature* 1993, **363**:637-640.

47. van de Weerdt BC, Medema RH: **Polo-like kinases: a team in control of the division**. *Cell Cycle* 2006, **5**:853-864.

48. Toyoshima-Morimoto F, Taniguchi E, Nishida E: **Plk1 promotes nuclear translocation of human Cdc25C during prophase**. *EMBO Rep* 2002, **3**:341-348.

49. Nakajima H, Toyoshima-Morimoto F, Taniguchi E, Nishida E: **Identification of a consensus motif for Plk (Polo-like kinase) phosphorylation reveals Myt1 as a Plk1 substrate**. *J Biol Chem* 2003, **278**:25277-25280.

50. van Vugt MA, Bras A, Medema RH: **Polo-like kinase-1 controls recovery from a G2 DNA damage-induced arrest in mammalian cells**. *Mol Cell* 2004, **15**:799-811.

51. Toyoshima-Morimoto F, Taniguchi E, Shinya N, Iwamatsu A, Nishida E: **Polo-like kinase 1 phosphorylates cyclin B1 and targets it to the nucleus during prophase**. *Nature* 2001, **410**:215-220.

52. do Carmo Avides M, Glover DM: **Abnormal spindle protein, Asp, and the integrity of mitotic centrosomal microtubule organizing centers**. *Science* 1999, **283**:1733-1735.

53. do Carmo Avides M, Tavares A, Glover DM: **Polo kinase and Asp are needed to promote the mitotic organizing activity of centrosomes**. *Nat Cell Biol* 2001, **3**:421-424.

54. Budde PP, Kumagai A, Dunphy WG, Heald R: **Regulation of Op18 during spindle assembly in Xenopus egg extracts**. *J Cell Biol* 2001, **153**:149-158.

55. Casenghi M, Barr FA, Nigg EA: **Phosphorylation of Nlp by Plk1 negatively regulates its dynein-dynactin-dependent targeting to the centrosome**. *J Cell Sci* 2005, **118**:5101-5108.

56. Casenghi M, Meraldi P, Weinhart U, Duncan PI, Korner R, Nigg EA: **Polo-like kinase 1 regulates Nlp, a centrosome protein involved in microtubule nucleation**. *Dev Cell* 2003, **5**:113-125.

57. McNally KP, Buster D, McNally FJ: **Katanin-mediated microtubule severing can be regulated by multiple mechanisms**. *Cell Motil Cytoskeleton* 2002, **53**:337-349.

58. Glover DM: **Polo kinase and progression through M phase in Drosophila: a perspective from the spindle poles**. *Oncogene* 2005, **24**:230-237.

59. Alexandru G, Uhlmann F, Mechtler K, Poupart MA, Nasmyth K: **Phosphorylation of the cohesin subunit Scc1 by Polo/Cdc5 kinase regulates sister chromatid separation in yeast**. *Cell* 2001, **105**:459-472.

60. Kotani S, Tugendreich S, Fujii M, Jorgensen PM, Watanabe N, Hoog C, Hieter P, Todokoro K: **PKA and MPF-activated polo-like kinase regulate anaphase-promoting complex activity and mitosis progression**. *Mol Cell* 1998, **1**:371-380.

61. Sumara I, Vorlaufer E, Stukenberg PT, Kelm O, Redemann N, Nigg EA, Peters JM: **The dissociation of cohesin from chromosomes in prophase is regulated by Polo-like kinase**. *Mol Cell* 2002, **9**:515-525.

62. Kraft C, Herzog F, Gieffers C, Mechtler K, Hagting A, Pines J, Peters JM: **Mitotic regulation of the human anaphase-promoting complex by phosphorylation**. *Embo J* 2003, **22**:6598-6609.

63. May KM, Reynolds N, Cullen CF, Yanagida M, Ohkura H: **Polo boxes and Cut23 (Apc8) mediate an interaction between polo kinase and the anaphase-promoting complex for fission yeast mitosis**. *J Cell Biol* 2002, **156**:23-28.

64. Zhou T, Aumais JP, Liu X, Yu-Lee LY, Erikson RL: **A role for Plk1 phosphorylation of NudC in cytokinesis**. *Dev Cell* 2003, **5**:127-138.

65. Strebhardt K, Ullrich A: **Targeting polo-like kinase 1 for cancer therapy**. *Nat Rev Cancer* 2006, **6**:321-330.

66. Takai N, Hamanaka R, Yoshimatsu J, Miyakawa I: **Polo-like kinases (Plks) and cancer**. *Oncogene* 2005, **24**:287-291.

67. Takai N, Miyazaki T, Fujisawa K, Nasu K, Hamanaka R, Miyakawa I: **Expression of polo-like kinase in ovarian cancer is associated with histological grade and clinical stage**. *Cancer Lett* 2001, **164**:41-49.

68. Kanaji S, Saito H, Tsujitani S, Matsumoto S, Tatebe S, Kondo A, Ozaki M, Ito H, Ikeguchi M: **Expression of polo-like kinase 1 (PLK1) protein predicts the survival of patients with gastric carcinoma**. *Oncology* 2006, **70**:126-133.

69. Weichert W, Kristiansen G, Schmidt M, Gekeler V, Noske A, Niesporek S, Dietel M, Denkert C: **Polo-like kinase 1 expression is a prognostic factor in human colon cancer**. *World J Gastroenterol* 2005, **11**:5644-5650.

70. Liu X, Erikson RL: **Polo-like kinase (Plk)1 depletion induces apoptosis in cancer cells**. *Proc Natl Acad Sci U S A* 2003, **100**:5789-5794.

71. Liu X, Lei M, Erikson RL: **Normal cells, but not cancer cells, survive severe Plk1 depletion**. *Mol Cell Biol* 2006, **26**:2093-2108.

72. Kappel S, Matthess Y, Zimmer B, Kaufmann M, Strebhardt K: **Tumor inhibition by genomically integrated inducible RNAi-cassettes**. *Nucleic Acids Res* 2006.

73. Matthess Y, Kappel S, Spankuch B, Zimmer B, Kaufmann M, Strebhardt K: **Conditional inhibition of cancer cell proliferation by tetracycline-responsive, H1 promoter-driven silencing of PLK1**. *Oncogene* 2005, **24**:2973-2980.

74. McInnes C, Mazumdar A, Mezna M, Meades C, Midgley C, Scaerou F, Carpenter L, Mackenzie M, Taylor P, Walkinshaw M, *et al*.: **Inhibitors of Polo-like kinase reveal roles in spindle-pole maintenance**. *Nat Chem Biol* 2006.

75. Gumireddy K, Reddy MV, Cosenza SC, Boominathan R, Baker SJ, Papathi N, Jiang J, Holland J, Reddy EP: **ON01910, a non-ATP-competitive small molecule inhibitor of Plk1, is a potent anticancer agent**. *Cancer Cell* 2005, **7**:275-286.

76. Warner SL, Gray PJ, Von Hoff DD: **Tubulin-associated drug targets: Aurora kinases, Polo-like kinases, and others**. *Semin Oncol* 2006, **33**:436-448.

77. Mundt KE, Golsteyn RM, Lane HA, Nigg EA: **On the regulation and function of human polo-like kinase 1 (PLK1): effects of overexpression on cell cycle progression**. *Biochem Biophys Res Commun* 1997, **239**:377-385.

78. Lindon C, Pines J: **Ordered proteolysis in anaphase inactivates Plk1 to contribute to proper mitotic exit in human cells**. *J Cell Biol* 2004, **164**:233-241.

79. Shirayama M, Zachariae W, Ciosk R, Nasmyth K: **The Polo-like kinase Cdc5p and the WD-repeat protein Cdc20p/fizzy are regulators and substrates of the anaphase promoting complex in Saccharomyces cerevisiae**. *Embo J* 1998, **17**:1336-1349.

80. Lee KS, Erikson RL: **Plk is a functional homolog of Saccharomyces cerevisiae Cdc5, and elevated Plk activity induces multiple septation structures**. *Mol Cell Biol* 1997, **17**:3408-3417.

81. Qian YW, Erikson E, Li C, Maller JL: **Activated polo-like kinase Plx1 is required at multiple points during mitosis in Xenopus laevis**. *Mol Cell Biol* 1998, **18**:4262-4271.

82. Qian YW, Erikson E, Maller JL: **Purification and cloning of a protein kinase that phosphorylates and activates the polo-like kinase Plx1**. *Science* 1998, **282**:1701-1704.

83. Kelm O, Wind M, Lehmann WD, Nigg EA: **Cell cycle-regulated phosphorylation of the Xenopus polo-like kinase Plx1**. *J Biol Chem* 2002, **277**:25247-25256.

84. Jang YJ, Ma S, Terada Y, Erikson RL: **Phosphorylation of threonine 210 and the role of serine 137 in the regulation of mammalian polo-like kinase**. *J Biol Chem* 2002, **277**:44115-44120.

85. Qian YW, Erikson E, Maller JL: **Mitotic effects of a constitutively active mutant of the Xenopus polo-like kinase Plx1**. *Mol Cell Biol* 1999, **19**:8625-8632.

86. Jang YJ, Lin CY, Ma S, Erikson RL: **Functional studies on the role of the C-terminal domain of mammalian polo-like kinase**. *Proc Natl Acad Sci U S A* 2002, **99**:1984-1989.

87. Elia AE, Cantley LC, Yaffe MB: **Proteomic screen finds pSer/pThr-binding domain localizing Plk1 to mitotic substrates**. *Science* 2003, **299**:1228-1231.

88. Elia AE, Rellos P, Haire LF, Chao JW, Ivins FJ, Hoepker K, Mohammad D, Cantley LC, Smerdon SJ, Yaffe MB: **The molecular basis for phosphodependent substrate targeting and regulation of Plks by the Polo-box domain**. *Cell* 2003, **115**:83-95.

89. Sumara I, Gimenez-Abian JF, Gerlich D, Hirota T, Kraft C, de la Torre C, Ellenberg J, Peters JM: **Roles of polo-like kinase 1 in the assembly of functional mitotic spindles**. *Curr Biol* 2004, **14**:1712-1722.

90. van Vugt MA, van de Weerdt BC, Vader G, Janssen H, Calafat J, Klompmaker R, Wolthuis RM, Medema RH: **Polo-like kinase-1 is required for bipolar spindle formation but is dispensable for anaphase promoting complex/Cdc20 activation and initiation of cytokinesis**. *J Biol Chem* 2004, **279**:36841-36854.

91. Cogswell JP, Brown CE, Bisi JE, Neill SD: **Dominant-negative polo-like kinase 1 induces mitotic catastrophe independent of cdc25C function**. *Cell Growth Differ* 2000, **11**:615-623.

92. Zink D, Fischer AH, Nickerson JA: **Nuclear structure in cancer cells**. *Nat Rev Cancer* 2004, **4**:677-687.

93. Ching YP, Qi Z, Wang JH: **Cloning of three novel neuronal Cdk5 activator binding proteins**. *Gene* 2000, **242**:285-294.

94. Chen J, Liu B, Liu Y, Han Y, Yu H, Zhang Y, Lu L, Zhen Y, Hui R: **A novel gene IC53 stimulates ECV304 cell proliferation and is upregulated in failing heart**. *Biochem Biophys Res Commun* 2002, **294**:161-166.

95. Xie YH, He XH, Tang YT, Li JJ, Pan ZM, Qin WX, Wan da F, Gu JR: **Cloning and characterization of human IC53-2, a novel CDK5 activator binding protein**. *Cell Res* 2003, **13**:83-91.

96. Li H, Zhu H, Xu CJ, Yuan J: **Cleavage of BID by caspase 8 mediates the mitochondrial damage in the Fas pathway of apoptosis**. *Cell* 1998, **94**:491-501.

97. Cryns VL, Byun Y, Rana A, Mellor H, Lustig KD, Ghanem L, Parker PJ, Kirschner MW, Yuan J: **Specific proteolysis of the kinase protein kinase C-related kinase 2 by caspase-3 during apoptosis. Identification by a novel, small pool expression cloning strategy**. *J Biol Chem* 1997, **272**:29449-29453.

98. Elbashir SM, Harborth J, Lendeckel W, Yalcin A, Weber K, Tuschl T: **Duplexes of 21-nucleotide RNAs mediate RNA interference in cultured mammalian cells**. *Nature* 2001, **411**:494-498.

99. Jin P, Hardy S, Morgan DO: **Nuclear localization of cyclin B1 controls mitotic entry after DNA damage**. *J Cell Biol* 1998, **141**:875-885.

100. Porter LA, Donoghue DJ: **Cyclin B1 and CDK1: nuclear localization and upstream regulators**. *Prog Cell Cycle Res* 2003, **5**:335-347.

101. Li J, Meyer AN, Donoghue DJ: **Nuclear localization of cyclin B1 mediates its biological activity and is regulated by phosphorylation**. *Proc Natl Acad Sci U S A* 1997, **94**:502-507.

102. Yang J, Bardes ES, Moore JD, Brennan J, Powers MA, Kornbluth S: **Control of cyclin B1 localization through regulated binding of the nuclear export factor CRM1**. *Genes Dev* 1998, **12**:2131-2143.

103. Yang J, Song H, Walsh S, Bardes ES, Kornbluth S: **Combinatorial control of cyclin B1 nuclear trafficking through phosphorylation at multiple sites**. *J Biol Chem* 2001, **276**:3604-3609.

104. Smits VA, Klompmaker R, Arnaud L, Rijksen G, Nigg EA, Medema RH: **Polo-like kinase-1 is a target of the DNA damage checkpoint**. *Nat Cell Biol* 2000, **2**:672-676.

105. van Vugt MA, Smits VA, Klompmaker R, Medema RH: **Inhibition of Polo-like kinase-1 by DNA damage occurs in an ATM- or ATR-dependent fashion**. *J Biol Chem* 2001, **276**:41656-41660.

106. Tsvetkov L, Stern DF: **Phosphorylation of Plk1 at S137 and T210 is inhibited in response to DNA damage**. *Cell Cycle* 2005, **4**:166-171.

107. Blank M, Lerenthal Y, Mittelman L, Shiloh Y: **Condensin I recruitment and uneven chromatin condensation precede mitotic cell death in response to DNA damage**. *J Cell Biol* 2006, **174**:195-206.

108. Kramer A, Mailand N, Lukas C, Syljuasen RG, Wilkinson CJ, Nigg EA, Bartek J, Lukas J: **Centrosome-associated Chk1 prevents premature activation of cyclin-B-Cdk1 kinase**. *Nat Cell Biol* 2004, **6**:884-891.

109. Ou YY, Zhang M, Chi S, Matyas JR, Rattner JB: **Higher order structure of the PCM adjacent to the centriole**. *Cell Motil Cytoskeleton* 2003, **55**:125-133.

110. Jackman M, Lindon C, Nigg EA, Pines J: **Active cyclin B1-Cdk1 first appears on centrosomes in prophase**. *Nat Cell Biol* 2003, **5**:143-148.

111. Leung-Pineda V, Ryan CE, Piwnica-Worms H: **Phosphorylation of Chk1 by ATR Is Antagonized by a Chk1-Regulated Protein Phosphatase 2A Circuit**. *Mol Cell Biol* 2006, **26**:7529-7538.

112. Wu RS, Kumar A, Warner JR: **Ribosome formation is blocked by camptothecin, a reversible inhibitor of RNA synthesis**. *Proc Natl Acad Sci U S A* 1971, **68**:3009-3014.

113. Ljungman M, Hanawalt PC: **The anti-cancer drug camptothecin inhibits elongation but stimulates initiation of RNA polymerase II transcription**. *Carcinogenesis* 1996, **17**:31-35.

114. Green PS, Leeuwenburgh C: **Mitochondrial dysfunction is an early indicator of doxorubicin-induced apoptosis**. *Biochim Biophys Acta* 2002, **1588**:94-101.

115. Lu X, Nannenga B, Donehower LA: **PPM1D dephosphorylates Chk1 and p53 and abrogates cell cycle checkpoints**. *Genes Dev* 2005, **19**:1162-1174.

116. Oliva-Trastoy M, Berthonaud V, Chevalier A, Ducrot C, Marsolier-Kergoat MC, Mann C, Leteurtre F: **The Wip1 phosphatase (PPM1D) antagonizes activation of the Chk2 tumour suppressor kinase**. *Oncogene* 2006.

117. Fujimoto H, Onishi N, Kato N, Takekawa M, Xu XZ, Kosugi A, Kondo T, Imamura M, Oishi I, Yoda A, *et al*.: **Regulation of the antioncogenic Chk2 kinase by the oncogenic Wip1 phosphatase**. *Cell Death Differ* 2006, **13**:1170-1180.

118. Dozier C, Bonyadi M, Baricault L, Tonasso L, Darbon JM: **Regulation of Chk2 phosphorylation by interaction with protein phosphatase 2A via its B' regulatory subunit**. *Biol Cell* 2004, **96**:509-517.

119. Doxsey S, McCollum D, Theurkauf W: **Centrosomes in Cellular Regulation**. *Annu Rev Cell Dev Biol* 2005, **21**:411-434.

120. Doxsey S, Zimmerman W, Mikule K: **Centrosome control of the cell cycle**. *Trends Cell Biol* 2005, **15**:303-311.

121. Verde F, Labbe JC, Doree M, Karsenti E: **Regulation of microtubule dynamics by cdc2 protein kinase in cell-free extracts of Xenopus eggs**. *Nature* 1990, **343**:233-238.

122. Kramer A, Lukas J, Bartek J: **Checking out the centrosome**. *Cell Cycle* 2004, **3**:1390-1393.

123. Dutertre S, Cazales M, Quaranta M, Froment C, Trabut V, Dozier C, Mirey G, Bouche JP, Theis-Febvre N, Schmitt E, *et al*.: **Phosphorylation of CDC25B by Aurora-A at the centrosome contributes to the G2-M transition**. *J Cell Sci* 2004, **117**:2523-2531.

124. Hirota T, Kunitoku N, Sasayama T, Marumoto T, Zhang D, Nitta M, Hatakeyama K, Saya H: **Aurora-A and an interacting activator, the LIM protein Ajuba, are required for mitotic commitment in human cells**. *Cell* 2003, **114**:585-598.

125. Tsvetkov L, Xu X, Li J, Stern DF: **Polo-like kinase 1 and Chk2 interact and co-localize to centrosomes and the midbody**. *J Biol Chem* 2003, **278**:8468-8475.

126. Oshimori N, Ohsugi M, Yamamoto T: **The Plk1 target Kizuna stabilizes mitotic centrosomes to ensure spindle bipolarity**. *Nat Cell Biol* 2006.

127. Yuan J, Horvitz HR: **A first insight into the molecular mechanisms of apoptosis**. *Cell* 2004, **116**:S53-56, 51 p following S59.

128. Li H, Yuan J: **Deciphering the pathways of life and death**. *Curr Opin Cell Biol* 1999, **11**:261-266.

129. Chen F, Kamradt M, Mulcahy M, Byun Y, Xu H, McKay MJ, Cryns VL: **Caspase proteolysis of the cohesin component RAD21 promotes apoptosis**. *J Biol Chem* 2002, **277**:16775-16781.

130. Chen F, Chang R, Trivedi M, Capetanaki Y, Cryns VL: **Caspase proteolysis of desmin produces a dominant-negative inhibitor of intermediate filaments and promotes apoptosis**. *J Biol Chem* 2003, **278**:6848-6853.

131. Kothakota S, Azuma T, Reinhard C, Klippel A, Tang J, Chu K, McGarry TJ, Kirschner MW, Koths K, Kwiatkowski DJ, *et al*.: **Caspase-3-generated fragment of gelsolin: effector of morphological change in apoptosis**. *Science* 1997, **278**:294-298.

132. Lazebnik YA, Kaufmann SH, Desnoyers S, Poirier GG, Earnshaw WC: **Cleavage of poly(ADP-ribose) polymerase by a proteinase with properties like ICE**. *Nature* 1994, **371**:346-347.

133. Gibson SB, Oyer R, Spalding AC, Anderson SM, Johnson GL: **Increased expression of death receptors 4 and 5 synergizes the apoptosis response to combined treatment with etoposide and TRAIL**. *Mol Cell Biol* 2000, **20**:205-212.

134. Liu X, Yue P, Khuri FR, Sun SY: **Decoy receptor 2 (DcR2) is a p53 target gene and regulates chemosensitivity**. *Cancer Res* 2005, **65**:9169-9175.

135. Kaneda Y, Shimamoto H, Matsumura K, Arvind R, Zhang S, Sakai E, Omura K, Tsuchida N: **Role of caspase 8 as a determinant in chemosensitivity of p53-mutated head and neck squamous cell carcinoma cell lines**. *J Med Dent Sci* 2006, **53**:57-66.

136. Zhou BB, Li H, Yuan J, Kirschner MW: **Caspase-dependent activation of cyclin-dependent kinases during Fas-induced apoptosis in Jurkat cells**. *Proc Natl Acad Sci U S A* 1998, **95**:6785-6790.

137. Clarke CA, Bennett LN, Clarke PR: **Cleavage of claspin by caspase-7 during apoptosis inhibits the Chk1 pathway**. *J Biol Chem* 2005, **280**:35337-35345.

138. Jiang H, Luo S, Li H: **Cdk5 activator-binding protein C53 regulates apoptosis induced by genotoxic stress via modulating the G2/M DNA damage checkpoint.** *J Biol Chem* 2005, **280**:20651-20659.

139. Tang J, Erickson RL, Liu X: **Ectopic Expression of Plk1 Leads to Activation of the Spindle Checkpoint.** *Cell Cycle* 2006, **5**:2484-2488.

140. Bowser R and Smith MA: **Cell cycle proteins in Alzheimer's disease: plenty of wheels but no cycle.** *J. Alzheimers Dis.* 2002 **4**:249–254.

141. Patrick GN, Zhou P, Kwon YT, Howley PM, Tsai LH: **Conversion of p35 to p25**

deregulates Cdk5 activity and promotes neurodegeneration. *Nature* 1999 **402**:615-22.

142. Lee MS, Tsai LH: **Cdk5: one of the links between senile plaques and neurofibrillary tangles?** *J. Alzheimers Dis.* 2003 **5**:127–137